Many facets of CPEB proteins in neurons and beyond: expression, mRNA recognition and phosphorylation

Dissertation

zur

Erlangung des Doktorgrades (Dr. rer. nat.)

der

Mathematisch-Naturwissenschaftlichen Fakultät

der

Rheinischen Friedrich-Wilhelms-Universität Bonn

vorgelegt von

Lech Kaczmarczyk

aus

Kraków

Bonn, November 2011

Angefertigt mit Genehmigung der Mathematisch-Naturwissenschaftlichen Fakultät der Rheinischen Friedrich-Wilhelms-Universität Bonn

1. Gutachter: Prof. Dr. Christian Steinhäuser

2. Gutachter: Prof. Dr. Walter Witke

Tag der Promotion: 8. Juni 2012
Erscheinungsjahr: 2013

Table of contents

Acknowledgments

I would like to thank:

My scientific advisor, **Dr. Martin Theis** for scientific advice, all support he has been giving me, and even more for scientific optimism he has been sharing with me.

The director of the Institute of Cellular Neurosciences, **Prof. Dr. Christian Steinhäuser**, for critical advice and giving me opportunity to work at the excellent scientific facility.

All the fellow students and co-workers at the Institute of Cellular Neurosciences, for help and support.

Glossary

µg	microgram
µl	microliter
°C	Centigrade
ADP	adenosindiphosphate
AMPA	α-amino-3-hydroxy-5-methyl-4-isoxazol propionic acid
AMPA-R	α-amino-3-hydroxy-5-methyl-4-isoxazol propionic acid receptor
ATP	adenosintriphosphate
BHQ-1	Black Hole Quencher-1
bp	basepair(s)
Ca^{2+}	calcium
CaMKIIα	Ca^{2+}/Calmodulin-dependent protein kinase II, alpha isoform
cAMP	cyclic adenosinmonophosphate
cm	centimeter
CMV	cytomegalovirus
CNS	central nervous system
CPE	cytoplasmic polyadenylation element
CPEB	cytoplasmic polyadenylation element-binding protein
CPSF	cleavage and polyadenylation specificity factor
$_{dd}H_2O$	double distilled water
DKO	double knockout
DMSO	dimethylsulfoxide
DN	dominant negative
DNA	desoxyribonucleic acid
DNAse	desoxyribonuclease
dNTP	2-desoxy-nucleoside-5- triphosphate
E. coli	*Escherichia coli*
e.g.	(for) example
EDTA	ethylenediaminetetraacetic acid
EGFP	enhanced green fluorescent protein
eIF	eukariotic initiation factor
ES-cells	embrionic stem cells
ESdM	embrionic stem cells-derived microglia
et al.	*et altera* (and others)
FAM	fluorescein amidite
FCS	fetal calf serum
FSC	forward scatter
GFAP	glial fibrillary acidic protein
GLAST	glutamate-aspartate transporter
GLT-1	glutamate transporter 1
GluR	glutamate receptor
h	hour(s)
i.e.	*it est*
ICC	immunocytochemistry
K^+	potassium
kb	kilo base pairs (1000 bp)
loxP	locus of crossing over of P1
LTD	long term depression
LTP	long term potentiation
M	molar
mg	milligram
MGB	Minor Groove Binder
min	minute(s)
ml	milliliter
mm	millimeter
mM	millimolar
n.c.	negative control
ng	nanogram
NG2	neuroglycan 2
nm	nanometer
NMDA	N-methyl-D-aspartate
NMDA-R	N-methyl-D-aspartate receptor
nt	nucleotide(s)
Ori	Origin of replication
PABP	poly(A)-binding protein
PARN	poly(A)-ribonuclease
PBS	phosphate buffered saline
PCR	polymerase chain reaction
PFA	paraformaldehyde
pH	a negative decimal logarithm of the hydrogen ions concentration
PKA	protein kinase A
pmol	picomol
Poly(A)	polyadenylation signal
RNA	ribonucleic acid
RNAse	ribonuclease
rpm	revolutions per minute
RT	room temperature / reverse transcription
s	second(s)
SDS	sodium dodecyl sulphate
SE	*status epilepticus*
SOE-PCR	splicing by overlap extension PCR
SSC	side scatter
SV40	Simian Virus 40
Taq	*Thermus aquaticus*
TBE	tris-borate-EDTA
TE	tris-EDTA
TetO	tetracycline operator
tPA	tissue plasminogen activator
Tris	tris-(hydroxymethyl)-aminomethane
tTA	tetracycline transactivator
U	enzyme unit
UTR	untranslated region
UV	ultraviolet
v/v	volume per volume
w/v	weight per volume
WT	wildtype

1 Introduction

The fundamental role of transcription in regulating gene expression is well established. However, the importance of post-transcriptional mechanisms has been increasingly acknowledged only in recent decades. These mechanisms involve alternative splicing and mRNA editing, specific subcellular targeting of mature mRNA, **translational regulation** and posttranslational modifications of proteins (Hovland *et al.*, 1996; Ashkenas, 1997; Macdonald, 2001; Routtenberg and Rekart, 2005; Xiao and Lee, 2010). Translational regulation plays a key role in controlling the process of protein synthesis (Merrick, 1992). It is fundamental for relatively basic mechanisms (e.g. mitosis) and the most complex biological functions (e.g. learning and cognition). The latter we just start to elucidate.

1.1 The initiation phase of translation

Most of the translational regulation occurs at the initiation phase. Probably due to this fact, the evolutionary mechanisms of initiation have diverged the most, allowing different organisms to adjust protein synthesis to their needs. Herein, the focus is put on 5' end-dependent mechanism of translation initiation in eukaryotes (Fig. 1-1). For simplicity reasons, several factors directly and indirectly involved in translation initiation were omitted. Modulation of translation efficiency in eukaryotes involves proteins, called **e**ukaryotic translation **i**nitiation **f**actors (eIFs) as well as proteins interacting with them and/or with mRNA. The magnitude of the regulation, as well as its direction (inhibition or activation), depends on the interplay between these proteins and mRNAs, as well as on auxiliary regulatory factors (i.e. protein kinases). Promotion of translation leads to recognition of the initiation codon and formation of the 48S complex (the complex of the S40 ribosomal subunit, initiation factors and mRNA) (Mendez and Richter, 2001; Jackson *et al.*, 2010). A simplified scheme of translation initiation steps, leading to S48 complex formation is presented in Fig. 1-1.

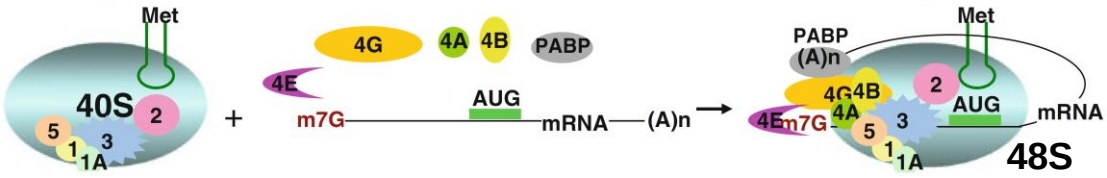

Fig. 1-1: "Canonical" 5' end-dependent mechanisms of translation initiation in eukaryotes. Eukaryotic initiation factors eIF1, eIF1A, eIF2, eIF3, eIF4A, eIF4B, eIF4E, eIF4G, and eIF5 are labelled 1, 1A, 2, 3, 4A, 4B, 4E, 4G, and 5, respectively; Met – methionyl-tRNA; m7G - **7**-**m**ethyl **g**uanine nucleotide (cap); PABP – **P**oly(**A**) **B**inding **P**rotein; AUG – start codon (encoding methionine); 40S – small ribosomal subunit; (A)n – poly(A) tail. Adapted from Malys and McCarthy (2011).

In cap-dependent translation initiation (shown in Fig. 1-1), most regulatory factors are nucleated around eIF-4A, eIF-4E and eIF-4G (together forming a cap-binding

complex eIF-4F) at the 5'end of mRNA. Assembly of eIF-4F facilitates binding to the S40 ribosomal subunit, via eIF-3. eIF-3, in turn, recruits eIF-2-GTP-Met-tRNA to the complex and promotes ribosomal scanning of the start codon (Jackson *et al.*, 2010). The detailed function of the initiation factors depicted on Fig. 1-1 is summarized in Tab. 1-1.

Factor	Number of subunits	Function
eIF-1	1	Ensures the fidelity of initiation codon selection, promotes ribosomal scanning, stimulates binding of eIF2–GTP–Met-tRNA$_i$ to 40S subunits, prevents premature eIF5-induced hydrolysis of eIF2-bound GTP and Pi release
eIF-1A	1	Stimulates binding of eIF2–GTP–Met-tRNAi to 40S subunits and cooperates with eIF1 in promoting ribosomal scanning and initiation codon selection
eIF-2	3	Forms an eIF2–GTP–Met-tRNA$_i$ ternary complex that binds to the 40S subunit, thus mediating ribosomal recruitment of Met-tRNA$_i$
eIF-3	13	Binds 40S subunits, eIF1, eIF4G and eIF5; stimulates binding of eIF2–GTP–Met-tRNA$_i$ to 40S subunits; promotes attachment of 43S complexes to mRNA and subsequent scanning; possesses ribosome dissociation and anti-association activities, preventing joining of 40S and 60S subunits
eIF-4A	1	ATP-dependent RNA helicase
eIF-4E	1	Binds to the 5′ cap structure of mRNA
eIF-4G	1	Binds eIF4E, eIF4A, eIF3, PABP, SLIP1 and mRNA and enhances the helicase activity of elF4A
eIF-4F	3	A cap-binding complex, comprising eIF4E, eIF4A and eIF4G, unwinds the 5′ proximal region of mRNA and mediates the attachment of 43S complexes to it, assists ribosomal complexes during scanning
eIF-4B	1	An RNA-binding protein that enhances the helicase activity of eIF4A
eIF-5	1	A GTPase-activating protein, specific for GTP-bound eIF2, that induces hydrolysis of eIF2-bound GTP upon recognition of the initiation codon
PABP	1	Binds to the 3′ poly(A) tail of mRNA and eIF4G, enhances binding of eIF4F to the cap, might facilitate recruitment of recycled post-termination 40S subunits back to the 5′ end of mRNA

Tab. 1-1: Selected translation initiation factors and their functions. PABP – Poly(A) Binding Protein (after Jackson *et al.*, 2010).

1.2 3'UTR-interacting proteins mediate mRNA sequence-specific translational regulation

Translation of polyadenylated mRNAs is promoted by interaction of the poly(A) tail with the capped 5'end of the mRNA, facilitating the 48S complex formation (Fig. 1-1). This occurs via the **P**oly(**A**) **B**inding **P**rotein (PABP) and involves physical interaction between eIF-4G and PABP (Tarun and Sachs, 1996). The resulting circularization of the mRNA structure (Fig. 1-2) leads to an increase in protein synthesis. Such circularization of transcripts may have at least three advantages, contributing to an increase in the overall translation efficacy: (i) promotion of reinitiation of translation at the 5' end, as the 3' end of mRNA is in close proximity, (ii) stabilization of the transcript due to simultaneous protection of both mRNA ends, (iii) prevention of translation of truncated transcripts (Johnstone and Lasko, 2001).

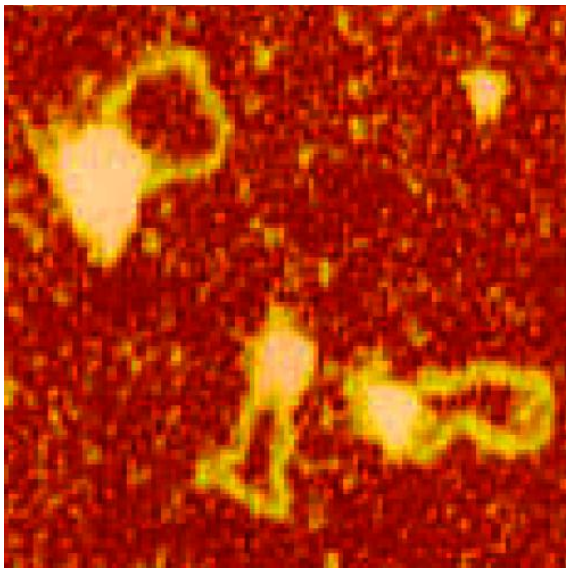

Fig. 1-2: Circular protein-RNA complexes. Atomic force microscopy visualization of circular, capped and polyadenylated double-stranded mRNAs in the presence of **P**oly(**A**) **B**inding **P**rotein (PABP), eIF-4G and eIF-4E (after Wells *et al.*, 1998).

The binding of PABP to eIF-4F is not the only example of the interaction between 3' and 5' mRNA ends. Protein factors interacting with mRNA in a sequence-specific manner can modulate synthesis of specific proteins by competing with the 5'mRNA end for PABP binding, by affecting its structural conformation, or by modulating the length of the poly(A) tail and thereby regulating the amount of PABP binding to it. This type of regulation involves non-canonical (i.e. required only in certain circumstances) auxiliary proteins, which by interacting with canonical (core) elements of the translational machinery, restrict the formation of the S43 complex (composed of a 40S subunit, eIF1, eIF1A, eIF3, eIF2–GTP–Metionyl-tRNA and probably eIF5) (Jackson *et al.*, 2010). Such sequence-specific regulators of translation initiation are most often binding to the 3'UTR region of the mRNA and prevent interaction of PABP with the cap-binding complex either directly or via intermediate proteins (Fig. 1-3).

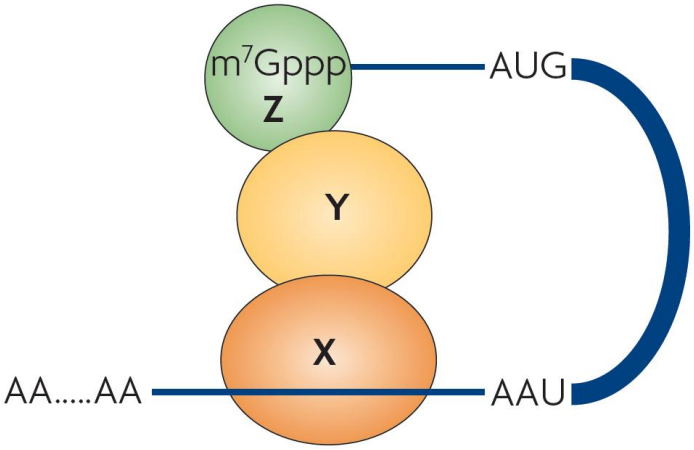

Fig. 1-3: Circular model of translational inhibition by 3'UTR-interacting proteins. A sequence specific translational factor X binds to the 3'UTR of mRNA and either directly or via an intermediate protein Y, interacts with the cap-binding protein Z. This results in translational inhibition by preventing the assembly of the cap-binding complex (eIF-4E + eIF-4G + eIF-4A). After Jackson *et al.* (2010).

In Tab. 1-2, examples of proteins X, Y, and Z (from Fig. 1-3) in *Xenopus laevis* oocytes and *Drosophila melanogaster* embryos are shown.

Organism	mRNA	Protein X	Protein Y	Protein Z
Xenopus laevis (oocytes)	Cyclin B1 (and others)	CPEB	eIF-4E-T/Maskin	eIF-4E1a/b
Drosophila melanogaster (embryos)	Nanos	Smaug	CUP	eIF-4E1b
	Oskar	Bruno	CUP	eIF-4E1b
	Caudal	**Bicoid**	**Bicoid**	eIF-4E-HP
	Hauchback	**Nanos**, **Pumilio**, and **Brat**	**Nanos**, **Pumilio**, and **Brat**	eIF-4E-HP

Tab. 1-2: Translational regulation by 3'UTR-interacting proteins. Selected examples of proteins involved in translational regulation in the 3'UTR in *Xenopus laevis* oocytes and *Drosophila melanogaster* embryos. Protein homologues, performing the function of proteins X, Y and Z (from Fig. 1-3), were shown (proteins fulfilling the function of both, X and Y were highlighted in **bold**). After Jackson *et al.* (2010).

1.3 Translational regulation: from development to synaptic plasticity and memory

In animal development, the regulation of gene expression occurs preferentially at the translation level, when a quick response to environmental cues is crucial. For example, translation of a pool of maternal mRNAs in the oocyte (transcribed during oogenesis) is rapidly triggered upon fertilization. Later, during development, translational regulation allows for a precise spatiotemporal restriction of protein expression, required for proper embryonic patterning (Curtis *et al.*, 1995; Tadros and Lipshitz, 2005). Translational regulation in development has been most extensively studied on two model organisms: *Xenopus laevis* (African clawed frog) and *Drosophila melanogaster* (Fruit fly). In both, it involves the regulation of Poly(A) tail length (Wilhelm and Smibert, 2005; Richter and Lasko, 2011). However oocyte maturation and embryonic development are not the only processes where translation regulation plays a key role. Translational mechanisms are also involved in strictly somatic processes, e.g. iron homeostasis (Muckenthaler *et al.*, 1998) or erythroid differentiation (Ostareck *et al.*, 2001). More recently, translational regulation has been shown critical for the functioning of the **c**entral **n**ervous **s**ystem (CNS). The increasing evolutionary complexity of animal nervous systems led to development of complex pre- and postsynaptic mechanisms, to allow appropriate responses to complex patterns of synaptic stimulation. These mechanisms are nowadays acknowledged as the basis for how the brain perceives and stores information (Kandel, 2001; Klann and Dever, 2004).

1.3.1 Translational regulation by the Cytoplasmic Polyadenylation Element Binding proteins

The **C**ytoplasmic **P**olyadenylation **E**lement **B**inding proteins (referred herein as CPEBs) are mRNA-binding translational factors. CPEBs in mammals comprise a family of four within-species paralogs, sharing considerable structural and functional similarities. All CPEBs contain an N-terminal regulatory domain (containing phosphorylation sites) and a C-terminal **R**NA **b**inding **d**omain (RBD), containing a **Z**n^{2+} **fi**nger (ZiF) motif (Fig. 1-4).

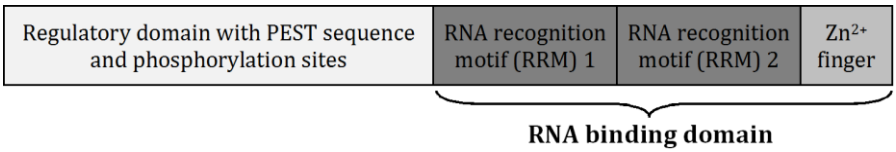

Fig. 1-4: Tertiary structure of CPEBs. All four CPEBs expressed in mouse brain are structurally similar, consisting of an N-terminal regulatory domain (containing phosphorylation sites) and a C-terminal RBD containing a ZiF motif.

On the basis of the RBD, CPEBs 2-4 can be regarded as a separate group, as they share more than 98% similarity in the amino acid sequence of their RBDs (Theis *et al.*, 2003b). CPEBs bind to a conserved nucleotide sequence (**c**ytoplasmic **p**olyadenylation **e**lement, CPE) located in the 3'UTR of the target mRNAs, and generally repress translation, unless activated. The recognition consensus site for CPEBs is the uracil-rich sequence UUUUUAU. However, the sequence specificity of CPEBs is not strictly defined and alternative binding sites have been widely reported (Hake *et al.*, 1998; Du and Richter, 2005). In addition to oogenesis and embryonic development, they are involved in the control of cellular senescence, synaptic plasticity, memory and learning. Seven percent of brain mRNAs are estimated to be CPEB targets based on the presence of a CPE, although only a small fraction has been experimentally confirmed so far.

1.4 Long term potentiation and synaptic plasticity

As synaptic plasticity we understand the changes in the synaptic efficacy induced by varying patterns of neuronal activity. This unique quality of synaptic connections and their interplay with astrocytes seem to be the basis for how neural circuits modulate their own activity. It is neuronal plasticity that allows the brain to perform most, if not all of its higher functions, including cognitive ones. One form of synaptic plasticity, thought to be especially related to memory and learning, is **l**ong **t**erm **p**otentiation (LTP) – a long lasting enhancement of synaptic efficacy. It represents an evolutionary conserved mechanism of memory storage (Kandel, 2001). The subcellular mechanisms of LTP formation remain to large extent unknown, however in recent years much progress has been made towards the delineation of how LTP is triggered and maintained, what proteins are involved in this process and how they interact with each other, allowing us to remember our own birthday date or significant events in our life. Depending on the

strength of the postsynaptic stimulation, we can distinguish an early phase of LTP (E-LTP), and a late phase of LTP (L-LTP). Unlike E-LTP, L-LTP requires new protein synthesis. Initial models suggested that synthesis of plasticity related proteins (PRPs) occurs in the cell body (together with the synthesis of other proteins) and these proteins are subsequently targeted specifically to the activated synapse(s). However, recent evidence suggest that protein synthesis occurs independently of transcription and be restricted to neuronal dendrites (reviewed by Klann and Dever, 2004). Moreover, the mechanisms involved are evolutionary conserved: **l**ong **t**erm **f**acilitation (LTF), a long-term form of synaptic plasticity in *Aplysia californica* is mechanistically very similar to L-LTP in the mammalian hippocampus (Kandel, 2001). These processes are the cellular correlates of learning and memory. Herein, selected regulatory mechanisms of local protein synthesis in brain involving CPEB proteins are described.

1.5 Subcellular mRNA targeting

As early as in 1965 David Bodian spotted a striking relationship of nerve cell RNA with specific synaptic sites (Bodian, 1965). Later on, dendritic spines were found to contain polyribosomes (Steward and Levy, 1982). Since this early works, a large number of neuronal transcripts distributed in a polarized fashion has been identified (Eberwine *et al.*, 2002). A genome-wide analysis of gene expression reveals that a significant number of messenger RNAs have a specific localization in neurons (Lein *et al.*, 2007). Dendritically localized mRNA is involved in certain types of synaptic plasticity (Kang and Schuman, 1996; Huber *et al.*, 2000; Jansen, 2001; Luscher and Huber, 2010). Particularly striking sub-regional differences in mRNA localization were observed for hippocampus and cerebellum. One of such dendrite-specific mRNA is the transcript encoding the alpha isoform of Ca^{2+}/**Cal**modulin-dependent protein **k**inase II (CaMKIIα), a key player in synaptic plasticity and a CPEB target.

1.6 CPEB in neural function

Local translation is a key mechanism controlling protein homeostasis of the synapse, and thereby synaptic plasticity (Wu *et al.*, 2007; Cajigas *et al.*, 2010). The molecular mechanism of CPEB function in this process has been extensively discussed (Mendez and Richter, 2001; Richter, 2007). Nonetheless, still very little is known about the nature of interactions between CPEBs and other elements of translational machinery. Several proteins were shown to functionally interact with CPEB in mouse hippocampus. These includes Neuroguidin (Ngd), a protein repressing translation in a CPE-dependent manner in *Xenopus* oocytes (Jung *et al.*, 2006). Importantly, neuroguidin is present in axon and dendrites, where it may have a function similar to maskin, with which it shares structural similarities. CPEB-1 also was shown to interact with the poly(A) polymerase Gld2 (Rouhana *et al.*, 2005). Gld2 expression in mammalian brain is most abundant in

cognitive and emotional learning-associated areas, further showing involvement of translational regulation in learning and memory mechanisms (Rouhana *et al.*, 2005). Other proteins which bind to CPEB and which are also present in neurons are the **c**leavage and **p**olyadenylation **s**pecificity **f**actor (CPSF), symplekin, and **p**oly(**A**)-specific **r**ibo**n**uclease (PARN) (see Fig. 1-5). CPSF is a crucial factor, recognizing the AAUAAA hexanucleotide, which is required for pre-mRNA polyadenylation (Takagaki *et al.*, 1990).

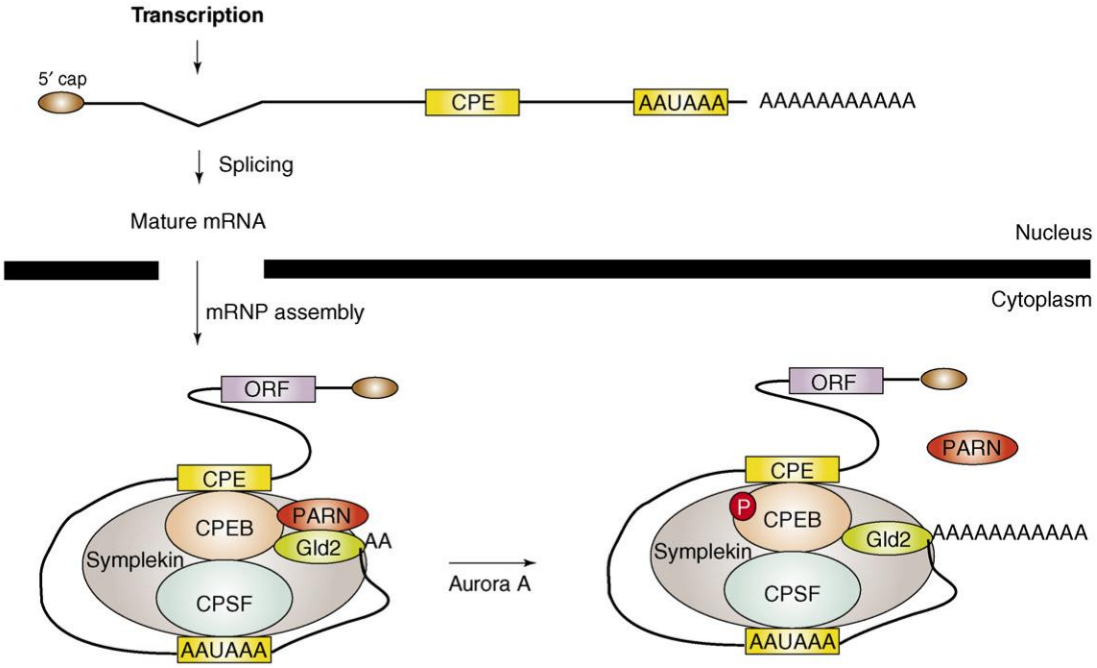

Fig. 1-5: General scheme of translational regulation by CPEBs. Following splicing and RNA export, a **r**ibo**n**ucleo**p**rotein (RNP) complex is nucleated by CPEB. Two proteins involved, PARN (deadenylase) and Gld2 (poly(A) polymerase) are competing with each other, with PARN overriding Gld2 activity, leading to poly(A) tail shortening. After CPEB phosphorylation by Aurora A kinase, a conformational change expulses PARN from the complex and allows polyadenylation of the mRNA by Gld2, ultimately resulting in increase in protein expression. See also description in the text (after Richter, 2007).

Symplekin is binding to CPSF and is a scaffold protein, serving as a nucleation factor for other members of the CPEB complex (Barnard *et al.*, 2004). PARN is a deadenylating enzyme, overriding Gld2 polymerase activity (Copeland and Wormington, 2001). After CPEB phosphorylation by Aurora A kinase, a conformational change leads to expulsion of PARN from the complex, allowing Gld2-mediated polyadenylation, ultimately resulting in an increase of protein expression. Several other factors are directly or indirectly involved in CPE-mediated polyadenylation in *Xenopus* (reviewed by Radford *et al.*, 2008). The most extensively studied function of CPEBs in neurons is sequestration of dendritic mRNAs, causing translational repression. Neuronal stimulation leads to activation of CPEBs, thereby leading to initiation of translation of plasticity-related proteins at the postsynaptic site (Fig. 1-6).

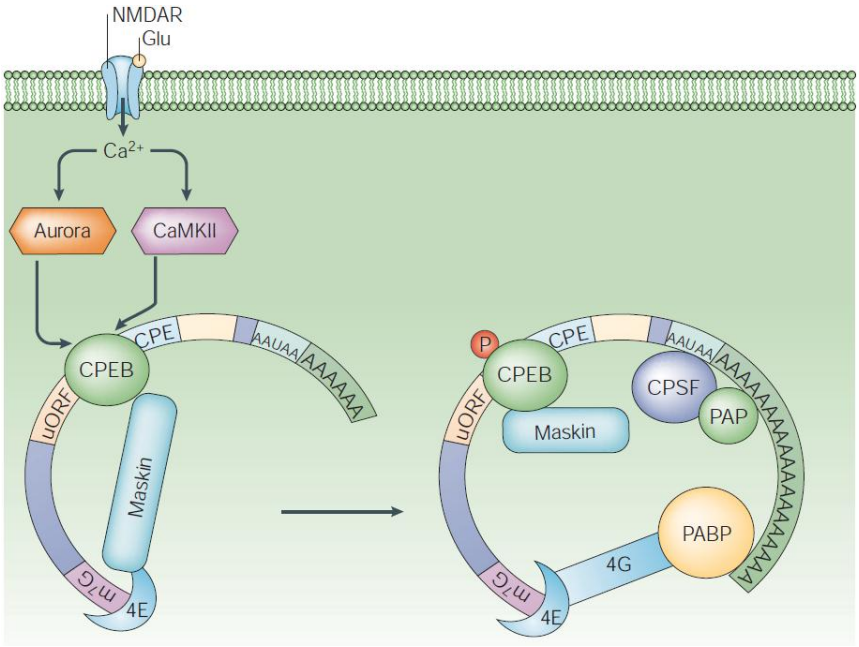

Fig. 1-6: Hypothetical scheme of CPEB function in neurons. Following N-methyl-D-aspartate (NMDA) receptor activation, kinases – Aurora and/or CaMKII (Atkins *et al.*, 2005) – are activated and phosphorylate CPEB1. Phosphorylation stabilizes the **C**leavage and **P**olyadenylation **S**pecificity **F**actor (CPSF) on the AAUAAA hexanucleotide, which attracts **p**oly(**A**) **p**olymerase (PAP) to catalyze polyadenylation. Maskin dissociates from eIF4E (cap binding protein). eIF4G then binds eIF4E and initiates translation. Adapted from Klann & Dever (2004).

One of the most intriguing examples of the neuronal function of CPEBs is their role in modulation of late-phase LTP, a phenomenon regarded as the cellular correlate of long term memory. As mentioned before, CPEBs primary function in neurons is the modulation of activity-dependent local protein synthesis in dendritic spines and, thereby, control of synaptic efficacy. One of the key players in synaptic plasticity is the CaMKIIα. The rat CaMKIIα mRNA contains 2 CPE elements and is bound by CPEB-1 (Wu *et al.*, 1998). In rat visual cortex, CaMKIIα is polyadenylated and upregulated following visual stimulation. Taken together, CPEB-1 may be involved in the plasticity of the visual cortex (Wu *et al.*, 1998). CPEB-1 is also phosphorylated upon **N**-**m**ethyl-**D**-**a**spartate **r**eceptor (NMDA receptor, NMDA-R) activation, via Aurora and CaMKII kinase (Huang *et al.*, 2002; Atkins *et al.*, 2005). NMDA-R is a major receptor of the neurotransmitter glutamate, involved in different forms of synaptic plasticity in most brain regions. Existence of a direct signalling pathway affirms the function of CPEB as synaptic modulator (Huang *et al.*, 2002).

CPEB-1 in neurons was shown to sequester **m**icrotubule **a**ssociated **p**rotein **2** (MAP2) mRNA while it was transported to dendrites, via direct or indirect interaction with molecular motors of the kinesin and dynein families (Huang *et al.*, 2003). Such sequestration would ensure temporal (NMDA-R activation) and spatial (dendritic spines) control of the translation of CPEB targets.

CPEB-1 was shown to bind **a**myloid-**p**recursor-**l**ike **p**rotein **1** (APLP1), as well as related proteins, including **a**myloid **p**recursor **p**rotein (APP) (Cao *et al.*, 2005). APLP1 is a paralog of APP, directly associated with the Alzheimer's disease pathology. Although it does not link CPEB directly to the pathology of Alzheimer's, APLP1 may serve as a membrane anchor for the complex of CPEB and CPEB-interacting proteins. Membrane proximity could ensure efficient phosphorylation upon synaptic stimulation.

Tissue **p**lasminogen **a**ctivator (tPA) – a serine protease produced in brain by neurons and microglia – is a key player in synaptic plasticity (Samson and Medcalf, 2006). tPA is also implicated in neurodegeneration following seizures in mouse brain (Tsirka *et al.*, 1995). In neurons, the production of tPA was demonstrated to be translationally regulated by CPEB-1 protein (Shin *et al.*, 2004).

In neuronal cultures, CPEB-3 represses the translation of the GluR2 subunit of the α-**a**mino-3-hydroxy-5-**m**ethyl-4-isoxazole**p**ropionic **a**cid (AMPA) receptor (AMPA-R) (Huang *et al.*, 2006) – a protein critical for many forms of synaptic plasticity (Jia *et al.*, 1996; Bassani *et al.*, 2009; Gainey *et al.*, 2009). Several transgenic mice were generated to address CPEB function *in vivo*. In the CPEB-1 **k**nock**o**ut (KO) mice, restricted deficits in **l**ong **t**erm **p**otentiation (LTP) were observed (Alarcon *et al.*, 2004). On the behavioral level, CPEB-1 KO mice show reduced hippocampal memory extinction (Berger-Sweeney *et al.*, 2006). Overexpression of an N-terminally truncated mutant form of CPEB-1 (lacking regulatory phosphorylation sites), termed dominant-negative CPEB1-4 (DN-CPEB1-4), in principal neurons led to deficits in stimulation induced protein synthesis and L-LTP, LTP induced by repeated trains of TBS (theta-burst stimulation), which correlated with impaired spatial reference memory tested in the Morris Water Maze task (Theis *et al.*, in revision). The latter finding is the first demonstration of target mRNA specificity overlap between CPEBs -2 to -4 and CPEB-1. Moreover, CPEB-3 translation might be regulated by CPEBs: CPEB-3 protein levels are strongly upregulated upon intraperitoneal kainate injection (Theis *et al.*, 2003b). Such upregulation is not observed in DN-CPEB1-4 mice (Theis *et al.*, in revision). In another *in vivo* model, mice overexpressing a kinase dead CPEB-1 mutant protein (mutations T171A and S177A) in Purkinje cells showed impaired cerebellar LTD and motor deficits (McEvoy *et al.*, 2007).

Other interesting insights into CPEB function in memory come from invertebrate research. Orb2, a *Drosophila melanogaster* homolog of CPEB-1 protein, is critical for long-term conditioning of male courtship behaviour (Keleman *et al.*, 2007). Aplysia CPEB (ApCPEB), a homolog of mouse CPEB-3 in *Aplysia californica*, is required in **l**ong **t**erm **f**acilitation (LTF) – the *Aplysia* correlate of long-term memory (Si *et al.*, 2003; Miniaci *et al.*, 2008; Si *et al.*, 2010).

Last but not least, CPEB-3 was found to play a role in memory formation in humans. In the intronic sequence of CPEB3 a self-cleaving ribozyme has been identified (Salehi-Ashtiani *et al.*, 2006). The polymorphic single nucleotide variation in sequence of this

ribozyme, influencing its enzymatic, self-cleaving activity, was related to the performance of human subjects in an episodic memory task (Vogler *et al.*, 2009).

1.7 CPEBs in glial function

CPEB proteins in brain are not restricted to neurons – they are expressed by all major cell populations, including astrocytes, NG2 cells, and microglia. Given increasing importance of glial cells and neuron-glia communication, it is conceivable that CPEBs may play an important role in glial contribution to CNS signalling. Astrocytic CPEB-1 is involved in cell motility and migration, via translational regulation of the actin-binding protein β-catenin (Jones *et al.*, 2008). β-catenin is a multifunctional protein, involved in cytoskeletal organization and cell signalling. In addition, neuronal targets of CPEBs may be (if present) likewise translationally regulated in glial cells. The AMPA-R subunit GluR2 might be an example, as it is expressed in NG2 glial cells. In the healthy brain, two subpopulations of cells with astroglial properties can be distinguished (Matthias *et al.*, 2003). One subpopulation – GluT cells or bona fide astrocytes – display passive electrical properties and express glutamate transporter-1 (GLT-1) protein. The other – GluR cells – express functional GluR2 subunit-containing AMPA-Rs (Matthias *et al.*, 2003) as well as GABA receptors (Jabs *et al.*, 2005). The population of GluR cells is, at least in the hippocampus, to large extent overlapping with the so-called NG2 glial cells (Karram *et al.*, 2008). In human subjects with Ammon's Horn Sclerosis (pathological changes in the hippocampus often associated with temporal lobe epilepsy (TLE)) the GluT cells disappear (Hinterkeuser *et al.*, 2000). Interestingly, both GluR and GluT cells possessed GLT-1 mRNA, but only GluT cells expressed functional transporters. And both GluR2 and GLT-1 mRNAs have CPEs in their 3'UTRs. It is therefore possible, that GLT-1 expression and, thereby, the cellular phenotype of glial populations is translationally regulated by CPEBs. Likewise, pathological alterations in epilepsy might occur, at least to a certain extent, on the translational level. Considering the reciprocal glutamatergic interaction of neurons and glial cells (Hansson and Ronnback, 2003; Lin and Bergles, 2004), CPEBs in astrocytes might thereby modulate both, normal and epileptiform neuronal activity. Finally, in neurons, production of tPA was demonstrated to be translationally regulated by CPEB-1 protein (Shin *et al.*, 2004). However, not the neuronal but the microglial tPA is critically involved in neurodegeneration following seizures in mouse brain (Siao *et al.*, 2003).

1.8 Transgenic approaches to study gene function

To study protein function in brain *in vivo*, several gene manipulation strategies have been developed during the last decades. The idea dates back to the early work conducted by the three Nobel Prize laureates, Mario R. Capecchi, Sir Martin J. Evans, and Oliver Smithies, ultimately leading to establishment of targeted gene manipulation methods in mice (Evans and Kaufman, 1981; Thomas *et al.*, 1986; Doetschman *et al.*, 1988; Capecchi, 2001).

1.8.1 Spatiotemporal control of gene deletion

Currently, the most common system for the *in vivo* genetic manipulation is an unrestricted deletion (knock-out) or modification of a specific gene. This is achieved by homologous recombination following transfection of mouse embryonic stem (ES) cells, selection of homologously recombined ES cell clones, and injection of ES cells into mouse embryos of the blastocyst stage (Capecchi, 2001). This strategy, however, is not free of limitations, as it affects every process (and at all developmental stages) in which the studied gene (protein) plays a role. Consequently, it is rather difficult to ascribe observed phenotypical abnormalities to a specific molecular pathway due to possible pleiotropic effects. The conditional gene deletion method is to a large extent circumventing this problem. It uses a Cre-*loxP* system, allowing deletion of genes in a specific cell type or region of the brain (Fig. 1-7) (Tsien *et al.*, 1996a). This system involves generation of two mouse lines. In one line, the Cre recombinase from bacteriophage P1 is expressed under the control of a cell-type specific promoter, e.g. the CaMKIIα promoter. In the second line, the target DNA region (usually a gene or a fragment thereof) is floxed (i.e. flanked by *loxP* sites), using homologous recombination-based gene targeting. Breeding the two mice together, leads to generation of the mouse with cell-type (or regionally) restricted deletion of the floxed allele. Using the Cre-*loxP* system, Tsien *et al.* generated a mouse with the NR1 subunit of receptor deleted almost exclusively in the CA1 region of the hippocampus (Tsien *et al.*, 1996a; Tsien *et al.*, 1996b). Severe learning impairments observed in this mouse confirmed and expanded the earlier-established hypothesis of the NMDA-Rs having crucial role in LTP and memory (Bliss and Collingridge, 1993).

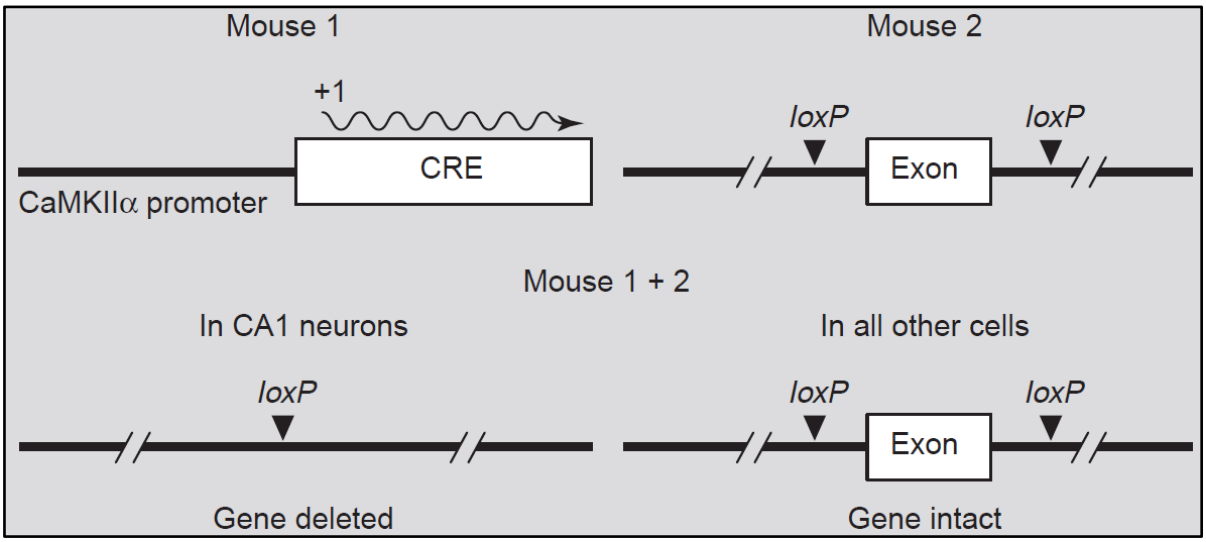

Fig. 1-7: Conditional gene deletion in neurons. Two transgenic mice are required. Mouse 1 expresses Cre recombinase under a forebrain neurons-specific CaMKIIα (or other cell-type specific) promoter. Mouse 2 expresses a floxed (i.e. flanked by *loxP* sites) target gene (to be deleted). Breeding mouse 1 and mouse 2 together leads to recombination exclusively in the cells where Cre is expressed (in this case forebrain neurons) (after Mayford and Kandel, 1999).

The Cre/Lox-P system (Sauer and Henderson, 1988) is nowadays the most common method for generation of cell-type-restricted knock-outs of genes in mice. Many Cre transgenes have been developed to spatiotemporally restrict Cre expression, including brain-specific (Tsien *et al.*, 1996a; Zhuo *et al.*, 2001; Casper *et al.*, 2007) and inducible systems (Hirrlinger *et al.*, 2006; Mori *et al.*, 2006; Slezak *et al.*, 2007; Gosejacob *et al.*, 2011). Despite obvious advantages, the Cre-*loxP* system still does not allow to unambiguously correlate the observed phenotype with the particular molecular mechanism. Although cell-type restricted, the deletion is achieved in a manner controlled only by the spatiotemporal activity pattern of the used promoter. Moreover, ectopic promoter activity has been reported for many Cre transgenes described to date (Eckardt *et al.*, 2004; Schmidt-Supprian and Rajewsky, 2007; Martens *et al.*, 2010; Wicksteed *et al.*, 2010). Several of the abovementioned pitfalls can be circumvented by using inducible Cre transgenes and/or Cre activated by the co-incidental activity of two promoters (Kellendonk *et al.*, 1999; Hirrlinger *et al.*, 2006; Hirrlinger *et al.*, 2009).

1.8.2 The Cre/LoxP system benefits from a direct linkage between gene deletion and reporter activation

As already mentioned, currently used Cre transgenes are not free of limitations (Schmidt-Supprian and Rajewsky, 2007). One way to validate Cre-recombination fidelity is by employing reporter genes, which are activated by Cre recombinase. The reporter gene may be ubiquitously expressed and activated by Cre-mediated excision of the floxed STOP codon located upstream of the reporter coding region (Cre-excision reporter). Alternatively, a gene deletion may be directly linked to reporter activation, resulting in a functional replacement of the deleted gene with a reporter gene (gene inactivation reporter) (Requardt, Kaczmarczyk *et al.*, 2009). Such a direct link between gene deletion and reporter activation has been previously described (Moon *et al.*, 2000). In astrocytes, such approach was used for reporting deletion status of connexin Cx43 (Theis *et al.*, 2003a). A direct link between gene deletion and reporter activation allows for a quick and easy estimation of the recombination status, specificity, and for a clear identification of gene deletion in the target cells while the adjacent cells still express the transgene at high levels (Requardt, Kaczmarczyk *et al.*, 2009). It also enables an ad-hoc, rigid verification of gene inactivation, to large extent eliminating the necessity of performing the post-experimental validation of recombination fidelity. Moreover, unlike the Cre-excision reporters, the gene inactivation reporters can be successfully used in multiple transgenic mice.

1.8.3 Spatiotemporal control of gene overexpression

Spatiotemporally-restricted overexpression of genes is alternative strategy to study their function *in vivo*. This can be achieved by using the bi-transgenic tTA/tetO system (Mayford and Kandel, 1999), employing tetracycline-responsive promoter elements to

drive the transgene expression (Gossen and Bujard, 1992). The system requires two transgenic mice lines: (1) expressing the tetracycline-responsive transcription factor (tTA) under control of cell-type specific promoter and (2) expressing the transgene under the tetracycline responsive promoter. Breeding the two lines together leads to generation of a double transgenic mouse line, expressing the transgene exclusively in the cells where tTA is expressed (e.g. forebrain neurons in case of CaMKIIα-driven tTA) (Fig. 1-8). Administration of doxycycline (tetracycline analogue) modulates the tTA activity, allowing for temporal control of transgene expression. Depending on the nature of tTA, the system (termed the "tet" system) has two varieties: (1) the tet-off system, where administration of doxycycline (dox) renders the tTA inactive, and (2) the tet-on system, where dox is required for tTA activation. The tet-off system has become more commonly used, and has been successfully applied to study the function of the CPEB1-4 protein family in forebrain neurons (see also section 1.6).

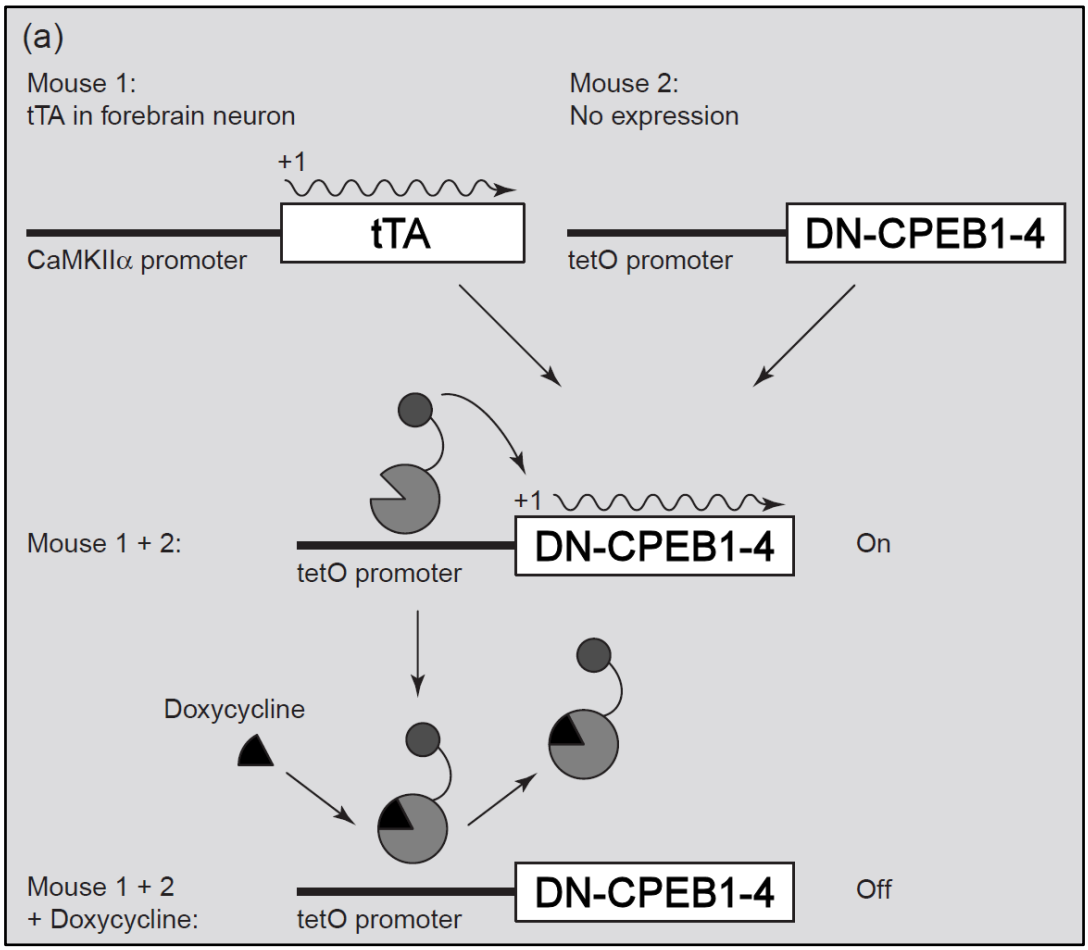

Fig. 1-8: Conditional gene overexpression in neurons. Two transgenic mice are required. In mouse 1, a cell-type-specific (e.g. forebrain-neurons specific CaMKIIα) promoter drives expression of the tTA. Mouse 2 expresses the transgene (in this example a dominant-negative CPEB1-4) under the minimal eukaryotic promoter and the tet operator (tetO). Breeding mouse 1 and mouse 2 together leads to a double transgenic mice which exhibit transgene expression exclusively in the cells where tTA is expressed (e.g. forebrain neurons in case of CaMKIIα-driven tTA). Administration of doxycycline renders tTA inactive, allowing for temporal control of transgene expression (after Mayford and Kandel, 1999, modified).

2 Experimental Goals

Goal of the thesis was to investigate the expression of CPEBs and their splice isoform in selected cell types in mouse brain, with special emphasis on microglial cells. I aimed at identification of novel CPEB targets present in astrocytes and microglia. I also embarked on establishing and optimizing appropriate methodologies (i.e. mRNA pull down) for assessment of mRNA binding specificity of CPEBs, in order to test the potential specificity overlap between CPEB family members. Focusing on the CPEB-3 protein, I have embarked on testing its function in transgenic mice overexpressing CPEB3a-EGFP fusion protein in principal neurons. Based on the hypothesis formulated by Theis *et al.* (2003b), I wanted to investigate the phosphorylation of CPEB-3 *in vitro* and *in vivo*, identify the protein kinases involved, and the function of the process. To this end, I also aimed at generating and characterizing a custom-made phosphospecific polyclonal antibody against CPEB-3. Using **e**mbryonic **s**tem-Cell-**d**erived **m**icroglia (ESdM), I intended to test the putative translational regulation of microglial tPA by CPEBs. To do so, I aimed at establishing a DN-CPEB1-4 overexpression, using retroviral gene targeting followed by **f**luorescence-**a**ctivated **c**ell **s**orting (FACS). Finally, I embarked on developing a quality control method for hGFAP-Cre mediated gene deletion.

3 Materials and Methods

3.1 Molecular biology

All the reagents for molecular biology work were of analytical grade, and were purchased from Sigma, Carl-Roth, Roche or Merck. Small volume (up to 1 ml) solutions and reaction mixtures were made with sterile water. Double distilled ($_{dd}H_2O$) or deionized water was used for larger volumes.

3.1.1 Solutions

DNA loading buffer (6x)

Component	Concentration
Glycerol	30% (v/v)
Xylene cyanol	0.1 % (w/v)
Bromophenol blue	0.1 % (w/v)

Coomassie staining solution (1x)

Component	Concentration
EtOH	40% (v/v)
Acetic Acid	10% (v/v)
Coomassie Brilliant Blue	0.1% (w/v)

TBE buffer (10x)

Component	Concentration
Tris-Cl	1 M
Boric acid	0.83 M
EDTA	10 mM

TBS-T buffer (1x)

Component	Concentration
Tris-Cl, pH 7.4	25 mM
NaCl	150 mM
Tween 20	0.05 % (v/v)

RIPA buffer (modified) (1x)

Component	Concentration
Tris-Cl, pH 7.4	50 mM
NaCl	150 mM
Nonidet P40	0.5 % (v/v)
Na-DOC	0.5 % (w/v)
Triton X-100	1 % (v/v)
SDS	0.5 % (w/v)
Complete Mini Protease Inhibitor Cocktail*	1 tab./50 ml

(*) Added directly before use

PIL (Phosphatase Inhibitor Lysis) buffer (1x)

Component	Concentration
Tris-Cl, pH 7.5	50 mM
NaCl	50 mM
NaF	50 mM
EDTA	2 mM
Triton X-100	1 % (v/v)
NP-40	1 % (v/v)
$NaVO_3$	2 mM
Sucrose	270 mM
Complete Mini Protease Inhibitor Cocktail*	1 tab./10 ml
PhosStop Phosphatase Inhibitor Cocktail *	1 tab./10 ml

(*) Added directly before use

Protein sample buffer (SDS-PAGE) (1x)

Component	Concentration
Tris-Cl, pH 6.8	50 mM
DTT	100 mM
SDS	2 % (w/v)
Glycerol	10 % (v/v)
Bromophenol blue	0.01 % (w/v)

Firefly luciferase substrate solution (1x)

Component	Concentration
Tricine, pH 7.8	30 Mm
$MgSO_4$	3.75 mM
ATP	0.75 mM
DTT	1.25 mM
Coenzyme-A	67 µM
D-luciferin, Na-salt	0.5 mM

(*) After addition of D-luciferin, 1x solution was stored at -80°C and protected from light

3.1.2 Solutions for RNA work

All solutions for RNA work were prepared from RNA work-designated reagents and sterilized by filtration (pore size 0.22µM).

RNA co-IP lysis buffer (1x)

Component	Concentration
HEPES	10 mM
NaCl	**200 mM**
EDTA	30 mM
Triton X-100	0.5% (v/v)
Complete Mini Protease Inhibitor Cocktail*	1 tab./10ml
RNAsin*	200 U/ml
tRNA*	5 µg/ml

(*) Added directly before use

RNA co-IP wash buffer (1x)

Component	Concentration
HEPES	10 mM
NaCl	**500 mM**
EDTA	30 mM
Triton X-100	0.5% (v/v)
Complete Mini Protease Inhibitor Cocktail*	1 tab./50ml
RNAsin*	100 U/ml

(*) Added directly before use

3.2 Cell culture reagents

Unless stated otherwise, all the solutions used for cell culture work were purchased from Invitrogen/Gibco, Germany.

3.2.1 Media formulations

Fetal Calf Serum (FSC) medium component was heat-inactivated at 56°C for 30min.

DMEM / FCS cell culture medium (500ml)

Component	Amount/Concentration
DMEM with 25mM Glucose	500 ml
FCS (heat-inactivated)	10%
Penicillin/Streptomycin (100x)*	1%

(*) optional

MEF cell culture medium (500ml)

Component	Amount/Concentration
DMEM with 25mM Glucose	500 ml
FCS (heat-inactivated)	**10%**
L-Glutamine	6 mM
MEM Non-Essential Amino Acids	0.1 mM
MEM Sodium Pyruvate	1 mM
Penicillin/Streptomycin (100x)*	1%

(*) optional

Trans-MEF cell culture medium (500ml)

Component	Amount/Concentration
DMEM with 25mM Glucose	500 ml
FCS (heat-inactivated)	**2%**
L-Glutamine	6 mM
MEM Non-Essential Amino Acids	0.1mM
MEM Sodium Pyruvate	1 mM
Chloroquine (Sigma, Germany)	50 μM

N2 cell culture medium (500ml)

Component	Amount/Concentration
DMEM / F12	500 ml
N2 supplement (100x)	1%
L-Glutamine	0.48 mM
D-Glucose (Sigma, Germany)	15.3 μg/ml
Penicillin/Streptomycin (100x)*	1%

(*) optional

3.2.2 Cell culture reagents

Reagent	Provider
PBS	Invitrogen
PBS (for FACS)	Lonza
Opti-MEM	Invitrogen
Trypsin-EDTA (0.05%)	Invitrogen
Lipofectamine 2000	Invitrogen
Polybrene	Sigma
Chloroquine	Sigma
Forskolin	New England Biolabs

3.2.3 Cell culture consumables

All cell culture consumables/plasticware were purchased from Sarstedt, Grainer Bio-One, and Carl Roth. ESdM cells were cultured in standard Tissue Culture (TC) dishes/flasks purchased from Greiner Bio-One.

3.2.4 Antibodies

Antigen	Coupling	Immunogen	Type	Host specie	Application	Source	Catalogue number/ reference
FLAG	-	synthetic peptide	M	Ms	IP, WB	Sigma	F3165
CPEB-1	-	synthetic peptide	P	Rb	IP, WB, ICC	Eurogentec	custom-made
CPEB-2	-	synthetic peptide	P	Rb	ICC	Eurogentec	custom-made
CPEB-3	-	synthetic peptide	P	Rb	IP, WB	Eurogentec	custom-made
CPEB-3	-	synthetic peptide	P	Rb	WB, ICC	Abcam	ab10883
CPEB-4	-	synthetic peptide	P	Rb	ICC	Eurogentec	custom-made
GAPDH	-	full length GAPDH protein	M	Ms	WB	Abcam	ab9484
Mouse IgG	HRP	mouse IgG (heavy + light chain)	M	Gt	WB	Pierce	31430
Rabbit IgG	HRP	rabbit IgG (heavy + light chain)	M	Gt	WB	Pierce	31460
Cx43	-	synthetic peptide (C-terminal)	P	Rb	WB	A gift from Radek Dobrowolski	(Theis *et al.*, 2001)
Phospho-CPEB3-S419/S420	-	syntetic peptide	P	Rb	WB	Eurogentec	custom-made
GluR2	-	recominant GluR2 fusion protein	M	Ms	WB	Millipore	MAB397
α-tubulin	-	microtubules from chicken embryo brain	M	Ms	WB	Sigma	T9026
β-actin	-	synthetic peptide (C-terminal)	M	Ms	WB	Sigma	A3853
Cre recombinase	-	bacteriophage P1 Cre protein	P	Rb	WB	Novagen	69050-3
CD11b	APC	glycosylated form of CD11b antigen	M	Rt	FACS	Invitrogen	CD11b05

Tab. 3-1: List of the antibodies used. IgG – immunoglobulin; Coupling: HRP – **H**orser**a**dish **p**eroxidase Type: M – monoclonal, P – polyclonal; Host specie: MS – Mouse, Rb – Rabbit, Gt – Goat, Rt – Rat; Application: IP – immunoprecipitation, WB – Western blot (immunoblot), ICC – immunocytochemistry, FACS – Fluorescence Activated Cell Sorting.

3.3 PCR and RT-PCR oligonucleotides

The majority of PCR oligonucleotides was designed using the Primer3 online tool (Rozen and Skaletsky, 2000). TaqMan primers and probes were designed with Primer Express 3.0 (Applied Biosystems).

3.3.1 3'RACE oligonucleotides

target gene	RACE primer sequence
CaMKIIα	5'-AACTGTCCAGAGCCCACCCTCATCTG-3'
Cx43	5'-AACAGGCTTGAACATCAAGCTGCCAATC-3'
tPA	5'-CAAAGAAAGCCCAGCTCCTTCAATCCAG-3'

Tab. 3-2: Gene-specific oligonucleotides used for 3'RACE amplification.

3.3.2 Primers for cloning and site directed mutagenesis of 3'UTRs

#	Oligonucleotide sequence	Target gene	Application
1	5'-GCACTCTAGACTCTCTCTCTTTCTTTTTTAATCTGTG-3'	CaMKIIα	Cloning of 3'UTR (forward)
2	5'-CGACGTCGACAAATTTGTAGCTATTTATTCCACTG-3'	CaMKIIα	Cloning of 3'UTR (reverse)
3	5'-GCACTCTAGACTCTCTCTCTTTC**GG**T**ACC**AATCTGTG-3'	CaMKIIα	Cloning of 3'UTR (forward) / Mutating proximal CPE
4	5'-GAAGAGATGTCTGGT**G**TA**C**TCTTGGCGTTTTCAG-3'	CaMKIIα	Mutating distal CPE by SOE PCR (forward)
5	5'-CTGAAAACGCCAAGA**G**TA**C**ACCAGACATCTCTTC-3'	CaMKIIα	Mutating distal CPE by SOE PCR (forward)
7	5'-GCACTCTAGACACTCCTCAACTCTTGGGACATA-3'	tPA	Cloning of 3'UTR (forward)
8	5'-CGACGTCGACAAAGTGTGAAAAATACCTCTGAATTTA-3'	tPA	Cloning of 3'UTR (reverse)
9	5'-GGAGAACTGTATGA**GG**T**C**A**CC**AATTGATGAATAAC-3'	tPA	Mutating proximal CPE by SOE PCR (forward)
10	5'-GTTATTCATCAATT**GG**T**G**A**CC**TCATACAGTTCTCC-3'	tPA	Mutating proximal CPE by SOE PCR (reverse)
11	5'-CACTAGTATATTTATA**GG**T**C**A**CC**CTATTTTAGTTTTTAC-3'	tPA	Mutating distal CPE by SOE PCR (forward)
12	5'-GTAAAAACTAAAATAG**GG**T**G**A**CC**TATAAATATACTAGTG-3'	tPA	Mutating distal CPE by SOE PCR (reverse)
13	5'-GCACTCTAGAATTGAAATGTCGAGTTATCATGTTT-3'	Cx43	Cloning of 3'UTR (forward)
14	5'-CGACGTCGACATTATACTAAATTAAAATTTTATTGAATAAAGAAC-3'	Cx43	Cloning of 3'UTR (reverse)
15	5'-GTCGACATTATACTA**GG**TT**GTCC**TTTTATTGAATAAAGAAC-3'	Cx43	Cloning of 3'UTR (forward) / Mutating distal CPE
16	5'- AATCTAGAGAAACCCTGGACCACCCAC-3'	GAPDH	Cloning of 3'UTR (forward)
17	5'- AAGTCGACGGGTGCAGCGAACTTTATTGAT-3'	GAPDH	Cloning of 3'UTR (reverse)

Tab. 3-3: PCR oligonucleotides used to generate wild-type and mutated 3'UTR luciferase reporter constructs. Introduced restriction sites (SalI: TCTAGA or XbaI: GTCGAC) were underlined. Nucleotides mutated with respect to wild-type genes were shown **in bold**.

3.3.3 Taq-Man sqRT-PCR oligonucleotides

Unless specified otherwise, Taq-Man oligonucleotides were designed using Primer Expert 3.0 software (Applied Biosystems) and synthetized by Eurogentec. In case of mouse β-actin, a commercial internal control assay with 6-carboxyfluorescein amidite/Minor Groove Binder (6-FAM/MGB) probe (Applied Biosystems) was used.

#		Oligonucleotide sequence	Target gene	Species
1	Forward	5'-GGCTCCCGCTGAATTGG-3'	Luciferase	Firefly
	Reverse	5'-GCGACACCTGCGTCGAA-3'		
	Probe	5'-ATCCATCTTGCTCCAACACCCCAACA-3'		
2	Forward	5'-ACACCTCCCAAGTCCTTTATGAAT-3'	β-catenin	Mouse
	Reverse	5'-CCCGTCAATATCAGCTACTTGCT-3'		
	Probe	5'-AGGCTTTTCCCAGTCCTTCACGCAA-3'		
3	Forward	5'-GCTATGAAGGATGGGCAACT-3'	Porphobilinogen deaminase (PBGD)	Human
	Reverse	5'-GTGATGCCTACCAACTGTGG-3'		
	Probe	5'-TGCCCAGCATGAAGATGGCC-3'		
4	Forward	5'-CGACAGTCAGCCGCATCTT-3'	Glyceraldehyde-3-phosphate dehydrogenase (GAPDH)	Human
	Reverse	5'-CCGTTGACTCCGACCTTCAC-3'		
	Probe	5'-CGTCGCCAGCCGAGCCACA-3'		
5	Forward	5'-GAGACGGCCGCATCTTCTTGT-3'	Glyceraldehyde-3-phosphate dehydrogenase (GAPDH)	Mouse
	Reverse	5'-CACACCGACCTTCACCATTTT-3'		
	Probe	5'-CAGTGCCAGCCTCGTCCCGTAGA-3'		
6	Forward	5'-ATTCAGCATAGAGAGAGAGGCTAGA-3'	CPEB1	Mouse
	Reverse	5'-CCAGGTACACGTAGCTTCATTCAC-3'		
	Probe	5'-TCCACCGGCAGGCTGCAGC-3'		
7	Forward	5'-TGCAGCAGAGGAACTCGTACA-3'	CPEB2	Mouse
	Reverse	5'-CCAACCGCTGTTCTGATGGT-3'		
	Probe	5'-CCACCACCAGCCTCTTCTGAAACAGTCT-3'		
8	Forward	5'-GCGCTCAGGTGGGACAGA-3'	CPEB3	Mouse
	Reverse	5'-GGGTTTTGCTTTTGTCCATCA-3'		
	Probe	5'-CAGCTGCGCAAACCATGCAGGA-3'		
9	Forward	5'-TTGAACAGGGCTGACAACATTT-3'	CPEB4	Mouse
	Reverse	5'-CCAGTGAGTGCATGTCAAACG-3'		
	Probe	5'-CCTTTTCCGGAACGCCCCAGG-3'		

Tab. 3-4: Taq-Man sqRT-PCR oligonucleotides. Except for the Porphobilinogen deaminase (PBGD), probes were labeled with carboxytetramethylrhodamine (TAMRA) (3'-end) and 6-FAM (5'-end). PBGD probe was labeled with TAMRA (3'-end) and Black Hole Quencher-1 (BHQ-1) (5'-end).

3.3.4 SYBR Green sqRT-PCR oligonucleotides

#		Oligonucleotide sequence	Target gene	Species
1	Forward	5'-TGTTGTTTTGGAGCACGGAA-3'	Luciferase	Firefly
	Reverse	5'-ACTCCTCCGCGCAACTTTT-3'		
2	Forward	5'-TGTGCCCATCTACGAGGGGTATGC-3'	β-actin	Mouse
	Reverse	5'-GGTACATGGTGGTGCCGCCAGACA -3'		

Tab. 3-5: SYBR Green sqRT-PCR oligonucleotides.

3.3.5 Oligonucleotides for generating lentiviral vectors

#	Oligonucleotide sequence	Target sequence	Application
1	5'- GACTGCAGCCGGATCCACCATGGACTACAAAGACCATGAC-3'	FLAG	Cloning of mCPEB-1/-3/-DN (forward)
2	5'- CGGTACCCGGGGATCCCGGTTCTTCTGGTTCCTCATTAG-3'	CPEB1 ORF	Cloning of mCPEB-1/-DN (reverse)
3	5'- CGGTACCCGGGGATCCCGGCTCCAGCGGAACGGGAC-3'	CPEB3 ORF	Cloning of mCPEB-3 (reverse)
4	5'- GATCCAGTTTGGTTAATTAATACCGGGTAGGGGAGGCGCTTTTC-3'	PGK promoter	Cloning of PGK promoter (forward)
5	5'- CGGTACCCGGGGATCCGGCTGCAGTCGAAAGGCCCGGA-3'	PGK promoter	Cloning of PGK promoter (reverse)

Tab. 3-6: PCR oligonucleotides used to generate lentiviral expression constructs. Restriction sites (PacI: TTAATTAA or BamHI: GGATCC) were underlined. In-Fusion overhangs, homologous to the target vector sequence, were highlighted.

3.3.6 Primers for sequencing of 3'UTR luciferase constructs

#	Oligonucleotide sequence	Target region
1	3'-AACTCGACGCAAGAAAAATCAGAGAG-5'	Upstream of XbaI restriction site (forward read)
2	3'-CACCTGTCCTACGAGTTGCATGATAAAG-5'	Downstream of SalI restriction site (reverse read)

Tab. 3-7: Primers used for sequencing of 3'UTR luciferase constructs.

3.3.7 Primers for sequencing of lentiviral vectors

#	Oligonucleotide sequence	Target region / purpose
1	5'-CGGGTTTATTACAGGGACAGC-3'	Binds upstream of PacI restriction site / promoter sequencing (forward)
2	5'-CACCTGTCCTACGAGTTGCATGATAAAG-3'	Binds in the PGK promoter / insert ORF sequencing (forward)
3	5'-CACCACCCCGGTGAACAG-3'	Binds in the GFP cds promoter / insert ORF sequencing (reverse)

Tab. 3-8: Primers used for sequencing of lentiviral constructs.

3.3.8 Primers for CPEB splice isoform analysis

		Oligonucleotide sequence
mCPEB-1	Forward	5'-GGATTGGTTAACACCTTCCGTGTTTTTGGC-3'
	Reverse	5'-AGGCCATCTGGGCTCAGCGGG-3'
mCPEB-2	Forward	5'-ATGTGTTCAGGACAGACAATAGTAACA-3'
	Reverse	5'-CAAGCTATCATCTATTGGAAATAGGGAAGA-3'
mCPEB-3	Forward	5'-GGATATGATAAGGACTGACCATGAGCCTCTGAAAG-3'
	Reverse	5'-CCATGGCTGTCATCCAAGAAGGCGTC-3'
mCPEB-4	Forward	5'-CAGACCACTATGAAGAGGTTGATCCCCACG-3'
	Reverse	5'-CCCAGGACGTTTGACATGCACTCACTG-3'

Tab. 3-9: Oligonucleotides used for CPEB splice isoform analysis, flanking alternatively spliced regions (Theis *et al.*, 2003b).

3.4 Mouse lines

All mice were bred and maintained under specific pathogen-free (SPF) conditions, by the House for Experimental Therapy, University of Bonn.

Genotype	Reference	Source
CX_3CR1kiGFP	(Jung *et al.*, 2000)	Kind gift from Prof. Harald Neumann, Institute of Reconstructive Neurobiology, University of Bonn
hGFAP-Cre	(Zhuo *et al.*, 2001)	Provided by Dr. Martin Theis, Institute of Cellular Neurosciences, University of Bonn
CaMKIIα-tTA	(Mayford *et al.*, 1996)	Provided by Dr. Martin Theis, Institute of Cellular Neurosciences, University of Bonn
tetO-CPEB3-EGFP	(unpublished)	Provided by Dr. Martin Theis, Institute of Cellular Neurosciences, University of Bonn
$Cx30^{-/-};Cx43^{fl/fl}$	(Wallraff *et al.*, 2006)	Provided by Dr. Martin Theis, Institute of Cellular Neurosciences, University of Bonn

Tab. 3-10: Transgenic mouse lines used.

3.5 Bacterial strains

Item	Genotype	Source
Top10 chemically competent *E.coli*	F^- *mcr*A Δ(*mrr-hsd*RMS-*mcr*BC) φ80*lac*ZΔM15 Δ*lac*X74 *rec*A1 *ara*D139 Δ(*ara-leu*) 7697 *gal*U *gal*K *rps*L (Str^R) *end*A1 *nup*G λ-	Invitrogen
Stbl3 chemically competent *E.coli*	F^- *mcr*B *mrr hsd*S20(r_B^-, m_B^-) *rec*A13 *sup*E44 *ara*-14 *gal*K2 *lac*Y1 *pro*A2 *rps*L20(Str^R) *xyl*-5 λ^- *leu mtl*-1	Invitrogen

Tab. 3-11: Bacteria strains used.

3.6 Kits and reagents

Item	Application	Provider
mMESSAGE mMACHINE T7 Ultra	*In vitro* transcription to yield translation-competent mRNA	Ambion
In-Fusion 2.0 Dry-Down PCR Cloning Kit	In-Fusion recombination-mediated cloning of PCR inserts	Clontech
Marathon-Ready Mouse Brain cDNA	3'RACE experiments	
Fast Link Ligation Kit	Ligating restriction fragments	Epicentre
Streptavidin-HRP	Chemiluminescent detection of biotin	GE Healthcare
AccuPrime *Taq* DNA Polymerase System	CPEB splice isoform analysis	Invitrogen
LIVE/DEAD Fixable Dead Cell Stain Kit	Dead cells discrimination in FACS	
PureLink HiPure Plasmid Midiprep Kit	DNA purification from bacterial cultures	
SuperScript III Reverse Transcriptase	Reverse transcription (RT-PCR and sqRT-PCR)	
TOPO XL PCR Cloning Kit	T/A cloning	

Item	Application	Provider
PKLight Assay Kit	Quantitation of *in vitro* phosphorylation	Lonza
T4 DNA Ligase	Ligation of restriction fragments	New England Biolabs
Quick Ligation Kit	Ligation of restriction fragments	
peqGOLD Gel Extraction Kit	Purification of DNA fragments from agarose gels	PeqLab
SuperSignal West Dura Substrate	Detection of HRP activity on immunoblots	Pierce
RNAsin	Prevention of RNA degradation	Promega
ADP-Glo Assay Kit	Quantitation of *in vitro* phosphorylation	
Wizard Plus SV Miniprep Kit	DNA purification from bacterial cultures	
Omniscripts Reverse Transcriptase	Reverse transcription (RT-PCR and sqRT-PCR)	Qiagen
PCR Clean-up Kit	DNA purification after enzymatic reactions	
Plasmid Maxi Kit	DNA purification from bacterial cultures	
RNeasy Mini-Kit	RNA purification	
RNase-Free DNase Set	Genomic DNA removal during RNA purification	
Expand High Fidelity PCR System	Amplification of restriction inserts, RACE	Roche
GC–Rich Polymerase Kit	CPEB3a OFR amplification	

Tab. 3-12: Commercial kits and reagents used.

3.7 Selected equipment

Item	Model	Provider
Bioanalyzer	2100	Agilent
FACS Cell Sorter	Customized FACS DiVa	Becton Dickinson
Flow Cytometer	FACS Canto II	Becton Dickinson
Microplate luminometer	Centro LB 960	Berdhold Technologies
Spectrophotometer (Nanodrop)	Pearl	Implen
Quantitative PCR System	7900HT	Applied Biosystems
Immunoblot documentation system	Gene Gnome HR	Syngene

Tab. 3-13: Laboratory equipment used.

3.8 Software

Item	Company / Reference
MS Excel 2010	Microsoft
SDS 5.0 sqRT-PCR software	Applied Biosystems
MultiAlign (web-tool)	(Corpet, 1988)
GeneSnap	Syngene
Lasergene Sequence Builder 7.0	Dynastar, Inc.
FlowJo 7.6	Tri Star, Inc.
Jalview 2.5.1	(Waterhouse *et al.*, 2009)
Graph Pad Prism 5.0	Graph Pad, Inc.
Primer3 (web-tool)	(Rozen and Skaletsky, 2000)
Bioedit 7.0.9	(Hall, 1999)

Tab. 3-14: Software used (including web-tools).

3.9 Molecular cloning

Unless specified otherwise, all basic molecular biology techniques were performed following product manufacturer's recommendations and/or according to the "Molecular Cloning" laboratory manual (Sambrook and Russell, 2001). All restriction enzymes were purchased from New England Biolabs. PCR reactions to amplify restriction inserts were done with the High Fidelity PCR system (Roche, Mannheim, Germany), unless stated otherwise. All the primer sequences can be found in section 3.3. The In-Fusion homologous recombination-mediated cloning technique (Clontech, Heidelberg, Germany) was also used as a cloning method for single-restriction enzyme cloning of long (>2kb) inserts. It was also used when an insert contained a target restriction site(s) of the cloning, and no suitable alternative sites on the vector existed. Vectors and cloning strategies were designed using Lasergene software (Dynastar, Inc.).

3.9.1 Rapid amplification of 3' cDNA ends (3'RACE)

To determine the 3'UTR termini of CPEB target mRNAs, the 3'RACE method was used. Gene specific primers used for 3'RACE experiments are listed in Tab. 3-2. Whole mouse brain "Marathon-Ready" cDNA (Clontech) served as a template. An anchor oligonucleotide (AP1) provided with the cDNA was used as a reverse primer. Reaction components and PCR temperature cycle conditions are listed in Tab. 3-15 and 3-16, respectively. 3'RACE PCR products were visualized on EtBr-stained agarose gels, purified, and inserted into the TA cloning vector XL-TOPO. Obtained clones were sequenced with vector-specific M13 forward and M13 reverse primers.

Reagent	Amount	Stock concentration
cDNA template	5µl	~0.1ng/µl
Polymerase Mix	0.5µl	3.5U/µl
dNTP mix	1µl	10mM
Gene-specific primer (GSP)	1µl	10µM
Anchor Primer (AP1)	1µl	10µM
Buffer with Mg^{2+}	10µl	5x
$_{dd}H_2O$	31.5µl	n/a
Total volume	**50µl**	

Tab. 3-15: 3'RACE of CPEB target cDNA – reaction mixture.

Temp.	Time	No. of cycles
94°C	1 min	
94°C 72°C	15 s 3 min	x 5
94°C 70°C	15 s 3 min	x 5
94°C 68°C	15 s 3 min	x 25
68°C	10 min	
4°C	hold	

Tab. 3-16: 3'RACE of CPEB target cDNA – temperature profile

3.9.2 Generation of luciferase reporter constructs

The pGL4.75[*hRluc*/CMV] Renilla luciferase-encoding plasmid (GenBank accession no. HC872744) was used as backbone for the generation of all CPE-containing reporter constructs, further used for RNA co-IP experiments and luciferase reporter assays.

3.9.2.1 Cloning of Firefly luciferase Open Reading Frame (ORF)

The firefly luciferase ORF was extracted from the pGL3-Control vector (GenBank accession no. U47296.2) using XbaI and HindIII restriction enzymes. The excised fragment was ligated to respective sites in pGL4.75[*hRluc*/CMV], replacing the *Renilla* luciferase ORF. The obtained vector was termed pGL4.75[*luc+*/CMV].

3.9.2.2 Cloning of T7 promoter

A T7 promoter-containing dsDNA insert was ligated into HindIII restriction site of the pGL4.75[*luc+*/CMV] and pGL4.75[*hRluc*/CMV] plasmids. This generated pGL4.75[*luc+*/T7/CMV] and pGL4.75[*hRluc*/T7/CMV] constructs, respectively. To this end, complementary oligonucleotides containing the T7 promoter flanked with compatible cohesive overhangs were used (see Tab. 3-17). The oligonucleotides contained 3' and 5' phosphate groups to facilitate ligation. An EcoRI restriction site was included for identification of positive clones and elimination of multiple insertions (via EcoRI digestion and re-ligation). The oligonucleotides were reconstituted in water and 25 mM stock solution in 10 mM Tris pH 7.4 was prepared. The mixture was boiled for 5 min at 95°C to ensure proper annealing. For ligation, a vector-to-insert ratio of 1:10 was used.

strand	sequence
sense	5'-P_i-AGCTTGAATTCTAATACGACTCACTATAGGGAGAA-P_i-3'
antisense	3'-P_i-ACTTAAGATTATGCTGAGTGATATCCCTCTTTCGA-P_i-5'

Tab. 3-17: Complementary oligonucleotides carrying the T7 promoter, with HindIII restriction site-compatible cohesive overhangs (underlined) and EcoRI restriction site (blue); P_i – phosphate groups.

3.9.2.3 Cloning of 3'UTR fragments

The pGL4.75[*luc+*/T7/CMV] plasmid was cut with XbaI and SalI restriction enzymes. Terminal fragments of 3'UTRs (determined by 3'RACE products) were PCR-amplified to generate compatible restriction overhangs (for reaction setup and temperature profile, refer to Tab. 3-18 and 3-19, respectively.

Reagent	Amount	Stock concentration
Plasmid template	1 µl	50-100ng/µl
Roche HF Polymerase Mix	0.5 µl	3.5U/µl
dNTP mix	1 µl	10mM
Primer mix (For + Rev)	1 µl	10µM each
Buffer with Mg^{2+}	10 µl	5x
$_{dd}H_2O$	35.5 µl	n/a
Total volume	**50 µl**	

Tab. 3-18: PCR amplification of 3'UTR fragments – reaction mixture (done with Roche High Fidelity (HF) PCR system).

Temp.	Time	No. of cycles
94°C	2 min	
94°C 53°C 70°C	15 s 30 s 1m:30s	x 30
70°C	10 min	
4°C	hold	

Tab. 3-19: PCR amplification of 3'UTR fragments – temperature profile.

PCR products were digested with XbaI and SalI restriction enzymes and cloned into respective sites of pGL4.75[*luc+*/T7/CMV], replacing the SV40 Poly(A) signal. A control vector containing GAPDH 3'UTR was generated in the same way.

3.9.3 Site-directed PCR mutagenesis

Splicing by overlap extension (SOE) PCR was used to mutate CPE elements in cloned 3'UTR fragments. SOE PCR was performed with the Advantage HF High Fidelity PCR Kit (Clontech, Heidelberg, Germany). Reaction setup and temperature conditions for both rounds of SOE PCR are summarized in Tab. 3-20 and 3-21, respectively.

Reagent	Amount	Stock concentration
Plasmid DNA template (1st round) / 1st round SOE PCR products (2nd round)	1 µl / 1 µl each	50-100 ng/µl
Polymerase Mix	0.5 µl	3.5 U/µl
dNTP mix	1 µl	10 mM
Primer mix (For + Rev)	1 µl	10 µM each
Buffer with Mg^{2+}	10 µl	5x
$_{dd}H_2O$	up to 50µl	n/a
Total volume	**50 µl**	

Tab. 3-20: 1st and 2nd round of SOE PCR reaction mixes.

Temp.	Time	No. of cycles
94°C	1 min	
94°C 56°C 68°C	15 s 30 s 90 s	x 35
68°C	10 min	
4°C	hold	

Tab. 3-21: 1st and 2nd round of SOE PCR - temperature profile.

3.9.4 Generation of a FLAG-EGFP control vector

The EGFP ORF was excised from pEGFP-N1 plasmid (Clontech) using HindIII and XbaI restriction enzymes, and then ligated in respective sites of the p3xFLAG-CMV-7.1 vector.

3.9.5 Generation of lentiviral protein expression vectors

A modified pFTM3GW (GenBank accession no. FJ797421) 3rd generation lentiviral transfer vector (Geller *et al.*, 2007), kindly provided by Dr. Elena Baron (AG Schoch, Institute of Neuropathology, University of Bonn), served as backbone for generation of lentiviral expression vectors. The vector lacked a synthetic transcription blocker TB (present in the original pFTM3GW plasmid) and contained an EGFP reporter. As a first step, the mouse PGK promoter (template kindly provided by Dr. Yiner Wang, AG Neumann) was cloned between PacI and BamHI restriction sites of the vector. Then, FLAG-tagged CPEB-1, DN-CPEB1-4 and CPEB-3 cDNA was cloned into the BamHI site of the vector, in frame EGFP ORF. As templates for amplification of the FLAG-tagged CPEBs, p3xFLAG-CMV-7.1 vectors (Sigma Aldrich, Munich, Germany) containing the respective CPEB ORFs were used. In case of hight GC content in the CPEB-3 DNA sequence, a GC-Rich PCR System (Roche, Mannheim, Germany) was used. The respective reaction setups and temperature profiles were summarized in Tab. 3-22 and 3-23 (CPEB-1 and DN-CPEB) and Tab. 3-24 and 3-25 (CPEB-3). Obtained positive clones were identified by colony PCR. The recombinase-deficient Stbl3 *E.coli* strain was used to propagate the

plasmids. To ensure that no undesirable recombination between Long Terminal Repeats (LTR) of the vector occurred during consecutive cloning steps, HindIII restriction endonuclease digestion was routinely performed to confirm the expected band pattern.

Reagent	Amount	Stock concentration
Plasmid template	1 µl	50-100 ng/µl
Roche HF Polymerase Mix	0.5 µl	3.5 U/µl
dNTP mix	1 µl	10 mM
Primer mix (For + Rev)	1 µl	10 µM each
Buffer with Mg^{2+}	10 µl	5x
$_{dd}H_2O$	35.5 µl	n/a
Total volume	**50 µl**	

Tab. 3-22: PCR amplification of CPEB-1 and DN-CPEB1-4 ORF fragment - reaction mixture.

Temp.	Time	No. of cycles
94°C	2 min	
94°C 60°C 70°C	15 s 30 s 3m+3s incr./cycle	x 35
70°C	10 min	
4°C	hold	

Tab. 3-23: PCR amplification of CPEB-1 and DN-CPEB1-4 ORF fragment - temperature profile.

	Reagent	Amount	Stock concentration
Reaction Mix 1	Plasmid template	1 µl	50-100 ng/µl
	Primer mix (For + Rev)	1 µl	10 µM each
	dNTP mix	1 µl	10 mM
	GC Rich resolving solution	15 µl	n/a
	$_{dd}H_2O$	17 µl	n/a
	Total volume	**35 µl**	
Reaction Mix 2	Enzyme mix	1 µl	3.5 U/µl
	GC Rich Polymerase Buffer	10 µl	5x
	$_{dd}H_2O$	4 µl	n/a
	Total volume	**15 µl**	
	Final reaction volume	**50 µl**	

Tab. 3-24: PCR amplification of CPEB-3 ORF fragment reaction mixtures (done with Roche GC-Rich Polymerase system).

Temp.	Time	No. of cycles
94°C	3 min	
94°C 55°C 70°C	30 s 30 s 2m:30s+5s incr./cycle	x 35
70°C	10 min	
4°C	hold	

Tab. 3-25: PCR amplification of CPEB-3 - temperature profile.

3.9.6 DNA sequencing

Sequencing of plasmid DNA and PCR products was done by Qiagen (Qiagen Genomic Services, Hilden, Germany). Obtained sequencing reads were of Phred20 quality. The company also provided standard sequencing primers. The critical sequencing reactions were confirmed by performing the opposite sequencing read of the same sequence. Additionally, in case of ambiguous bases/mismatches, the sequencing chromatograms were manually inspected for errors, using Bio-Edit software (Hall, 1999).

3.10 Generation of custom polyclonal antibodies

Custom polyclonal antibodies directed to CPEBs 1-4 were generated by Eurogentec GmbH (Cologne, Germany). The service included peptide synthesis, rabbit immunization and affinity purification of the obtained antibodies from the crude serum. Peptides (16-

18 amino acids long) were chosen on the basis of hydrophobicity (Kyte and Doolittle, 1982), antigenic index (Jameson and Wolf, 1988) and surface probability (Emini *et al.*, 1985). The following peptides were chosen (cysteine residues added to the sequences for coupling purpose were underlined): RGIHDQLPDFQDSEETVT and CTWSGQLPPRNYKNPI (CPEB-1), CLQQRNSYNHHQPLLK and LQLPAWGSDSLQDSWC (CPEB2), LSFHQPPQQPPPPQEPTA and QPPQPAQPPQAQPSQQ (CPEB-3), and SENSNGKEKLRIESPC and KPPSPWSSYQSPSPTP (CPEB-4). **K**eyhole **l**impet **h**emocyanin (KLH) was used as a carrier protein. Peptide coupling was done via cysteine –(SH) groups or (where applicable) –(NH_2) groups, using *m*-**M**aleimido**b**enzoyl-N-hydroxy**s**uccinimide (MBS) or glutaraldehyde methods, respectively. For each CPEB, two specific pathogen-free (SPF) rabbits were injected 4 times, with 200μg of each of both peptides, in 2-week intervals. 87 days after the first immunization, the animals were sacrificed and bled, and affinity purification was performed.

3.11 Generation of CPEB-3a phosphospecific antibodies

Custom polyclonal antibodies directed to the phosphorylated form of CPEB3a was generated by Eurogentec GmbH (Germany). The antibody was directed to a region surrounding the serine residues S419 and S420. The service included peptide synthesis, rabbit immunization and cross-affinity purification of the obtained antibodies from the crude serum. The RRGRSSLFPFEDC peptide was chosen for immunization (cysteine residue added to the sequences for coupling purpose was underlined). Bi-phosphorylated, two mono-phosphorylated (with either S419 or S420 phosphorylated) and non-phosphorylated versions of the peptide were synthetized. KLH was used as a carrier protein. Two SPF rabbits were immunized with the mixture of 3 peptides: the bi-phosphorylated and the two mono-phosphorylated. The better responsive animal (as determined by indirect ELISA) was chosen for further production steps. The affinity purification was performed on Toyopearl AF-Amino-650 matrix, sequentially on 2 columns. On the first column, containing immobilized bi-phosphorylated peptide, antibodies recognizing phosphorylated and non-phosphorylated peptides were captured. On the second column, containing immobilized non-phosphorylated peptide, the first column eluate was depleted of the antibodies non-specific to phosphorylation (the final product was the second column flow-through). Elution was performed with 100 mM Glycine, pH 2.5. The performance of the obtained antibody fractions was assessed by indirect ELISA.

3.12 Western blotting

Tissue and cell culture lysates were prepared in a modified RIPA lysis buffer supplemented with protease inhibitor cocktail (Roche, Mannheim, Germany). Tissue was homogenized with a pestle in a 1.5-ml tube. Cultured cells were scraped with a cell scraper in ice-cold RIPA modified lysis buffer. Samples were subsequently disrupted with a 27-gauge needle, and incubated on ice for 10 min. Supernatants were collected after 20-min centrifugation at 13.000 g at 4°C. Total protein content was assayed with a BCA kit (Pierce) and 10-100 μg of total protein per loading was used. Lysates were mixed with denaturing sample buffer and heated for 6 min at 95°C. Proteins were separated by discontinuous SDS-PAGE (Laemmli, 1970) in denaturing conditions and electroblotted onto a PVDF membrane. Membranes were blocked with 5% milk powder in TBS-T buffer, pH 7.4, and incubated O/N at 4°C with primary antibodies on an orbital shaker. For membrane reprobing, "Restore" stripping buffer (Pierce) was used. Membranes were usually re-blocked after stripping for 0.5–2 h. For detecting HRP activity, "West Dura" substrate (Pierce) was used and generated chemiluminescence was detected with the Gene Gnome digital documentation system (Synoptics, Cambridge, UK). Raw data analysis and densitometry were performed with GeneTools quantification software (Synoptics). Normalized values obtained were tested for significant differences with nonparametric Mann-Whitney test and where applicable with Student's t-test.

3.13 Immunocytochemical staining of the BV-2 cells

BV-2 cells were seeded on glass coverslips and grown for 48 hours (or until confluence). Cell culture medium was removed, coverslips were washed with PBS and fixed for 10 min with 4% PFA (in PBS) at room temperature. After fixation, cell membranes were permeabilized by incubation in 0.5% Triton X-100, followed by 1 h blocking with 5% normal goat serum (NGS) at room temperature. Cells were stained with affinity purified primary polyclonal antibodies directed to CPEBs 1-4, at the following dilutions: CPEB1 (custom-made) – 1:100, CPEB2 (custom-made) – 1:250, CPEB3 (Abcam) – 1:100, CPEB4 (custom-made) – 1:100. Antibodies were diluted in PBS supplemented with 2.5% NGS. Cells were incubated with primary antibody for 2 h at room temperature (or overnight at 4°C), followed by 1 h incubation with Alexa594-coupled goat-anti-rabbit secondary antibody at 1:500 dilution (in PBS). Counterstaining was performed with Hoechst dye for 5 min. Coverslips were mounted using the PermaFluor mounting medium (Thermo Scientific).

3.14 Cell culture maintenance and transfection

Transfection was performed with Lipofectamine 2000 (Invitrogen), according to the manufacturer's protocol. Cells were usually transfected at 80-95% confluence. Amounts of DNA and lipofectamine used were individually optimized for each experiment.

3.14.1 HeLa cell culture

HeLa cells (kindly provided by Dr. Bernd Evert, Department of Neurology, University of Bonn) were cultured as a monolayer in DMEM supplemented with 10% FCS. Cells were grown at 37°C in a 5% CO_2 atmosphere. When confluent, cells were split by trypsinization. For cryopreservation, 2-4 x 10^6 cells were suspended in 1 ml FCS supplemented with 10% DMSO, frozen in a freezing box, and stored in liquid N_2.

3.14.2 HEK-293FT culture

HEK-293FT cells were cultured in MEF cell culture medium (see section 3.2.1) and grown at 37°C in a 5% CO_2 atmosphere. When confluent, cells were split by trypsinization at 1:5 - 1:20 ratio. For cryopreservation cells were suspended in HEK-293FT medium supplemented with 40% FCS and 10% DMSO, frozen in a freezing box, and stored in liquid N_2.

3.14.3 BV-cells culture

The murine BV2 cell line (Blasi *et al.*, 1990) (kindly provided by Prof. Dr. Jochen Walter, Molecular Cell Biology Department of Neurology, University Hospital Bonn) was cultured in DMEM supplemented with 10% FCS. Cells were grown at 37°C in 5% CO_2 atmosphere and split by trypsinization when confluent. Cryopreservation was done as for HeLa cells (section 3.14.1).

3.14.4 ESdM cell culture

Liquid N_2-stored stocks (kindly provided by Prof. Dr. Harald Neumann, Institute of Reconstructive Neurobiology, University of Bonn, LIFE & BRAIN Center) were rapidly thawed at 37°C and cultured in standard N2 medium on standard TC-dishes or TC-flasks. Medium was replaced every 2-3 days. When confluent (80%), cells were split at a 1:3-1:8 ratio by scraping in PBS. Cells were grown at 37°C in a 5% CO_2 atmosphere. For cryopreservation, 4 x 10^6 of cells were suspended in 1ml of N2-medium supplemented with 10% DMSO and 40% FCS, frozen in a freezing box, and stored in liquid N_2.

3.15 RNA co-immunoprecipitation (RNA co-IP)

The procedure for the RNA co-IP experiments was initially adapted from Jones *et al.* (2008) and then modified. In case of anti-FLAG antibody co-IPs, the procedure involved a FLAG-EGFP fusion as a control bait protein.

3.15.1 Co-IP of endogenous β-catenin mRNA

3.15.1.1 Co-IP by overexpressed mCPEB-1 and mCPEB-3 proteins

FLAG-tag expression vectors containing ORFs of bait proteins mCPEB-1 and mCPEB-3 (p3xFLAG-CMV-7.1 backbone, cloned by Dr. Martin Theis) were chemically transfected into HeLa cells, typically seeded on 10 cm TC-dishes. 8 μg of total DNA and 20 μl of Lipofectamine 2000 was used per dish. Cells were harvested 24 h post-transfection by scraping in ice cold RNA co-IP lysis buffer, and finally disrupted with a 27G needle. Cell debris was pelleted by centrifugation at 15.000g at 4°C for 15 min. Subsequent incubation steps were performed at 4°C on a rotator (10-15 rpm). Lysates were precleared via 1 h incubation with 30 μl of protein A Sepharose (PAS) slurry (Invitrogen). Precleared lysates were incubated overnight with custom-made anti-CPEB-1 or anti-CPEB-3 rabbit sera (1:20, Eurogentec, Cologne, Germany). To capture immunoprecipitated complexes, the lysates were incubated with 40 μl of PAS slurry for 2 h. In each case, a 30 μl sample was taken before the IP step, to determine input RNA levels. The beads were washed 8 times with ice cold RNA wash buffer and retained RNA was extracted using the RNeasy Mini kit (Qiagen, Hilden, Germany). The on-column genomic DNA digestion step was included. To detect co-immunoprecipitated mRNA, conventional RT-PCR for β-catenin and GAPDH was performed. mRNA enrichment in analyzed samples was further validated with SYBR Green chemistry-based sqRT-PCR.

3.15.1.2 Co-IP by overexpressed mCPEB-2 and corresponding Zn^{2+} finger deletion mutant

The experiments were done as described in the section 3.15.1.1 with the following modifications: 1) The M2 anti-FLAG mouse monoclonal antibody (1:100, Sigma, Germany) was used for antigen binding in case of FLAG-tagged fusions; 2) Protein G Dynabeads (Invitrogen, Germany) were used to capture antigen-antibody complexes in case of co-IPs done with M2 anti-flag antibody; 3) Taq-Man chemistry-based sqRT-PCR was employed to quantitate mRNA levels in the input and output material.

3.15.2 Co-IP of 3'UTR luciferase constructs

Bait proteins (FLAG-tagged CPEB) and prey RNA constructs (luciferase gene appended with CPE-containing 3'UTRs - see section 3.9.2) were co-transfected and co-expressed in HeLa cells. As a control prey, a GAPDH 3'UTR construct was used. Typically, per 10 cm TC-dish, 6 μg of bait and 2 μg of prey constructs were used with 20 μl of lipofectamine. Cells were harvested 24 h post-transfection by scraping in ice cold RNA co-IP lysis buffer, and finally disrupted with a 27G needle. Cell debris was pelleted by centrifugation at 15.000 g at 4°C for 15 min. Subsequent incubation steps were performed at 4°C on a rotator (10-15 rpm). Lysates were precleared by 1 h incubation

with 30 µl of Protein G Dynabeads (Invitrogen). In the same time, an appropriate aliquot of the beads was blocked for 1 h with the RNA co-IP lysis buffer supplemented with 3% bovine serum albumin (BSA) and 15 µg of tRNA per 30 µl of the beads. Precleared lysates were incubated overnight with M2 anti-FLAG mouse monoclonal antibody (1:100, Sigma) and 40 µl of blocked protein G Dynabeads, in the presence of RNAsin (Promega). In each case, a 30 µl sample was taken before the IP step, to determine the input RNA levels, and to verify transfection efficacy by immunoblot. The beads were washed 8 times with ice cold RNA co-IP wash buffer and retained RNA was extracted using the RNeasy Mini kit (Qiagen, Hilden, Germany). The on-column genomic DNA digestion step was included. Taq-Man chemistry-based sqRT-PCR was used to quantitate luciferase, PBGD and GAPDH levels in the input and output material.

3.16 Analysis of CPEB-3 isoform expression pattern

Total RNA purification and cDNA production were performed according to the manufacturers guidelines, using (respectively) RNeasy kit (Qiagen) and SuperScript III reverse transcriptase system (Invitrogen). CPEB-3 was amplified using a set of primers flanking alternatively spliced region, yielding amplicons corresponding to different isoforms (Theis *et al.*, 2003b). Obtained PCR products were purified from gel, T/A-cloned into Topo-XL vector (Invitrogen) and sequenced. Sequences were aligned using Jalview software (Waterhouse *et al.*, 2009).

3.17 Semi-quantitative Real Time PCR (sqRT-PCR)

3.17.1 SYBR Green sqRT PCR

For verification of RNA co-IP results done with conventional RT-PCR, SYBR Green chemistry-based sqRT-PCR was performed (in a 2-step procedure). The RT-reaction (1st step) was done with Omniscript reverse transcriptase (Qiagen), using oligo-d$(T)_{15}$ for priming and up to 2 µg of total RNA as template, in a 20 µl total reaction volume. Prior to the RT reaction, the co-IP-input RNA amount was normalized to the concentration of the least abundant sample. For co-immunoprecipitated (output) material, normalization was not performed. SYBR Green PCR (2nd step) was performed using SYBRGreen 2x Supermix (Biorad) and 1 µl of RT reaction mix was used as template in 25 µl total reaction volume. Each reaction was done in duplicate. Relevant master-mixes were always prepared to minimize pipetting errors. The reactions were carried out in 96-well plates, in the IQ5 optical system (Bio-Rad). All primers were optimized for use at an annealing temperature of 59°C. See Tab. 3-26 and 3-27 for (respectively) the reaction setup and temperature profile. The appearance of primer dimers was ruled out by melt curve analysis. Data was analyzed using $\Delta\Delta C_t$ method using human β-actin gene as a reference.

Reagent	Amount	Stock concentration
2x SYBR Green Supermix	12.5 µl	2x
Template cDNA	1 µl	variable
Primer mix (F+R)	1 µl	10µM each
$_{dd}H_2O$	10.5 µl	n/a
Total volume	**25 µl**	

Tab. 3-26: SYBR Green sqRT-PCR reaction mixture.

Temp.	Time	No. of cycles
95°C	5 min	
95°C	30 s	x 40
59°C	30 s	
72°C	30 s	
55-95°C (+0.5°C/cycle) Melt curve	30 s	x 81

Tab. 3-27: SYBR Green sqRT-PCR temperature profile.

3.17.2 Taq-Man sqRT PCR

TaqMan sqRT-PCRs were performed as a 2-step procedure. The RT-reaction (1st step) was done with SuperScript III reverse transcriptase (Invitrogen), using up to 2 µg of total RNA template, and 250 ng of random hexamers for priming, in a 20 µl total reaction volume. Prior to the RT-reaction, the RNA amount was normalized to the concentration of the least abundant sample (except for co-immunoprecipitated material, when normalization was not performed). Taq-Man reaction (2nd step) was performed using Gene Expression Master Mix (Applied Biosystems), and 0.5 µl of RT reaction mix was used as template in 12.5 µl total reaction volume. Each reaction was done in duplicate. The reactions were carried out in Optical 384-Well Reaction Plate PCR plates (Applied Biosystems, Darmstadt, Germany) in the 7900HT Fast Real-Time PCR System (Applied Biosystems). See Tab. 3-28 and 3-29 for (respectively) the PCR reaction setup and temperature profile. Primer and probe design was done with Primer Express 3.0 software, using default parameters. Primers overlapping exon-exon boundaries and with the lowest penalty score were chosen preferentially. All probes were labeled with TAMRA (3'-end) and 6-FAM (5'-end), unless specified otherwise. For each reaction, critical threshold cycle (C_t) value was determined using SDS 5.0 Software (Applied Biosystems). Efficiency of the primer/probes sets was calculated according to the serial dilution method (Higuchi *et al.*, 1993; Souaze *et al.*, 1996). All expression data represent the statistical mean of at least three independent experiments. Error bars are standard errors of the mean (SEM). Data was analyzed with $\Delta\Delta C_t$ method, using human GAPDH, PBGD and/or β-actin reference genes. In the co-IP experiments, mRNA retention by the bait proteins was calculated using normalized input mRNA value.

Reagent	Amount	Stock concentration
Gene Expression Master Mix	6.25 µl	2x
Template cDNA	0.5 µl	variable
TaqMan Assay	0.5 µl	primers: 10 µM; probe: 5 µM
$_{inj}H_2O$	5.25 µl	n/a
Total volume	**12.5 µl**	

Tab. 3-28: TaqMan sqRT-PCR – reaction mixture.

Temp.	Time	No. of cycles
50°C	2 min	
95°C	10 min	
95°C	15 s	x 40
60°C	60 s	

Tab. 3-29: TaqMan sqRT-PCR temperature profile.

3.17.3 Conventional RT-PCR

The reverse transcription (RT step) was done as described in section 3.17.2. The PCR step was performed with the Platinum Taq hot start polymerase system (Invitrogen), using 2 µl of cDNA (RT reaction mix), in a C1000 thermal cycler (Bio-Rad). Obtained products were analyzed on 2% agarose gels stained with EtBr.

3.18 *In vitro* phosphorylation

3.18.1 Peptide synthesis

CPEB-3-derived peptides were used as substrates for *in vitro* phosphorylation reactions. Peptide synthesis was done by Peptide Specialty Labs (PSL, Heidelberg, Germany). Peptides were synthesized with free carboxy termini, starting with an L-resin. For PEG-biotinylated peptides, a Biotin-PEG-Nova Tag-resin (Merck) was used. Peptides were synthesized on a continuous flow peptide synthesizer according to the F-moc chemistry by starting with the Fmoc-L amino acid attached to Wang resin (loading 0.54 mM/g) and stepwise addition of the amino acids from C- to N-terminus. For facilitating the synthesis, pseudoproline dipeptides (Merck) were used for the following amino acids: N-T (9 and 10), S-S (20 and 21), D-S (32 and 33), and L-S (39 and 40). The other amino acids have been used as tBu-protected (D, E, S, T, Y), Trt-protected (H, N, Q), and Pbf-protected (R) amio acids. The peptides were cleaved off the resin by a mixture of 95% TFA, 4% triethylsilane and 1% water at room temperature for a period of 2 h. During the cleavage process all protecting groups have been removed from the corresponding amino acids and the pseudoproline dipeptides have been converted to the corresponding L-amino acids. The raw material was lyophilized and purified by HPLC by dissolving the peptides in 30% acetonitrile in 0.1% aqueous TFA and passing the solution over a Gemini Axia (Phenomenex) column (260x25 mm). Peptides were eluted with 30-75% acetonitrile gradient in 0.1% TFA, in a time period of 20 min, at a flow rate of 20 ml/min. Eluted fractions have been analyzed by analytical HPLC using the same column material (100 x 4.6 mm) and the same gradient, and have been assessed by MALDI-TOF mass spectrometry. Fractions containing the material with the correct mass have been combined and lyophilized to yield the peptides as TFA-salts.

3.18.2 *In vitro* phosphorylation reactions

In vitro phosphorylation reaction mixes comprised active kinase: CaMKII or protein kinase A (PKA) catalytic subunit α (PKA-C_α), ATP, kinase buffer (all from New England Biolabs), and peptide substrate. CaMKII was activated in the presence of Ca^{2+} and calmodulin (refer to Tab. 3-30 for the respective setup). Peptide substrate, ATP, and enzyme amounts were optimized, depending on the nature of downstream assay: MALDI-TOF-based assay, PKLight assay and ADP-Glo assay (for respective reaction

setups refer to section 3.18.3, 3.18.4 and 3.18.5). Relevant master mixes were prepared whenever possible to minimize pipetting errors. Control reaction mixes included water instead of kinase (no-kinase control) or peptide (no-substrate control).

reagent	amount	stock concentration
CaMKII kinase	4 µl	**500U/µl**
ATP	2 µl	**10 mM**
Calmodulin	2 µl	12 µM
$CaCl_2$	2 µl	20 mM
CaMKII buffer	2 µl	10x
water	8 µl	n/a
total volume	**20 µl**	
reaction conditions: 15min at 30°C		

Tab. 3-30: CaMKII preactivation reaction mix.

3.18.3 MALDI-TOF – based phosphorylation assay

MALDI-TOF (**m**atrix-**a**ssisted **l**aser **d**esorption/**i**onization – **t**ime-**o**f-**f**light) mass spectrometry (MALDI-TOF-MS) was used for qualitative determination of *in vitro* phosphorylation of peptide substrates (experiments were performed in the group of Prof. Hans-Georg Sahl, Institute of Microbiology and Biotechnology, Bonn). PKA and CaMKII phosphorylation reaction setups for MALDI-TOF-MS analysis were summarized in Tab. 3-31 and 3-32, respectively.

reagent	amount	stock concentration
PKA kinase	3.75 µl	**500U/µl**
ATP	4 µl	**10mM**
kinase buffer	4 µl	10x
peptide	8 µl	**500µM**
water	20.25 µl	n/a
total volume	**40 µl**	
reaction conditions: 1 h at 37°C		

Tab. 3-31: PKA phosphorylation for MALDI-TOF-based assay.

reagent	amount	stock concentration
CaMKII pre-activated mix	4 µl	**25U/µl**
ATP	1 µl	**10mM**
CaMKII buffer	1.6 µl	10x
peptide	2 µl	**500µM**
water	11.4 µl	n/a
total volume	**20 µl**	
reaction conditions:	**1 h at 30°C**	

Tab. 3-32: CaMKII phosphorylation for MALDI-TOF assay.

Prior to the MALDI-TOF-MS analysis, phosphorylation reaction mixes were desalted on the C18 resin-packed pipette tips (ZipTips) (Millipore). The following steps were performed via slowly aspirating and dispensing the solution through the C18 resin:

ZipTip was equilibrated with 0.1% TFA and an aliquot (~6 µl) of peptide-containing reaction mix was applied. The ZipTip was washed with excessive volume of 0.1% TFA. C18-bound peptides were eluted with 5 µl of the matrix, and applied on the spot of a ground steel MALDI target plate using a dried droplet method. As the matrix α-HCCA saturated in TA (33.3% acetonitrile/0.1%TFA) was used. Samples were dried at room temperature analyzed on the Biflex III MALDI-TOF MS spectrometer (Bruker Daltonik GmbH, Bremen, Germany), using the following parameters: IS1: 19 kV, IS2: 17.2 kV, lens: 8.8 kV, PIE: 200ns, gating: maximum. Spectra were recorded in the linear positive mode at a laser frequency of 20 Hz, within a mass range from 1,000 to 6,000 Da. For each spectrum, at least 300 laser shots in 30 shot steps were collected. Each sample was analyzed at least in duplicate. Visual estimation of the mass spectra, raw data smoothing and baseline subtraction was performed using the FlexAnalysis 1.0 software. Obtained data was analyzed and graphically presented using the GraphPad Prism 5.0 software.

3.18.4 PKLight phosphorylation assay

The PKlight assay (Lonza, Cologne, Germany) was used for quantitative analysis of *in vitro* phosphorylation by PKA (refer to Tab. 3-33 for the respective reaction setup).

reagent	amount	stock concentration
PKA kinase	3 µl	**50 U/µl**
ATP	4 µl	**10 µM**
kinase buffer	4 µl	10x
peptide	16 µl	**500 µM**
water	13 µl	n/a
total volume	**40 µl**	
reaction conditions:	**15 min at 37°C**	

Tab. 3-33: PKA phosphorylation for PKLight assay.

The assay was performed in white, flat-bottom, 96-well, polypropylene plates. In each well, 20 µl of the phosphorylation reaction (see section 3.18.2) was mixed with 20 µl of ATP detection reagent (kit component). The plate was gently vortexed and incubated for 10 min at RT. The firefly luciferase signal was measured on a luminometer, using 0.1 s integration time. Each reaction was performed at least in duplicate and each experiment was repeated at least 4 times. The data was normalized to „no-kinase" control levels and tested for significance with student's t-test.

3.18.5 ADP-Glo phosphorylation assay

The ADP-Glo assay (Promega, Mannheim, Germany) was used for quantitative determination of *in vitro* phosphorylation by CaMKIIα (refer to Tab. 3.34 for the respective reaction setup). The assay was performed in white, flat-bottom, 96-well, polypropylene plates, according to the manufacturers recommendations. In brief, in each well, 10 µl of phosphorylation reaction mix was mixed with 10 µl of ADP-Glo. The

plate was vortexed, briefly centrifuged, and incubated at RT for 40 min. After that time, 20 µl of Kinase Detection Reagent (KDR) was applied to each well and mixed by vortexing. The plate was incubated at RT for 40 min and firefly luciferase signal was measured on a luminometer, using an integration time of 0.5 s. Each reaction was performed at least in duplicate and each experiment was repeated at least 4 times. The data was normalized to „no-substrate" control levels and tested for significance with student's t-test.

reagent	amount	stock concentration
CaMKII pre-activated mix	4.5µl	**25U/µl**
ATP	not incl.	n/a
CaMKII buffer	1.55µl	10x
peptide	8µl	**2mM**
water	5.95µl	n/a
total volume	**20µl**	
reaction conditions:	**1 h at 30°C**	

Tab. 3-34: CaMKII phosphorylation for ADP-Glo assay.

3.19 Stimulation of HEK-293 cells

HEK-293 cells were seeded on 6-well TC-culture plates (800.000 cells/well) and transfected on the next day with 3µg of CPEB3a-EGFP plasmid, using Lipofectamine 2000 reagent (Invitrogen). 50 mM forskolin stock was prepared in DMSO. 24 h post transfection medium was supplemented with 50 µM forskolin (New England Biolabs, Frankfurt, Germany) or identical amount of DMSO without forskolin in case of control wells. After 1h incubation, cells were washed with ice-cold PBS and lysed in PIL buffer supplemented with protease and phosphatase inhibitors. Lysates were sonicated for 10min. Supernatants were collected after 10min centrifugation at 10.000 g at 4°C. Total protein content was assayed with a BCA kit (Pierce) and 10-100 µg of total protein per loading was used. Lysates were mixed with denaturing sample buffer and heated for 5 min at 95°C. Immunoblot procedure and analysis was performed as described in section 3.12, except that membranes were blocked with 5% BSA (instead of milk powder) in TBS-T buffer, pH 7.4, at 4°C, and incubated O/N at 4°C with custom-made primary phospho-CPEB-3a antibody (Eurogentec).

3.20 Brain tissue dissociation and FACS sorting

For analysis of CPEB expression in primary microglia and enzymatic tissue dissociation procedure follow by FACS cell sorting was applied. To visualize microglial cells, a transgenic mouse line $CX_3CR1^{GFP/GFP}$ (Jung *et al.*, 2000) was used. A $CX_3CR1^{GFP/GFP}$ parent was bred with C57BL/6 to obtain 100% heterozygous litter. To visualize NG2 cells and astrocytes simultaneously from one litter, homozygous $NG2^{kiYFP/kiYFP}$ mice (Karram *et al.*, 2008) were crossbred with $Cx43^{kiCFP/+}$ (Degen, Dublin *et al.*, unpublished)

to generate double transgenic littermates, expressing YFP in all and CFP in 50% of the progeny. Obtained littermate animals were sacrificed at postnatal day 5. Brains were surgically removed and placed in ice-cold PBS. Meninges were removed and the brain was dissociated with trypsin-based Brain Tissue Dissociation Kit (Miltenyi Biotec), according to the manufacturer's protocol. Dissociated cell suspension was diluted to ~5 x 10^6 cells/ml. An aliquot was stained with APC-coupled anti-CD11b antibody. The cell suspension was filtered through 70 μM pore size cell strainer and GFP+ cells were FACS-sorted. Sorted cells were centrifuged and total RNA was isolated using RNeasy mini kit (Qiagen) with on-column gDNA removal.

3.21 RNA purification

Total RNA was isolated using RNeasy mini kits (Qiagen) with on-column gDNA removal. Cells were lysed in 350 μl RLT buffer supplemented with β-mercaptoethanol (1% v/v final conc.) and disrupted with a 27G needle. Total RNA was eluted with 20-30 μl of TE-buffer, depending on the expected yield.

3.22 *In vitro* transcription

To allow for T7 polymerase-driven *in vitro* transcription of a luciferase reporter gene, a T7 promoter was inserted into the pGL4.75[luc+/CMV] and pGL4.75[hRluc/CMV] vectors, as described in section 3.9.2.2. Plasmid templates containing luciferase reporter appended with fragments 3'UTRs containing CPE elements (and their mutated counterparts) (see also section 3.9.2.3) were linearized with SalI restriction endonuclease and purified with DNA Clean-up kits (Qiagen). Transcription reactions, capping and polyadenylation were performed using mMESSAGE mMACHINE kit (Ambion, Darmstadt, Germany) following the manufacturer's protocol. 1 μg of linearized plasmid DNA was used as a template. Obtained products were purified and recovered using the MEGAclear RNA Purification Kit (Ambion). The RNA concentration was determined by the absorbance measurement at 260 nm, using a Pearl NanoSpectrophotometer (Implen, Schatzbogen, Gemany). The size and integrity of obtained transcripts was verified with on-chip electrophoresis using Agilent 2100 Bioanalyzer (Agilent, Waldbronn, Germany). RNA was kept on ice for immediate use, or frozen for long-term storage.

3.23 Luciferase assay

HeLa cells were seeded on 24-well TC culture plates and transfected on the next day with 50ng of *in vitro*-transcribed mRNA per well. mRNA transfection was performed with Lipofectamine 2000 reagent (Invitrogen) according to the manufacturers' protocol (0.5 μl of the lipofectamine per well was used). Five hours post transfection cells were

washed 3x with PBS and lysed in the passive lysis buffer (Promega), supplemented with 1000U of RNAsin (Promega) per 1 ml of the buffer; 100 µl of lysis buffer per well was used. To ensure complete lysis, plates were incubated at room temperature with orbital shaking for 10 min. After that time, a 50 µl aliquot of the sample was immediately mixed with 350 µl of RLT buffer (Qiagen) for RNA isolation for the Taq-Man chemistry-based sqRT-PCR determination of luciferase mRNA levels. RNA isolation was performed using RNeasy mini kits (Qiagen), with on-column gDNA removal, according to the manufacturers' protocol. The remainder of the lysate was used to determine firefly luciferase reporter activity. Luciferase reactions were performed in 96-well, white, flat-bottomed polypropylene plates. 20 µl of lysate was applied to the wells. Plates were analyzed on the Centro LB960 luminometer (Berdhold Technologies, Bad Wildbach, Germany) set for the following event sequence: 20 µl substrate (see section 3.1.1) injection, 2 s delay, and 1 s measurement. Experiment was repeated three times, each in triplicate. Each luciferase measurement was performed in duplicate. Values obtained were normalized to the luciferase reporter mRNA levels (GADPH and β-actin genes were used as internal controls). Obtained data was tested for statistical significance using student's t-test.

3.24 Lentiviral infection of ESdM

Lentiviral transfer vector of the 3rd generation, pFTM3GW (GenBank accession no. FJ797421) was used to deliver and express DN-CPEB1-4 and CPEB-3 genes in ESdM cells (see also section 3.9.5). HEK-293FT cells were used as a packaging cell line. Lentiviral packaging was achieved through chemical (Lipofectamine 2000) transfection of 4 plasmids. The cells were transfected at 90% confluence, on 14 cm TC-dishes. The lentiviral expression module (in the pFTM3GW) was co-transfected along with the 3 helper vectors pLP1 (containing the gag-pol genes), pLP2 (containing the Rev gene) and pLP/VSV-g (containing the VSV-g gene) (all components of the ViraPower kit, Invitrogen). The vectors were mixed at 1:1:1:1 molar ratio, and 46 µg of total DNA with 150 µl of Lipofectamine per dish was used for transfection. Medium was collected after 48 and 72 h (second harvest), and filtered (0.45 µm pore size). For storage, viral particles were concentrated by 90-min ultracentrifugation at 25.000 rpm, and recovered by re-suspension in PBS (gentle shaking for 3-4 h at 4°C). ESdM cells were transduced at 80% confluence on 10 cm TC-dishes. Before addition of viral particles, ESdM cells were placed in N2-medium containing polybrene (10 µg/ml). Transduction was performed with concentrated particles or crude harvest (diluted 1:1 with N2 medium on the cells). After overnight incubation, medium was replaced with standard N2 culture medium. Transduced ESdMs were incubated for additional 72 h before GFP-fluorescent cells were FACS-sorted.

3.25 FACS cell sorting and analysis

Transduced ESdM cells, primary microglia, NG2 cells and astrocytes were FACS sorted in the Flow Cytometry Core Facility, Institute for Molecular Medicine and Experimental Immunology, University of Bonn. Sorting was performed on a customized BD FACS DiVA (BD Biosciences, Heidelberg, Germany). EGFP was excited with a 488 nm (blue) solid state laser (200 mW), using a 530/30 nm bandpass emission filter. After sorting, selected populations of ESdM cells were brought back to culture by resuspending in N2 medium in T75 TC-flasks. Primary microglia were deep-frozen or immediately lyzed for RNA extraction using RLT buffer (Qiagen) supplemented with 1% (v/v) β-mercaptoethanol. For FACS-sorting, cells were collected from the culture TC-dishes by scraping in PBS. Live/Dead Far Red Fixable Dead Cell Stain (Invitrogen) was added at 1µl/10^6 cells to discriminate dead cells. Cell suspensions were diluted to ~5 x 10^6 cells/ml, and kept on ice until analyzed. Data was acquired using FACS Canto II flow cytometer (BD Biosciences) and analyzed using Diva 5.0 (BD Biosciences) and FlowJo 7.6 (Tri Star, Inc.) software. For astrocytes (Cx43ki-ECFP) and NG2 cells (NG2ki-EYFP), respectively 488 nm (blue, 200 mW) and 403 nm (violet, 70 mW) were used. After FACS total RNA was isolated using RNeasy mini kit (Qiagen) with on-column gDNA removal. mRNA expression levels were determined using TaqMan qRT-PCR, on 7900HT Fast Real-Time PCR System (Applied Biosystems, Darmstadt, Germany), following manufacturer's recommendations.

3.26 Transgenic mice breeding and genotyping

The quality-control of Cre-mediated gene deletion (section 5.6) was performed using Cx30/Cx43 double knockout mice (previously described by Wallraff *et al.*, 2006). These mice were raised by cross-breeding the mice with astrocyte-directed Cx43 gene deletion (Theis *et al.*, 2003a) with the mice bearing unrestricted deletion of Cx30 gene (Teubner *et al.*, 2003). Astrocyte-directed of Cx43 deletion was achieved using the hGFAP-Cre transgene (Zhuo *et al.*, 2001). The genotypes used were $Cx30^{-/-}$;$Cx43^{fl/fl}$:hGFAP-Cre (termed **d**ouble **k**nock**o**ut, or DKO mice), $Cx30^{-/-}$;$Cx43^{fl/fl}$ (control mice). The mice were analysed at the age of 30-90 postnatal days. Mouse genotyping was performed by PCR. DNA was isolated from the tail tips as previously described (Laird *et al.*, 1991).

4 Results

4.1 Specificity of CPEBs to target mRNA

4.1.1 Defining 3'UTR termini of selected CPEB targets

The positioning of the CPE element with respect to the cleavage and polyadenylation site is a determinant of direction and magnitude of cytoplasmic polyadenylation (Hake *et al.*, 1998). To define the functional cleavage and polyadenylation sites of CPEB target mRNAs, CaMKIIα, tPA and Cx43 (putative target), a 3'RACE was performed. For tPA and Cx43, results were unambiguous; however in case of CaMKIIα, the reaction yielded two distinct bands (Fig. 4-1).

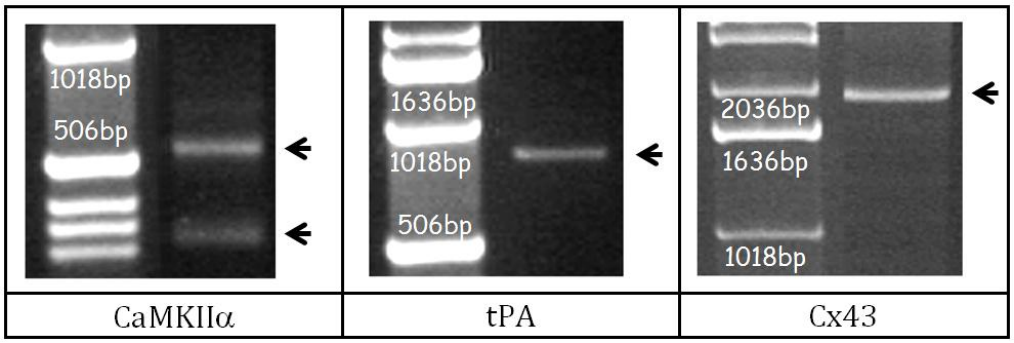

Fig. 4-1: **3'RACE results (CaMKIIα, tPA and Cx43), as analyzed by agarose gel electrophoresis.** Two distinct bands obtained in case of CaMKIIα suggest co-existence of long and short forms of mRNA (see also Fig. 5-8).

Results of the tPA and Cx43 3'RACE products sequencing revealed 3'UTR termini matching the records in the NCBI (accession no. NM_008872 and NM_010288, respectively). In case of CaMKIIα, the longer form (upper band) corresponded with the NCBI sequence (accession no. NM_009792). However, the shorter form seemed to be a specific RACE product as well. Firstly, because there was the AATAAA hexanucleotide in close proximity to the polyadenylation site. Secondly, because the 3'cDNA end was located in the homologous position to 3'cDNA terminus of the rat sequence (according to the NCBI record, accession no. AB056125) (Fig. 4-2). A fragment of the rat CaMKIIα 3'UTR, containing proximal and distal CPE elements, was found to be recognized by CPEB-1, CPEB-3, and CPEB-4 in electrophoretic mobility shift assay (EMSA) (Theis *et al.*, in revision). In the short variant of the mouse CaMKIIα 3'UTR, the position of CPE elements with respect to the 3'UTR terminus (and the AATAAA hexanucleotide) was the same, as in the rat 3'UTR. Consequently, this shorter variant, and not the long one, was chosen for further interaction studies.

Fig. 4-2: **Alignment of mouse CaMKIIα 3'RACE product sequences (long and short) with the rat 3'cDNA end.** Two distinct bands obtained for CaMKIIα 3'RACE (Fig. 4-1) suggest co-existence of long and short forms of mouse CaMKIIα mRNA. Alignment with rat 3'UTR sequence (GenBank accession no. AB056125) shows, that the mouse short form terminates in the position homologous to where the rat sequence ends. Poly(A) hexanucleotides were shown in orange. CPE-elements were depicted in blue. Discrepancies between mouse and rat sequences were marked in rat sequence in grey.

4.1.2 β-catenin mRNA is specifically recognized by different CPEBs

As already mentioned, all CPEBs have a distinct RBD, essential for mRNA recognition, comprising a ZiF and RNA-recognition motifs (RRMs) (Hake *et al.*, 1998). Similarity between the RBDs of CPEBs 2-4 is high (>97%) (Theis *et al.*, 2003b), suggesting overlapping target specificity between these proteins. On the other hand, the similarity between CPEB-1 RBD and CPEB-2-4 RBDs is considerably lower (<45%). β-catenin mRNA was previously shown to be regulated by CPEB-1 (Jones *et al.*, 2008). Regulation of this ubiquitous actin-binding protein implicates CPEB-1 in basic cell motility and adherence functions, as described in cultured astrocytes (Jones *et al.*, 2008). We wanted to find out, if other members of the CPEB family modulate β-catenin mRNA translation as well.

Endogenous β-catenin mRNA co-immunoprecipitated with CPEB-1 and CPEB-3 proteins in transiently transfected HeLa cells (Fig. 4-3). As a negative control, immunoprecipitated material was tested for GAPDH mRNA (the GAPDH 3'UTR does not contain CPE-elements).

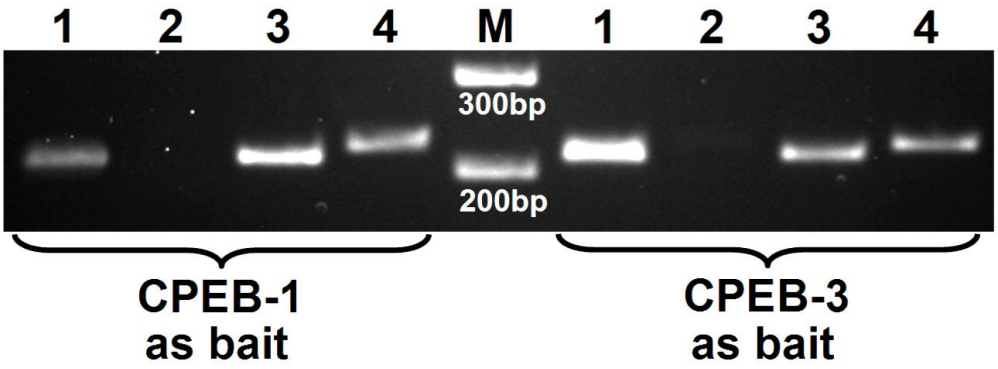

Fig. 4-3: **Co-IP of endogenous CPE-containing mRNAs in HeLa cells**. Endogenous β-catenin mRNA co-immunoprecipitates with overexpressed CPEB-1 (left) and CPEB-3 (right) proteins, as shown by RT-PCR from the co-immunoprecipitated material; line 1 – β-catenin; 2 – GAPDH; 3 and 4 – respective inputs of 1 and 2.

Likewise, CPEB2 was specifically binding to the endogenous β-catenin mRNA in HeLa cells (Fig. 4-4).

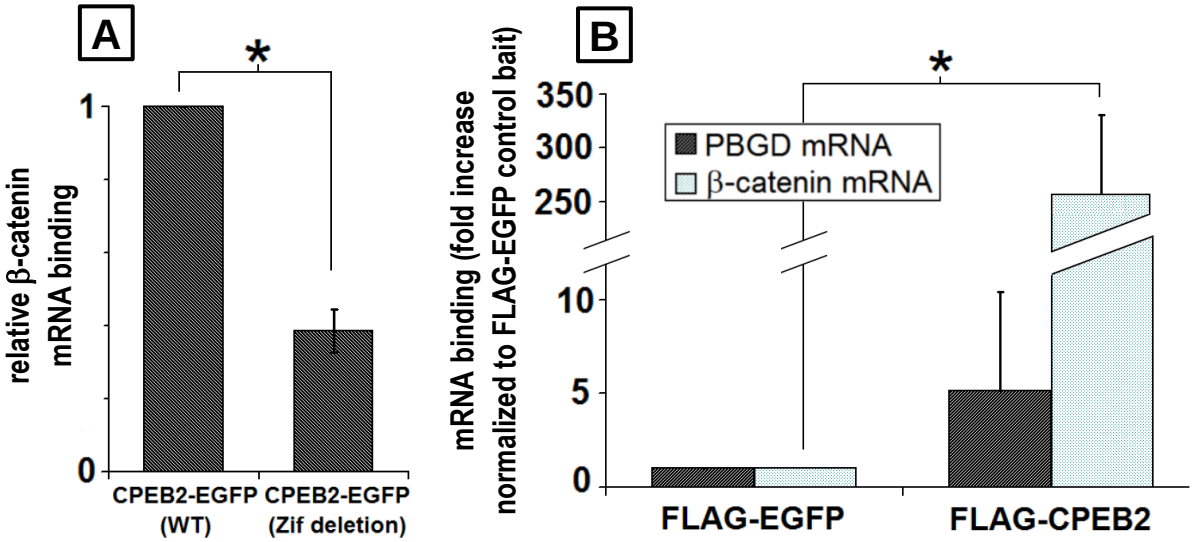

Fig. 4-4: Endogenous mRNA Pull Down experiments in cultured HeLa cells transfected with recombinant CPEB2 protein variants. (**A**) Deletion of Zn^{2+} finger significantly reduces CPEB2-EGFP fusion protein binding to β-catenin mRNA. (**B**) The binding is CPE-specific, as shown by comparison of PBGD (not containing any CPEs) and β-catenin 3'UTRs binding to FLAG-CPEB2 (graph on the right). EGFP-FLAG was used as a non-specific protein control (bait), to which the results were normalized (values set to 1 on the graph). *P<0.05, student's t-test.

The binding was mRNA specific, as shown via comparing porphobilinogen deaminase (PDGD) (not containing CPE-elements) and β-catenin mRNAs retention by CPEB-2 bait protein. A full-length- and a Zn^{2+} finger-truncated variant of the CPEB-2 protein (both as EGFP fusion proteins) were additionally used to test the importance of the Zn^{2+} finger in mRNA binding. ZiF deletion significantly reduced the binding of β-catenin mRNA. Results were normalized to the EGFP-FLAG fusion bait protein (non-specific protein control). Altogether, CPEB-2-4 are able to bind CPEB-1 protein targets, i.e. CaMKIIα, β-catenin, and CPEB3 mRNAs (Theis *et al.*, in revision) and the binding is ZiF-dependent.

4.1.3 CaMKIIα mRNA is specifically recognized by different CPEBs

In neurons of the mouse visual cortex, CPEB-1 was shown to modulate the experience-dependent translation of CaMKIIα (Wu *et al.*, 1998). CaMKIIα, in turn, is a well-established player in synaptic plasticity (Lisman *et al.*, 2002). Interestingly, CPEBs 2-4 contain a putative CaMKIIα phosphorylation site (Theis *et al.*, 2003b). Moreover, they are phosphorylated *in vitro* by recombinant kinase, as shown in the peptide phosphorylation assays (see section 4.3). This suggests that CPEBs might be activated by a protein, which is a CPEB target itself, resulting in a positive feedback loop. That might be one of the mechanisms underlying long term modifications of synaptic morphology and function occurring during LTP and/or LTD. Nonetheless, it was tempting to find out, if other members of CPEB family modulate CaMKIIα mRNA translation as well. Therefore I cloned the mouse CaMKIIα 3'UTR and performed co-IP experiments to compare the interaction of CPEB-1, DN-CPEB1-4 and CPEB-3 with CaMKIIα mRNA. For prey mRNA expression, a luciferase reporter vector appended with the 143bp fragment of the CaMKIIα 3'UTR, containing one consensus CPE (UUUUUUAAU) and one non-canonical CPE (UUUAUU) was used (Fig. 4-5D). DN-CPEB1-4, CPEB-1 and CPEB-3 were used as bait proteins. HeLa cells were co-transfected with respective bait protein expression vector and the pGL4.75[*luc+*/T7/CMV] vector encoding firefly luciferase appended with mCaMKIIα 3'UTR (with WT or MUT CPEs). I was able to co-immunoprecipitate mCaMKIIα 3'UTR with each of the three tested proteins (Fig. 4-5). In case of DN-CPEB1-4 and CPEB-1, conventional RT-PCR results were verified with SYBRGreen-based sqRT-PCR. For CPEB-3 co-IP, results were analyzed and quantified using TaqMan-based sqRT-PCR. In each case, I observed a decreased mRNA retention after replacing the wild-type (WT, with CPEs) fragment with the mutated one (MUT, without CPEs). This suggests that the binding is to a large extent CPE specific, and that the specificity of CPEB-1 and CPEB-3 is indeed overlapping.

4.1.4 CPEB-3 mRNA is a CPEB target

The CPEB3 3'UTR was another CPEB target tested in RNA co-IP experiments. A 3'RACE (performed by Vamshidhar Vangoor, Institute of Cellular Neurosciences, University of Bonn) revealed existence of two CPEB3 mRNA transcripts, with the poly(A) site at a distance of 3.5 kb or 0.8 kb from the STOP codon (termed distal and proximal, respectively). In co-IP experiments (performed similarly as for the CaMKIIα 3'UTR experiments), CPEB-1 and DN-CPEB1-4 proteins interacted with (i) the distal CPEB-3 3'UTR fragment (447bp, containing two consensus CPEs (UUUUAU) and one non-canonical CPE (UUUUCAU)) (Fig. 4-6) and (ii) the proximal CPEB-3 3'UTR fragment (271bp, with one canonical CPE) (Fig. 4-7).

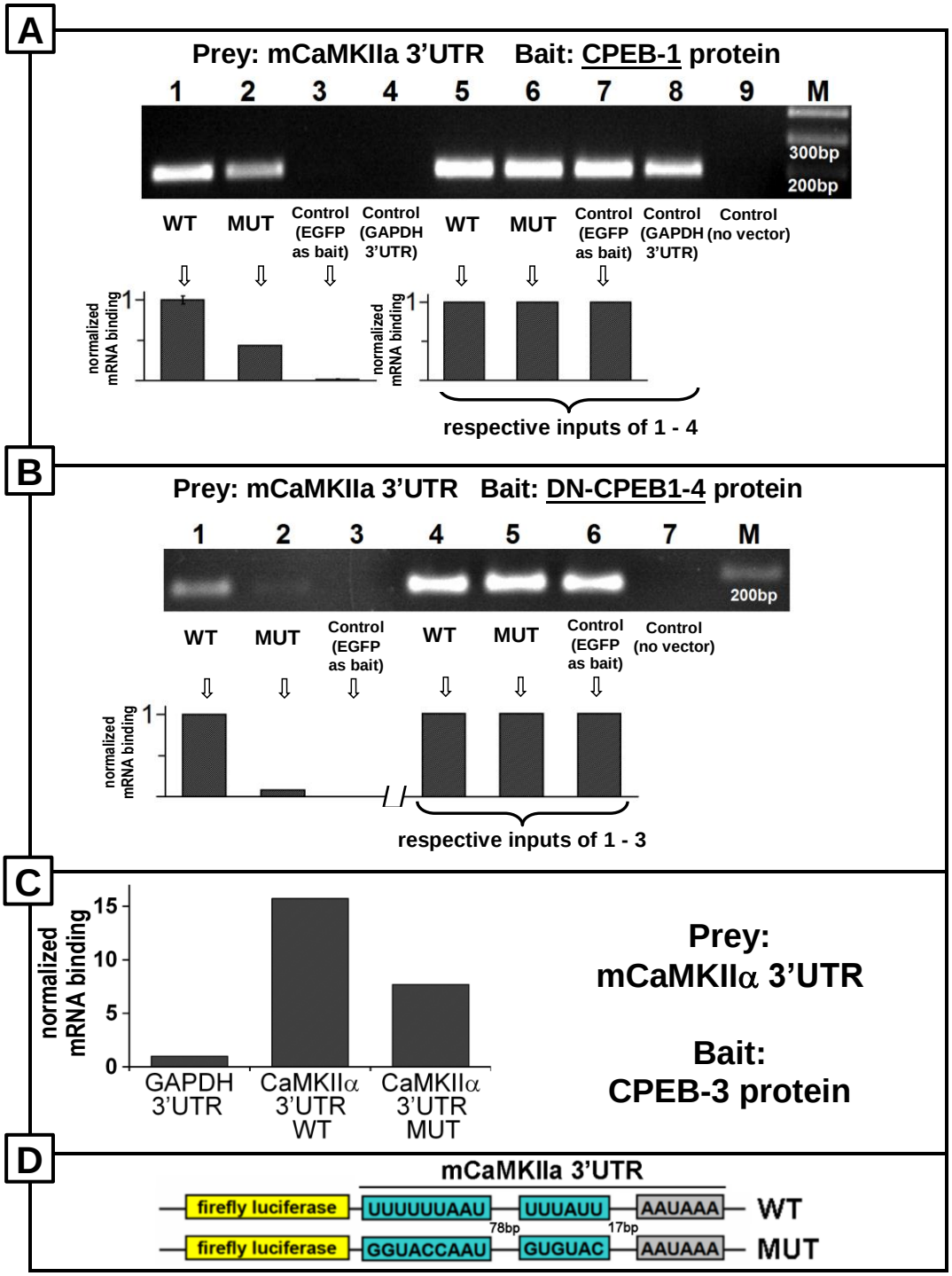

Fig. 4-5: **CPEB1, DN-CPEB1-4 and CPEB-3 bind specifically to the mouse CaMKIIα 3'UTR.** (**A**) Binding of CPEB-1 to mouse CaMKIIα shown by co-IPs: line 1 – co-IP of WT mCaMKIIα 3'UTR; 2 – co-IP of MUT mCaMKIIα 3'UTR (lacking CPEs); 3 – mock co-IP of WT mCaMKIIα 3'UTR with EGFP-FLAG fusion protein; 4 - co-IP of GAPDH 3'UTR construct (not-containing CPEs); 5, 6, 7 and 8 – respective inputs of 1, 2, 3, and 4; 9 – negative control (n.c.) (untransfected cell lysate). (**B**) Binding of DN-CPEB1-4 to mouse CaMKIIα shown by co-IPs: line 1 – co-IP of WT mCaMKIIα 3'UTR; 2 – co-IP of MUT mCaMKIIα 3'UTR; 3 – mock co-IP of WT mCaMKIIα 3'UTR with EGFP-FLAG fusion protein; 4, 5, and 6 – respective inputs of 1, 2, and 3; 7 – n.c. (untransfected cell lysate). (**A** and **B**) All bands represent RT-PCR for luciferase. SYBR Green sqRT-PCR quantitation of the corresponding immunoprecipitates was shown (data was normalized to the input control levels). (**C**) Binding of CPEB-3 to mouse CaMKIIα shown by co-IPs: TaqMan quantification of mCaMKIIα 3'UTR co-IP with CPEB-3 protein. Data represent normalized mRNA retention, with GAPDH (control) 3'UTR retention set to 1. (**D**) Schematic of wild-type and mutated mCaMKIIα 3'UTR fragments used in A, B and C.

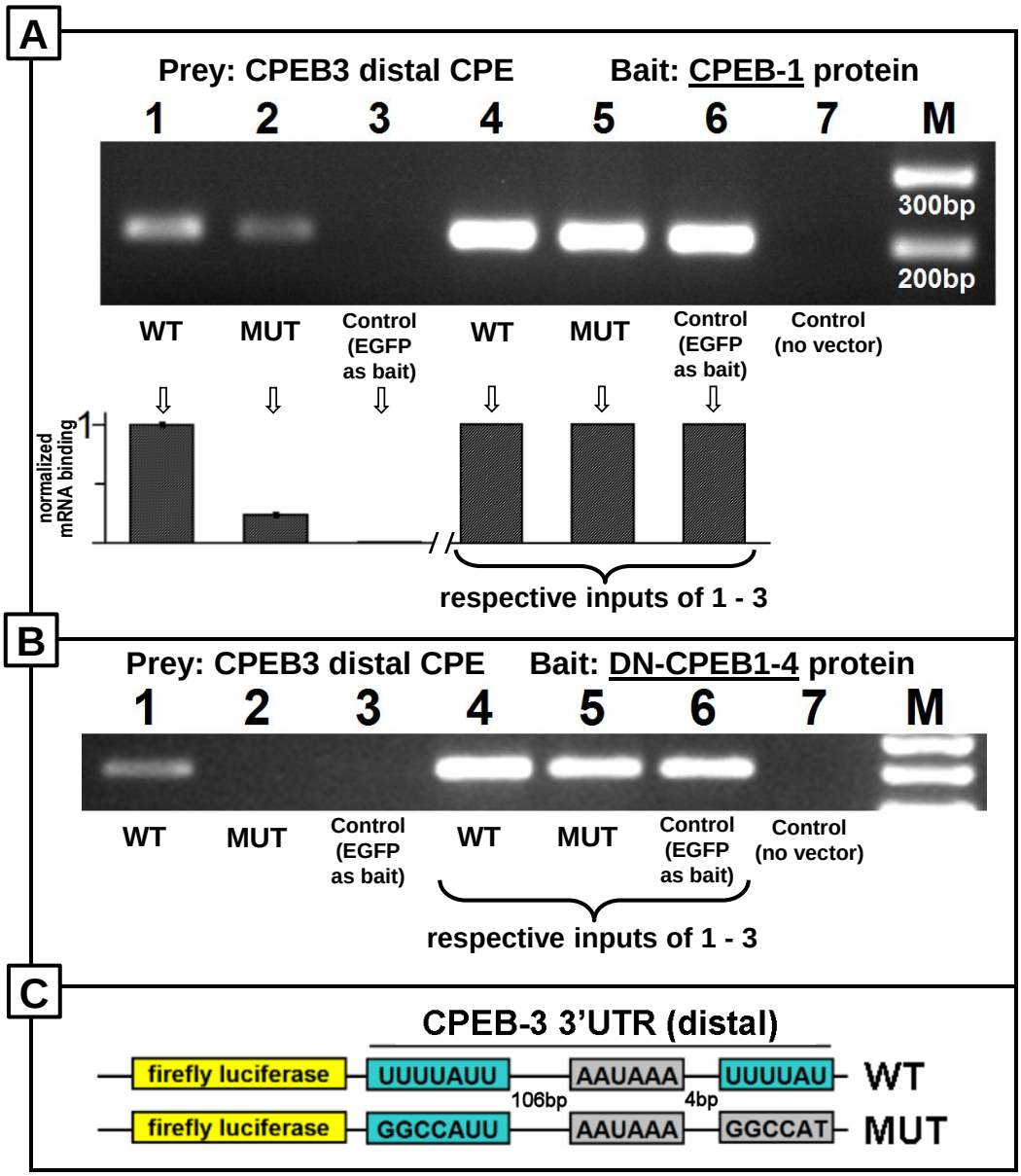

Fig. 4-6: CPEB-1 (**A**) and DN-CPEB1-4 (**B**), bind specifically to the CPEB3 3'UTR (fragment containing 2 canonical CPEs, distal to coding region). (**A**, **B**): Line 1 – co-IP of WT 3'UTR; 2 – co-IP of MUT 3'UTR (lacking CPEs); 3 – mock co-IP of WT 3'UTR with EGFP-FLAG fusion protein; 4, 5 and 6 – respective inputs of 1, 2 and 3; 7 – n.c. (untransfected cell lysate). All bands represent RT-PCR for luciferase. (**A**) SYBR Green sqRT-PCR quantitation of the corresponding immunoprecipitates was shown (data was normalized to the input control levels). (**C**) Schematic of wild-type and mutated fragments of CPEB3 3'UTR (distal) used in A and B.

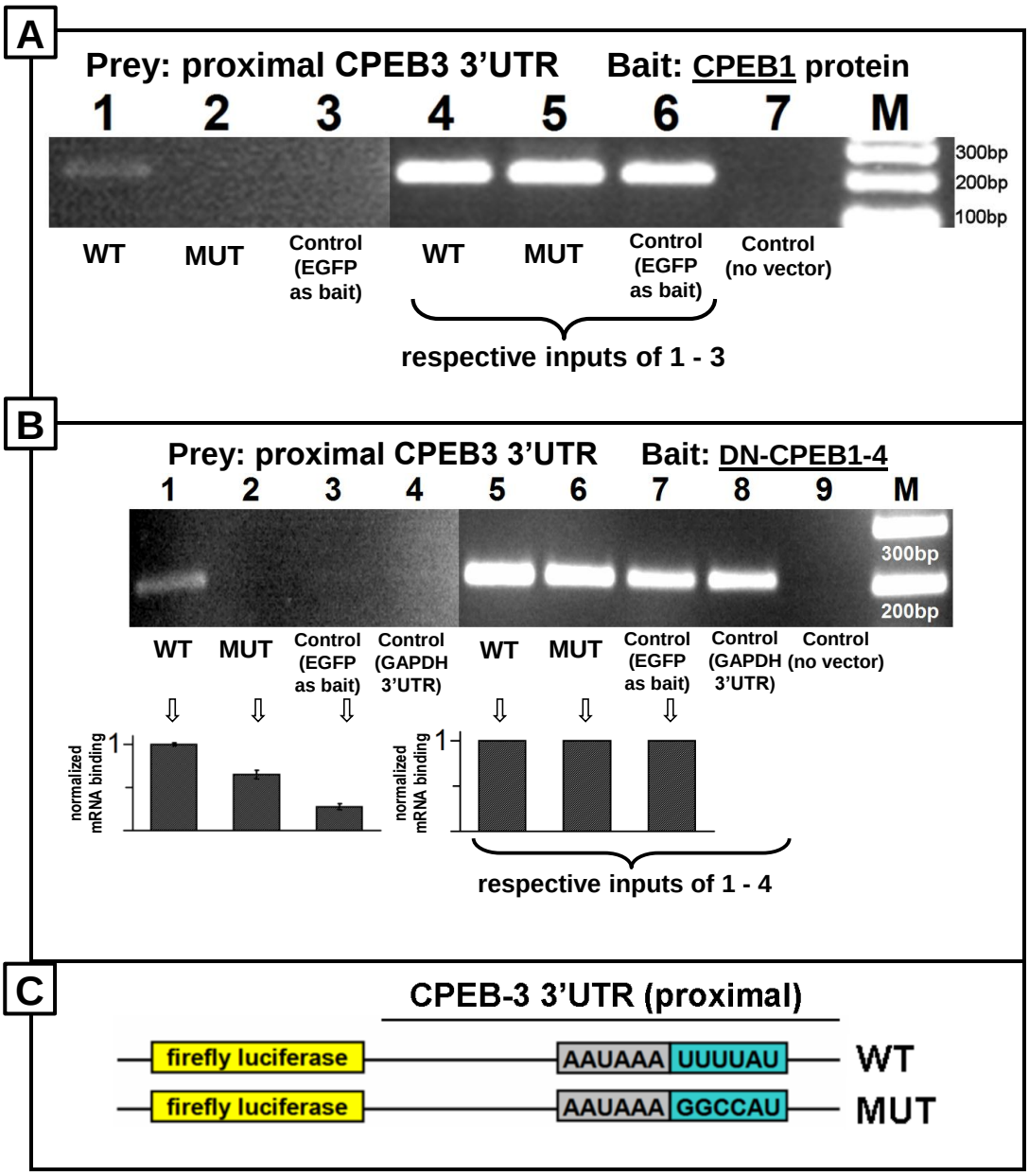

Fig. 4-7: **CPEB1 (A) and DN-CPEB1-4 (B) bind specifically to the CPEB3 3'UTR (fragment containing one canonical CPE element, proximal to coding region).** (**A**) Binding of CPEB1 to the proximal 3'UTR of CPEB3 shown by co-IP: line 1 – co-IP of WT 3'UTR; 2 – co-IP of MUT 3'UTR (lacking CPE); 3 – mock co-IP of WT 3'UTR with EGFP-FLAG fusion protein; 4, 5 and 6 – respective inputs of 1, 2 and 3; 7 – n.c. (untransfected cell lysate). All bands represent RT-PCR for luciferase. (**B**) Binding of DN-CPEB1-4 to the proximal 3'UTR of CPEB3 shown by co-IP: line 1 – co-IP of WT 3'UTR; 2 – co-IP of MUT 3'UTR (lacking CPE); 3 – mock co-IP of WT 3'UTR with EGFP-FLAG fusion protein; 4 - co-IP of GAPDH 3'UTR construct (not-containing CPEs); 5, 6, 7 and 8 – respective inputs of 1, 2, 3, and 4; 9 – n.c. (untransfected cell lysate); SYBR Green-based sqRT-PCR quantitation of the corresponding immunoprecipitates was shown (data was normalized to the input control levels). (**C**) Schematic of wild-type and mutated fragments of CPEB3 3'UTR (proximal) used in A, B and C.

4.2 Translational regulation of the GluR2 AMPA receptor subunit by the CPEB-3 protein

In cultured primary hippocampal neurons, siRNA-mediated knock-down of CPEB-3 protein led to upregulation of the GluR2 AMPA-R subunit (Huang *et al.*, 2006). The GluR2 protein plays a key role in modulating AMPA-R properties (Isaac *et al.*, 2007), and thereby contributes to the multifunctional role of the AMPA-Rs in the CNS (Kessels and Malinow, 2009), (Derkach *et al.*, 2007). As already mentioned, mice overexpressing DN-CPEB1-4 display deficits in activity-induced translation, late-phase LTP and spatial memory formation (Theis *et al.*, in revision). We wanted to explore the hypothesis that CPEB-3, via translational regulation of the GluR2 subunit, accounts for the electrophysiological and behavioral phenomena observed in DN-CPEB1-4 mice. To this end, we took advantage of the tet-off system (see section 1.8.3) to overexpress CPEB-3-EGFP fusion protein in principal neurons. We used the CaMKIIα-tTA driver (Mayford *et al.*, 1996) and the tetO-CPEB3-EGFP overexpressor (tetO-CPEB3-EGFP construct generation and immunohistochemical screening of founder animals was done by Vamshidhar Vangoor). We cross-bred the CaMKIIα-tTA and the CPEB3-EGFP-tetO transgenic mice, to obtain the CaMKIIα-tTA/CPEB-3EGFP-tetO double transgenic (DT) progeny and littermate controls. The mice were sacrificed at the postnatal age of 3 months and the hippocampus, cortex and cerebellum were surgically dissected and analyzed by immunoblotting. Expression of the CPEB3-EGFP transgene was clearly detectable, as shown by immunoblots (Fig. 4-8A) of selected brain areas of DT mice. Expression in the cerebellum was much weaker compared to the cortex and the hippocampus, which was in line with the reported spatial pattern of CaMKIIα-promoter activity (Odeh *et al.*, 2011). We then assessed the GluR2 protein levels in the hippocampus and observed a decrease of expression to 48.5 ± 9.2%, compared to single transgenic (tTA+/tetO-) littermate controls (DT: n=4, control: n = 4) (Fig. 4-8B,C). This observation was in line with the previous findings (Huang *et al.*, 2006). Nevertheless, the experiments by Huang *et al*. (2003) were performed in cell culture. Here, using the *in vivo* paradigm of a transgenic mouse, we further demonstrated the relevance of CPEB-3 for the GluR2 expression, a protein critical for neuronal function.

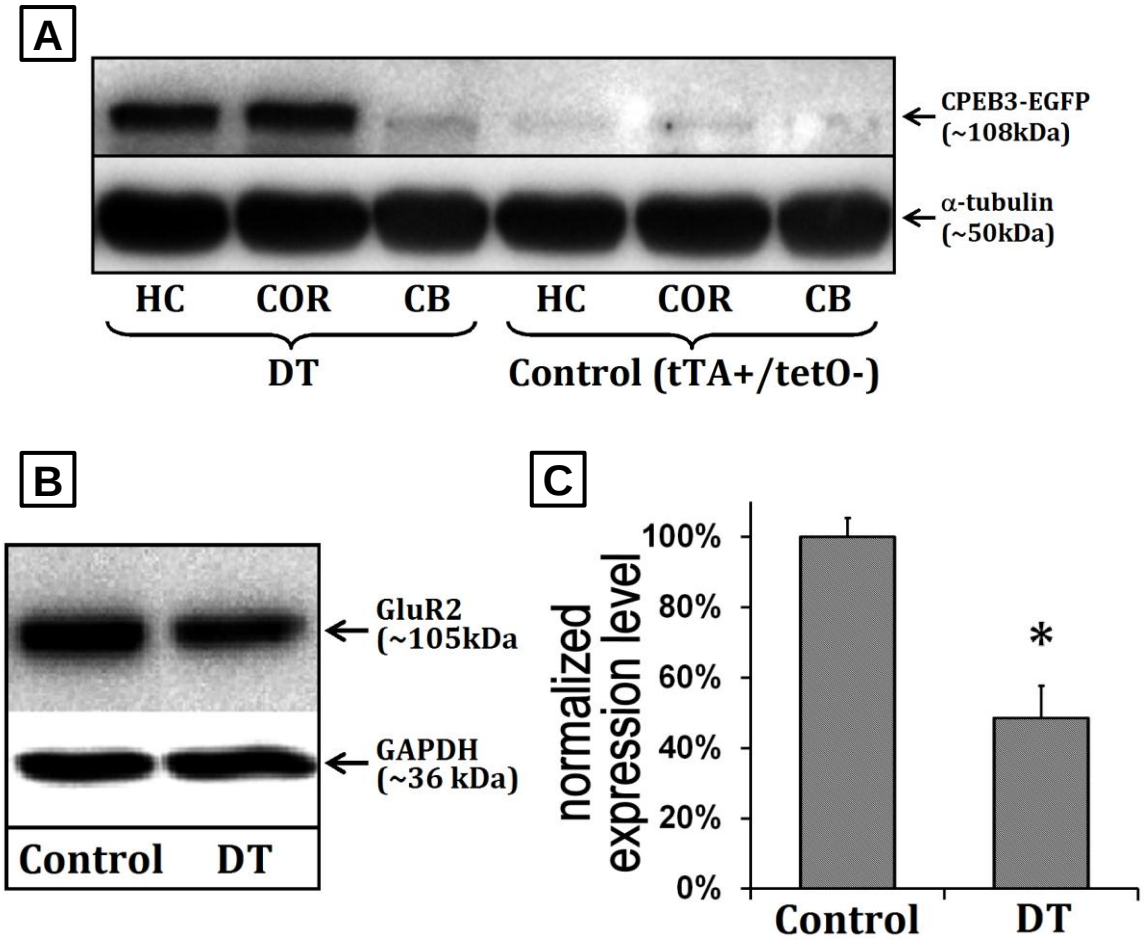

Fig. 4-8: Neuron-specific overexpression of the CPEB-3 protein suppresses translation of the GluR2 AMPA-R subunit. (**A**) Representative immunoblot of selected brain subregions (HC-hippocampus, COR-cortex, CB-cerebellum) showing overexpression of the CPEB3-EGFP transgene exclusively in double transgenic (DT) animals (CaMKIIα-tTA/tetO-CPEB3-EGFP). No expression was observed in the cerebellum, as expected from the spatial distribution of the CaMKIIα-promoter activity, and in single transgenic controls. For each sample, α-tubulin was used as an internal control. (**B**) Representative immunoblot showing downregulation of the GluR2 protein in the hippocampus of the CPEB3-EGFP overexpressing mice (DT: tTA+/tetO+; control: tTA+/tetO-). GAPDH was used as an internal control for normalizing expression levels. (**C**) Densitometric analysis of the representative immunoblot shown in A. DT mice show hippocampal GluR2 levels decreased to 48.5 ± 9.2% of the littermate controls. DT: n=4, control: n = 4. (*) P<0.01 (student's t-test).

4.3 CPEB-3 is phosphorylated by PKA and CaMKII

4.3.1 In vitro peptide phosphorylation assays

A set of 43 amino acids-long peptides was synthesized to test if the putative phosphorylation site (serine residues S419 and S420) in CPEBs 2-4 (Theis *et al.*, 2003b) undergoes phosphorylation. The peptides included wild-type CPEB-3a and CPEB-3b isoforms (respectively, containing and lacking phosphorylation consensus motif), as well as the serine-to-alanine mutants of CPEB-3a isoform peptide. An overview of the peptides used for experiments in this section is presented on Fig. 4-9.

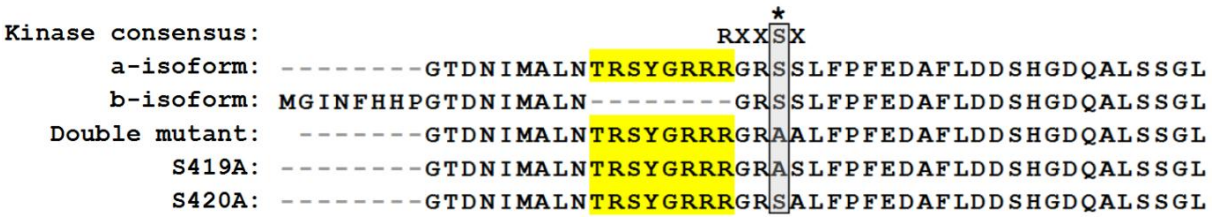

Fig. 4-9: Aligned sequences of the synthetic peptides used in *in vitro* phosphorylation experiments. Alternatively spliced exon (termed a-domain) was highlighted in yellow. Putative phosphorylation site was marked with an asterisk.

For qualitative determination of phosphorylation, the a-isoform and the corresponding S419A/S420A double mutant were phosphorylated in the *in vitro* reaction, and then analyzed by MALDI-TOF-MS. Both, CaMKII, and PKA phosphorylated CPEB-3-derived peptides. PKA activity led to a mass shift of the a-isoform peptide peak, as would be expected by addition of one (80Da) or two (160Da) phosphate (P_i) groups (Fig. 4-10A). This may suggest that during the *in vitro* reaction, both serine residues (S419 and S420) are being phosphorylated by the enzyme. No shift was observed in case of the S419A/S420A double mutant peptide (Fig. 4-10B). For CaMKII phosphorylation, a mass shift was observed in case of the a-isoform peptide, and was equal to the molecular weight of one P_i group (Fig. 4-11A). No shift was observed in case of the S419A/S420A double mutant (Fig. 4-11B).

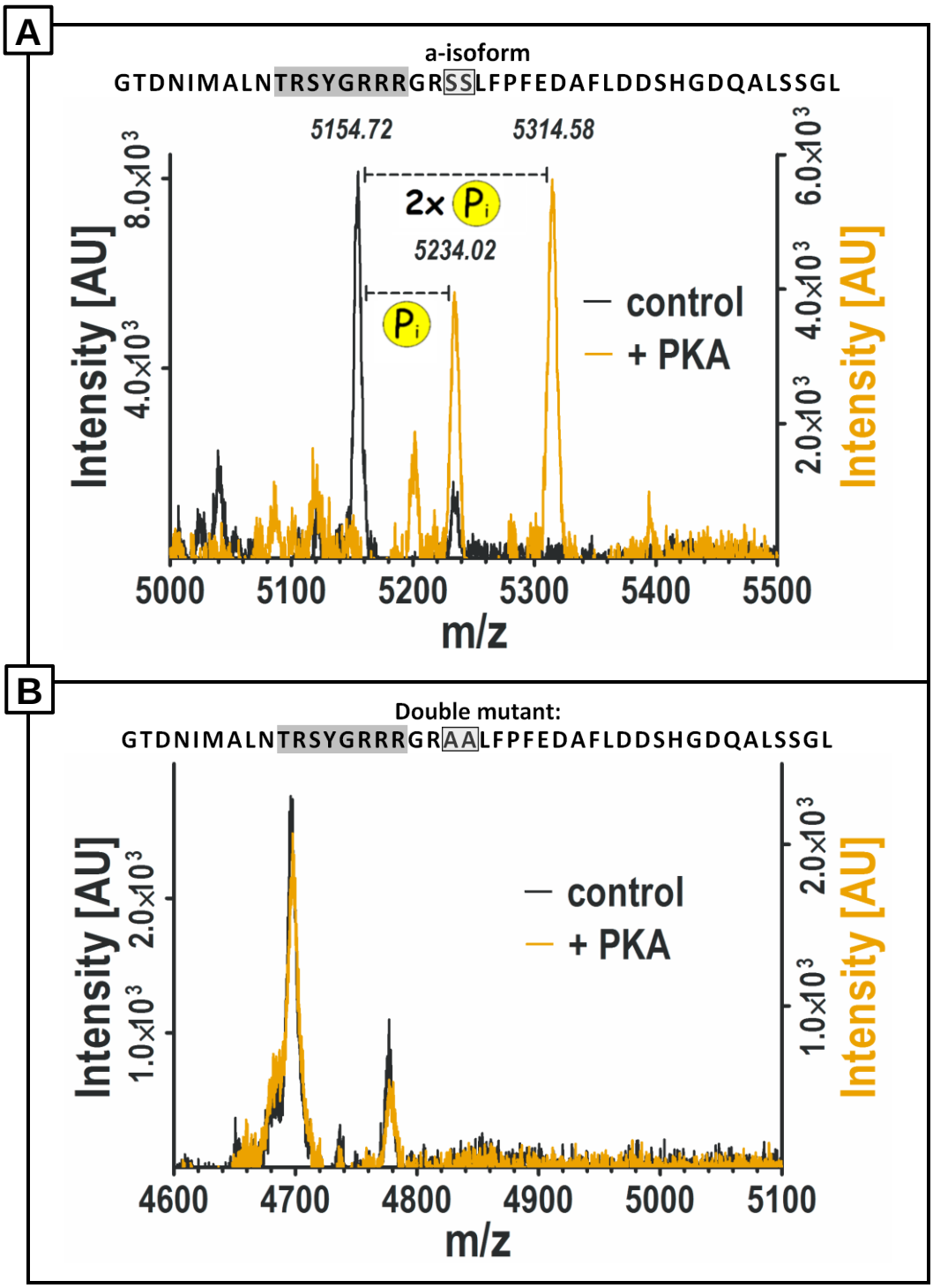

Fig. 4-10: MALDI-TOF-MS spectra of CPEB-3-derived peptides phosphorylated by PKA-C_{α}. (**A**) a-isoform peptide spectrum: the peak shift corresponds to incorporation of 1 or 2 phosphates. (**B**) S419A/S420A double mutant peptide spectrum: no shift was observed after phosphorylation. (**A**, **B**) orange trace – spectrum after phosphorylation; black trace – no-kinase control spectrum; m/z – mass to charge ratio.

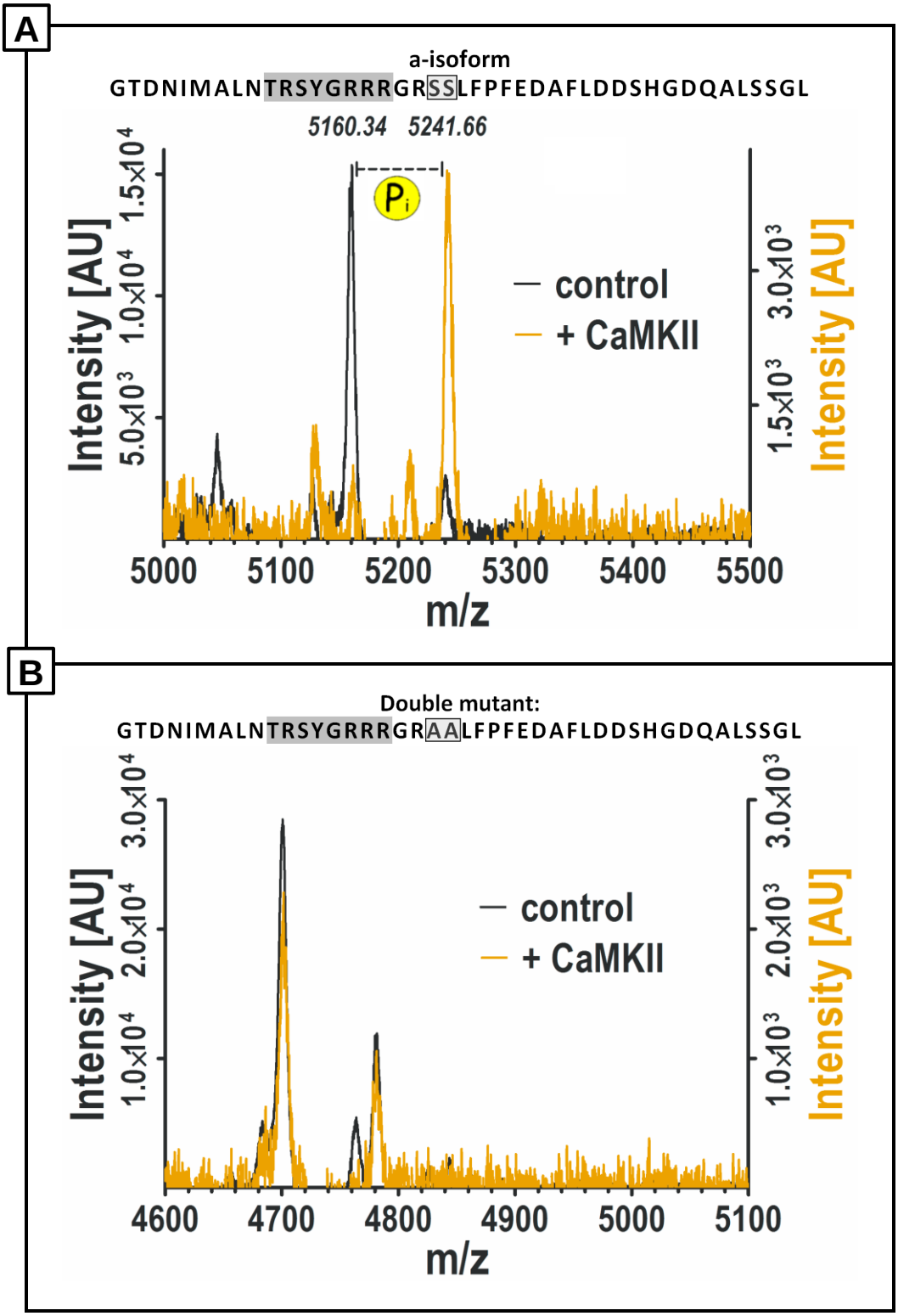

Fig. 4-11: MALDI-TOF-MS spectra of CPEB-3-derived peptides phosphorylated by CaMKII. (**A**) a-isoform peptide spectrum: peak shift corresponding to incorporation of 1 phosphate was observed. (**B**) S419A/S420A double mutant peptide spectrum: no shift was observed after phosphorylation. (**A**, **B**) orange trace – spectrum after phosphorylation; black trace – no-kinase control spectrum; m/z – mass to charge ratio.

To confirm the MALDI-TOF results, and to quantitatively compare the propensity of different peptide variants to phosphorylation, the PKLight assay (Lonza) was used for PKA reactions and the ADP-Glo assay (Promega) was used for CaMKII reactions. In addition to the peptides used for MALDI-TOF, the serine-to-alanine single mutants (S419A and S420A) and the b-isoform peptide were included in the analysis. This allowed determining, respectively, which of the two critical serine residues was phosphorylated preferentially, and if the alternative splicing affects the CPEB3 protein propensity for phosphorylation. The a-isoform, and the S419A, and S420A mutant peptides were phosphorylated by PKA-C_α kinase at a significantly higher rate compared to the S419A/S420A double mutant (Fig. 4-12). The observed phosphorylation in case of the b-isoform was not significantly different. PKA preferentially phosphorylated serine 420, as shown by the decreased phosphorylation rate in case of the S420A mutant peptide compared with the S419A substitution ($p<0.01$). Importantly, no significant differences were observed between no-kinase and no-substrate control, to which the data was normalized. Quantitative results of the PKA phosphorylation are summarized in Fig. 4-12. Note that due to the nature of the PKLight assay (in which post-reaction ATP levels are a read-out) the measured signal is inversely proportional to the phosphorylation rate.

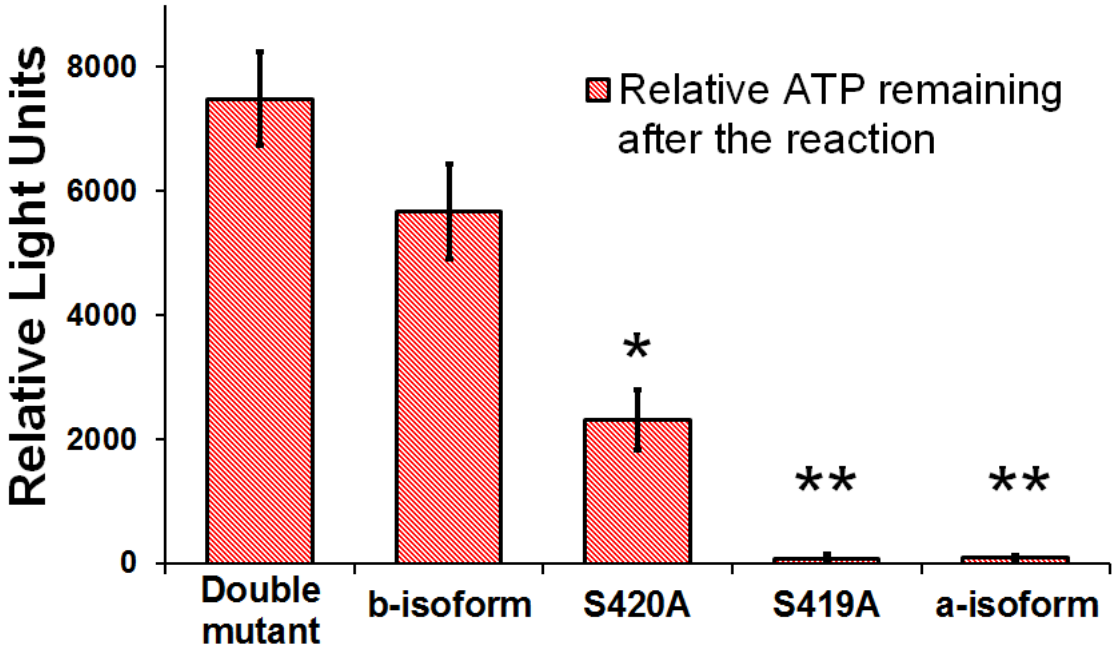

Fig. 4-12: Quantitation of peptides phosphorylation by PKA-C_α (PKLight assay). The a-isoform, S419A, and S420A mutant peptides were phosphorylated at a significantly higher rate compared to the S419A/S420A double mutant, while the b-isoform phosphorylation was not significantly different from the double mutant. Serine 420 is phosphorylated preferentially, as shown by decreased phosphorylation rate in case of S420A mutant peptide compared with S419A substitution ($p<0.01$). Values were normalized to no-substrate control levels (not shown on the graph). Values show relative levels of unused ATP after the phosphorylation reaction. Error bars are SEM. *P<0.005, **P<0.001 (student's t-test).

For CaMKII, the a-isoform mutant peptide was phosphorylated at a significantly higher rate than the S419A/S420A double mutant peptide and the b-isoform (p-values <0.001 and <0.01, respectively) (Fig. 5-13A). Serine 420 was phosphorylated preferentially, as shown by the decreased phosphorylation rate in case of the S420A mutant peptide compared with the S419A substitution (p-value <0.05) (Fig. 5-13B). Note that in case of CaMKII reactions, a different type of phosphorylation assay was used. This was necessary, as the CaMKII kinase required pre-activation (by phosphorylation) in the presence of excessive ATP levels. Such excessive ATP could interfere with the PKLight assay. Instead, an ADP-Glo assay was used, where the ADP (and not ATP) post-reaction level is the read-out parameter. In this case, the magnitude of the signal is directly proportional to the phosphorylation rate.

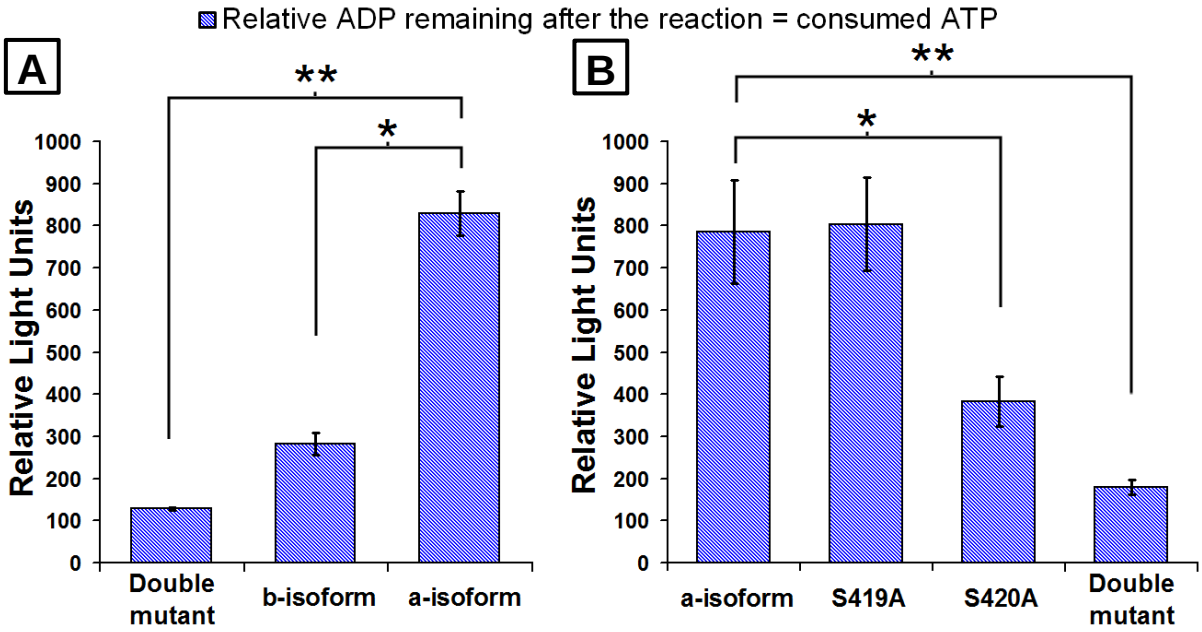

Fig. 4-13: Quantitation of peptide phosphorylation by CaMKII (ADP-Glo assay). (**A**) a-isoform is phosphorylated at significantly higher rate compared with b-isoform and S419A/S420A double mutant. (**B**) Serine 420 is phosphorylated preferentially, as shown by decreased phosphorylation rate in case of S420A mutant peptide. (**A**,**B**) Values show relative ADP levels after the phosphorylation reaction, normalized to no-substrate control levels (not shown on the graphs). Error bars are SEM. *P<0.01, **P<0.001, ***P<0.05 (student's t-test).

4.3.2 Generation of phosphospecific antibodies directed to CPEB-3a/c

A phosphospecific CPEB-3a/c antibody directed to serine residues S419 and S420 (pCPEB3-S419-S420) was generated by Eurogentec (Germany), as described in section 3.11. The performance of the antibody was tested by immunoblotting. Both, the phosphospecific fraction (column flow-through obtained after the second purification step against non-phosphorylated peptide), and the non-phosphospecific fraction (corresponding eluate) were tested. As a test antigen, the PKA-phosphorylated a-isoform peptide (see Fig. 4-9) was used. The phosphospecific antibody detected the phosphorylated form of the peptide, but showed no reactivity against the non-phosphorylated control peptide (Fig. 4-14).

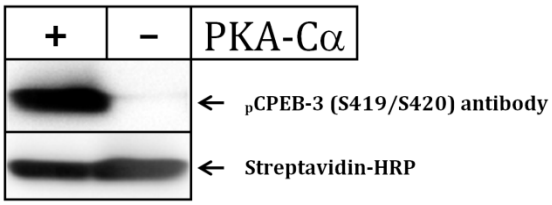

Fig. 4-14: Immunoblot test of the pCPEB3 S419/S420 polyclonal antibody raised against a synthetic phosphopeptide derived from the region flanking Ser419 in the CPEB-3a/c. A PKA *in vitro*-phosphorylated a-isoform peptide was used as a test antigen. Streptavidin-HRP, detecting biotynylated peptides, was used to control for equal loading.

4.3.3 Phosphorylation of CPEB-3a by PKA in cultured cells.

HEK-293 cells transiently overexpressing CPEB3a-EGFP fusion protein were subjected to a forskolin stimulation paradigm (50 μM for 1 h), following immunoblot assessment of CPEB3a-EGFP phosphorylation (Fig. 5-15A). Forskolin-treated cells showed a signal increment amounting to 654 ± 80% of untreated control levels (Fig. 4-15B).

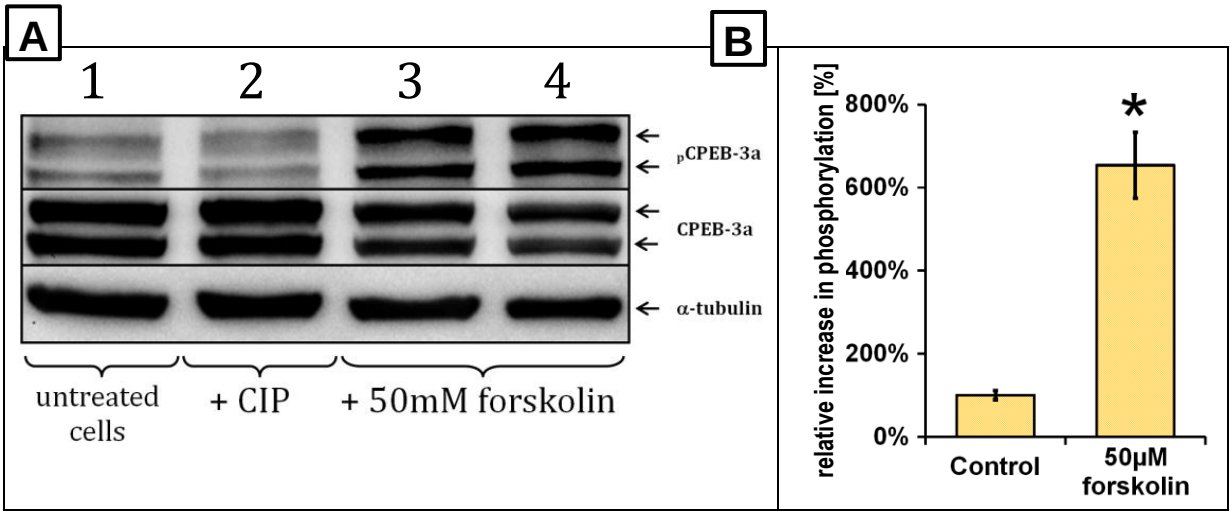

Fig. 4-15: CPEB-3a phosphorylation in cultured cells. HEK-293 cell line was transiently transfected with the CPEB-3a protein and (24 h post transfection) treated with 50μM forskolin (adenylate cyclase activator) for 1 h. (**A**) A representative immunoblot showing increased phosphorylation state of CPEB-3a protein after forskolin stimulation. Lysate in lane 2 was additionally treated with calf intestine phosphatase (CIP) and showed a modest decrease of signal as compared with the control lysate (lane 1). (**B**) Cumulative densitometric analysis of the immunoblots of the forskolin-treated (n=5) and control (n=4) HEK-293 cells. Values were normalized to mean control level, which was set to 100%. After stimulation relative phosphorylation increased to 654 ± 80% of control. α-tubulin and β-actin (not shown) were used to normalize for the total protein content. Error bars are SEM. *P<0.01 (student's t-test).

4.4 Microglial CPEBs and their splice isoforms

4.4.1 Microglial cell lines are positive for CPEBs 1-4

To confirm expression of CPEB1-4 genes in microglial cell lines, ESdM and BV-2 cells, RT-PCR analysis, followed by immunoblot immunocytochemical staining were performed. On the transcript level, the cells were tested for the presence of CPEB1-4 mRNA. The primers used for the analysis flanked the alternatively spliced region (in each of the CPEBs, resulting in multiple RT-PCR bands in case more than one isoform was present (Fig. 4-16A). All four CPEBs were detected. Mouse Whole Brain Marathon Ready cDNA (Clontech) was used as a reference sample. In case of CPEB2-4, the obtained splice isoform band pattern was different in the cell lines, as compared to the reference (whole brain cDNA). This may suggest, that (some) isoforms are specific for microglial cells, or at least point on quantitative differences in isoform distribution between the cell types. In addition, the presence of CPEB2-4 proteins in ESdM and BV-2 cells was confirmed by immunoblot (Fig. 4-16B). CPEB1 was not detected probably due to insufficient affinity of the antibody used.

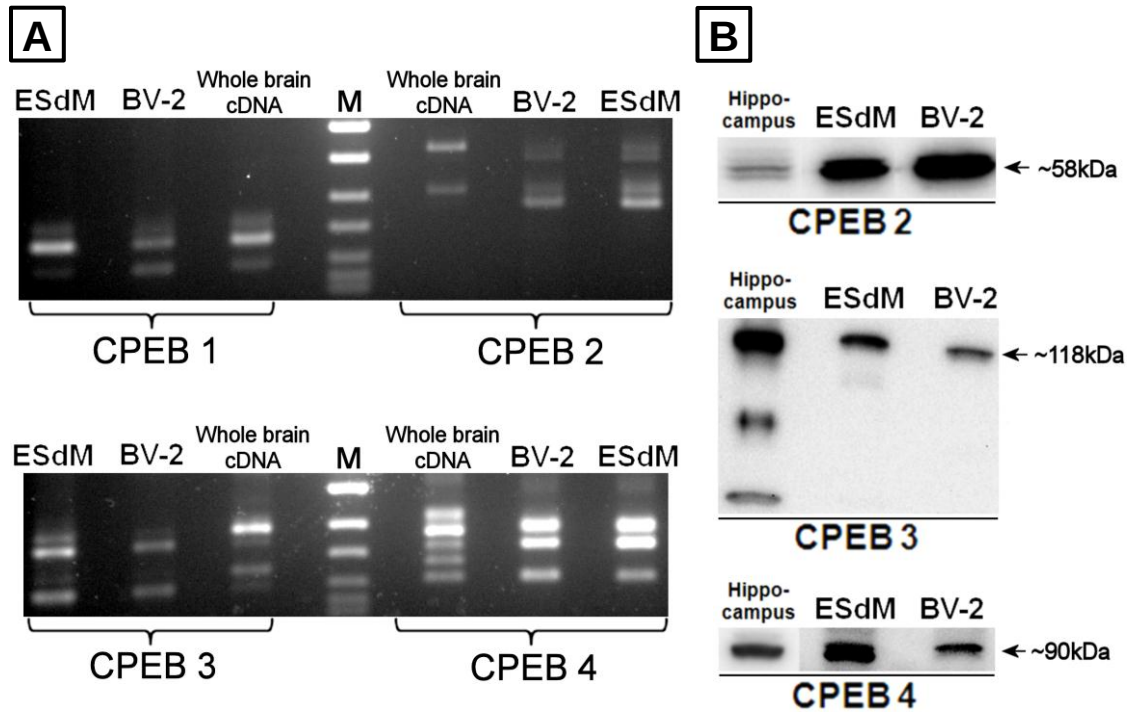

Fig. 4-16: **CPEB expression in microglial cell lines and mouse hippocampus.** (**A**) RT-PCR of BV-2 immortalized microglial cells and ES-cell derived microglia (ESdM) reveals expression of all 4 CPEB1-4 transcripts in both analyzed cell types (n=2 experiments). Multiple bands observed correspond to different splice isoforms. β-actin was used as a positive control (not shown). (**B**) Immunoblot analysis of the abovementioned cell lines. CPEB-2-4 proteins were detected in both cell lines. CPEB-1 was not detectable, possibly due to insufficient specificity of the anti-CPEB-1 antibody used (not shown).

Immuno**c**yto**c**hemical (ICC) staining of BV-2 cells showed immunoreactivity to CPEB1-4 antibodies, confirming the RT-PCR and immunoblot results (Fig. 4-17). Immunoreactivity to CPEB-1 antiserum was lower, as compared with the CPEB2-4 antibodies. This may suggest that the affinity of the CPEB-1 antibody used is lower (as compared to CPEBs -2 to -4) and explain its suboptimal performance in the immunoblot analysis.

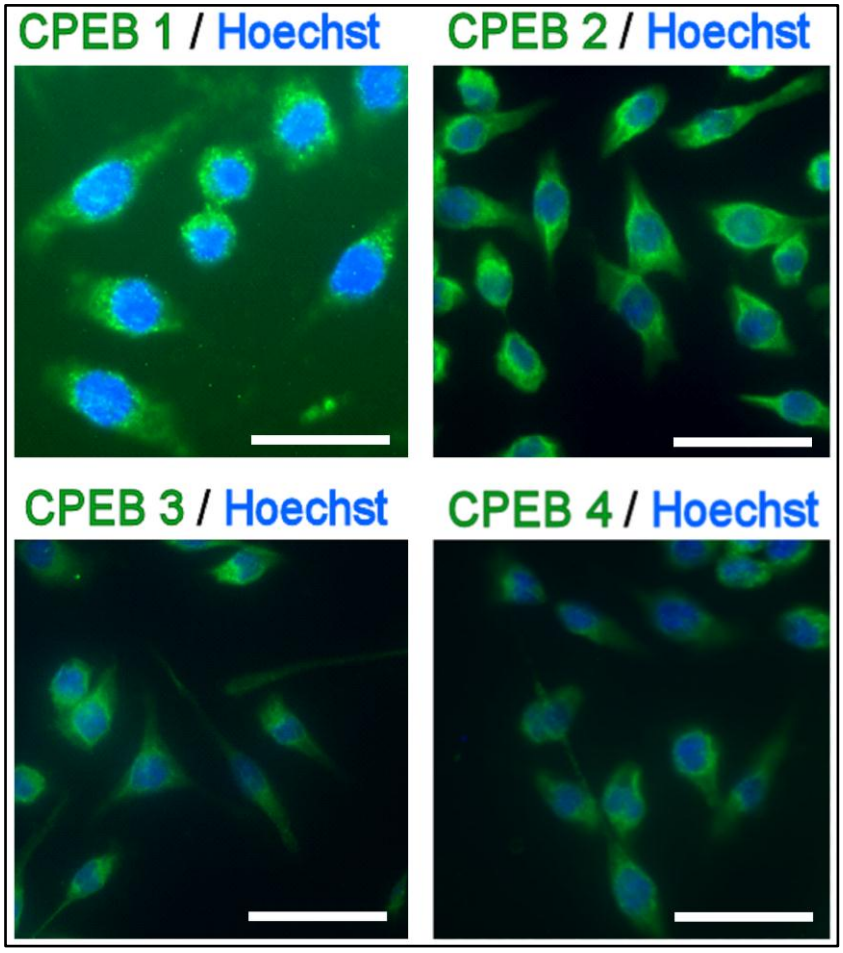

Fig. 4-17: Immunofluorescent antibody staining of BV2-immortalized microglia for CPEB1-4. Cells showed immunoreactivity to antibodies against all four CPEB proteins. Scale bar: 50µm.

To detect and quantify the distribution of CPEBs 1-4 in mouse primary microglia, astrocytes and NG2 cells, enzymatically dissociated mouse brains were subjected to FACS cell sorting. To facilitate identification of microglial cells, transgenic mice expressing GFP in the fraktalkine receptor (CX_3CR1) locus were used (Jung *et al.*, 2000). Mice were sacrificed at postnatal day 5. Brains were removed and enzymatically dissociated using the trypsin-based Neural Tissue Dissociation Kit (Miltenyi Biotec). To minimize contamination with blood monocytes (positive for the CX_3CR1 receptor as well), meninges were removed prior to the procedure. In case of primary microglia, detection specificity was validated by FACS, using allophycocyanin (APC)-coupled anti-CD11b antibody (Fig. 4-18).

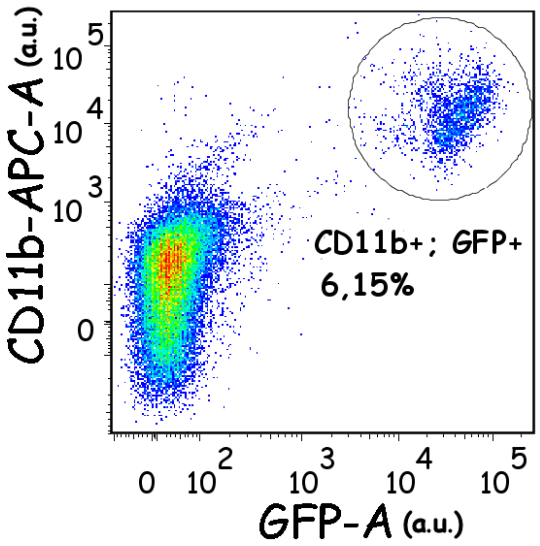

Fig. 4-18: Fluorescent-activated cell sorting (FACS) analysis of microglia from $CX_3CR1^{GFP/+}$ knock-in transgenic mice (Jung *et al.*, 2000). GFP versus allophycocyanin (APC) dot-plot showing dissociated brain cells of $CX_3CR1^{GFP/+}$ knock-in transgenic mice stained with APC-coupled anti CD11b-antibody. APC – **a**llo**p**hyco**c**yianin (labelling of CD11b positive cells with APC-coupled monoclonal anti-CD11b antibody).

After isolation of RNA from the sorted population, sqRT-PCR was performed, using Taq-Man primers/probes for CPEBs 1-4. All four CPEBs were detected in FACS-sorted primary microglia. Results are presented in Fig. 4-19.

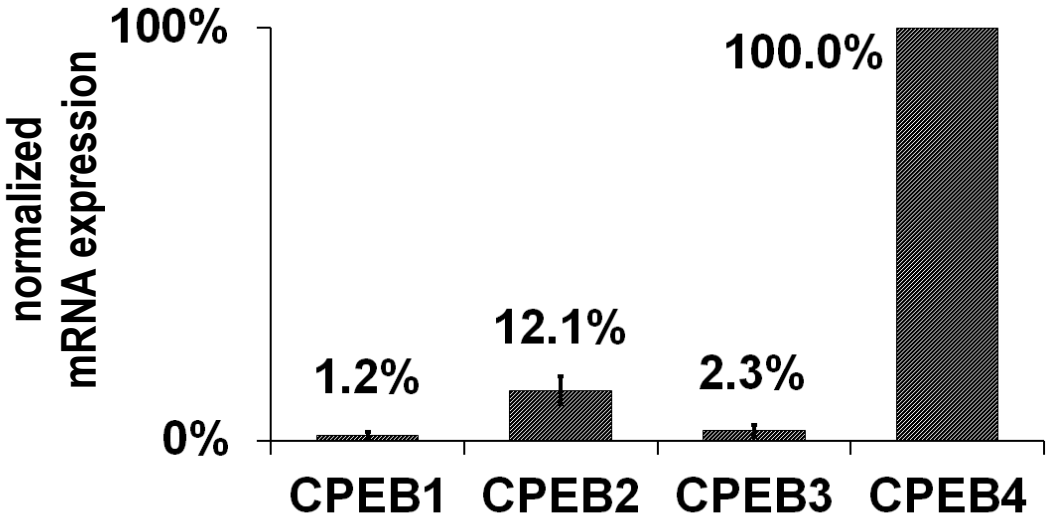

Fig. 4-19: sqRT-PCR analysis of relative expression of CPEBs -1 to -4 in FACS-sorted primary microglia. Total RNA was extracted from FACS-sorted microglial cells from mouse brain (postnatal day 5) and the relative expression of CPEBs -1 to -4 was analyzed using Taq-Man-based sqRT-PCR system. Highest level (CPEB4) was set to 100%. Error bars are SEM; n=4.

4.4.3 CPEB-3 isoforms containing the B-region were not detected in ESdM cells

RT-PCR analysis of the CPEB-3 transcripts in Embryonic Stem Cells-derived Microglia, followed by sequencing of the obtained PCR products revealed expression of the b/d isoforms, but not the a/c isoforms. Note that the b-region, present in the a/c isoforms contains the putative phosphorylation consensus site. This region corresponds to exon 5 in the CPEB-3 gene (accession no. NM_198300). Modulation of the rate of exon 5 skipping during alternative splicing would affect the propensity of the cellular pool of CPEB-3 for phosphorylation (and activation). Lack of the a/c isoforms may be a cell culture-specific phenomenon. It is possible that skipping of exon 5 is a default alternative splicing setting for CPEB-3 in resting conditions, and the specific stimulation leads to inclusion of this exon. Therefore cultured cells, lacking the physiological signalling partners, might preferentially skip it (see also section 5.2).

4.4.4 tPA mRNA is a CPEB target

Sequence analysis of the tPA 3'UTR revealed the presence of CPE element(s) in the vicinity of the polyadenylation signal. tPA was previously described as a CPEB-1 target (Shin *et al.*, 2004). Before testing new CPEB targets, I decided to confirm the interaction between CPEB-1 protein and tPA 3'UTR by co-IP. A terminal 215bp fragment of tPA 3'UTR was used as bait (Fig. 4-20B). CPEB-1 co-immunoprecipitated the tPA 3'UTR WT fragment with significantly higher affinity than it did in case of the corresponding mutated 3'UTR, control bait protein (FLAG-EGFP), or control prey mRNA (GAPDH 3'UTR, not-containing CPE elements) (Fig. 4-20A).

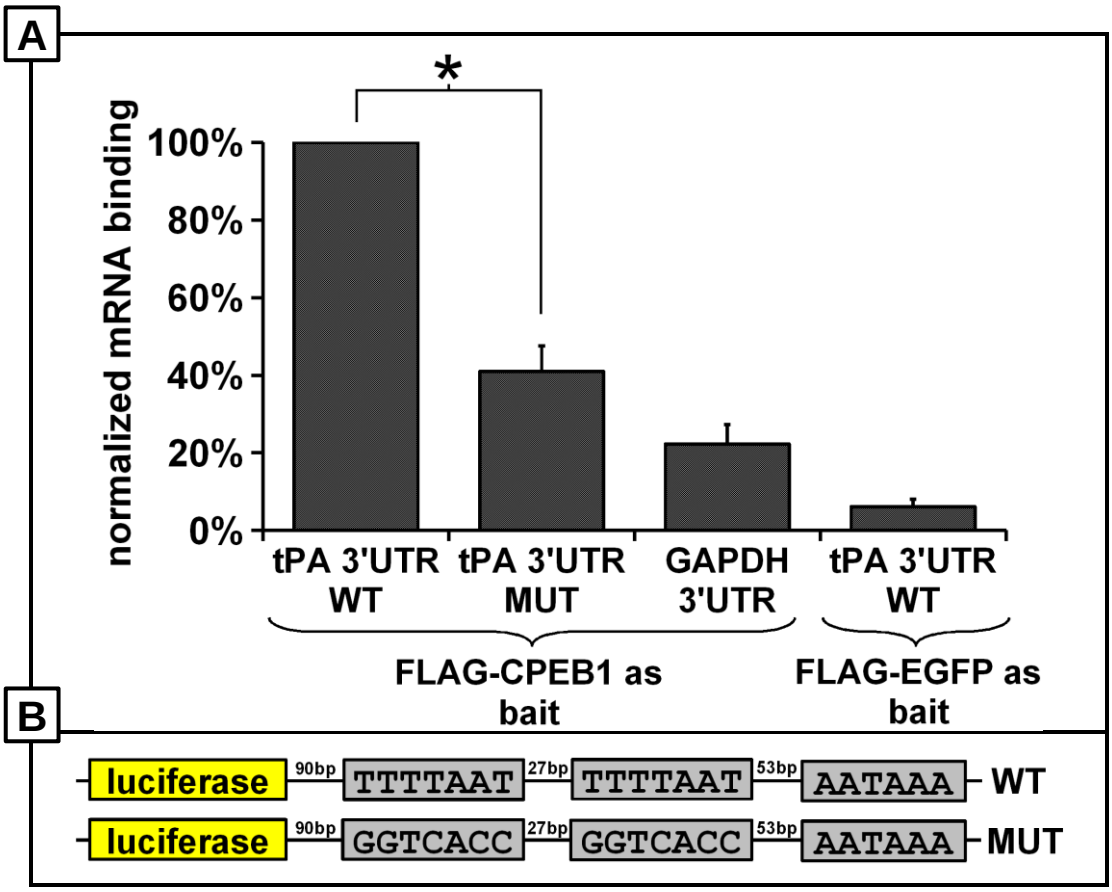

Fig. 4-20: The CPEB-1 protein interacts with the tPA 3'UTR. (**A**) Co-IP of overexpressed 3'UTR derived from tPA luciferase reporter mRNA appended with wild-type (WT) or mutated (MUT) 3'UTR (TaqMan-based sqRT-PCR quantification using luciferase-gene specific oligonucleotides). FLAG-CPEB1 or FLAG-EGFP (control) fusion proteins were used as baits. (**B**) Schematic of wild-type and mutated 3'UTR constructs used in A. * P<0.05 (student's t-test).

4.5 Luciferase Reporter Assays to study CPEB-mediated translational regulation

The luciferase reporter assay was done to demonstrate the functional relevance of the CPEs in the tPA 3'UTR. Experiments were performed on HeLa cells transfected with the *in vitro*-transcribed mRNA encoding the luciferase reporter construct. The constructs used contained the luciferase reporter Open Reading Frame (ORF) appended with the tPA 3'UTR in its wild-type form (WT) and with mutated CPEs (MUT). The *in vitro* transcription was driven by T7 polymerase, using the Message Machine T7 Ultra kit (Ambion) (see section 3.22). The schematic of the construct is depicted in Fig. 5-21.

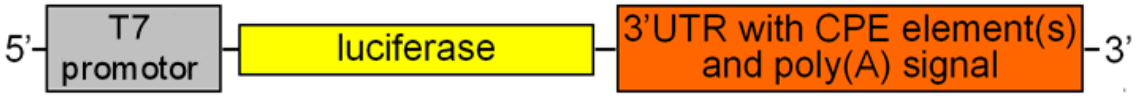

Fig. 4-21: **Schematic of the tPA 3'UTR luciferase reporter constructs used in the luciferase reporter experiments.** The T7 promoter drives expression of the luciferase reporter. The reporter coding sequence is appended with the tPA 3'UTR containing wild type or mutated CPEs, thereby allowing to assess their impact on gene expression.

The mRNA transfection was chosen to exclude the impact of the modifications of the 3'UTR on nuclear polyadenylation, which would lead to changes in reporter expression unrelated to the CPEB-mediated cytoplasmic polyadenylation. Prior to transfection of the HeLa cells, the mRNA integrity was assessed by the Agilent 2100 Bioanalyzer, according to manufacturer's protocol. The result of the analysis is shown in Fig. 4-22.

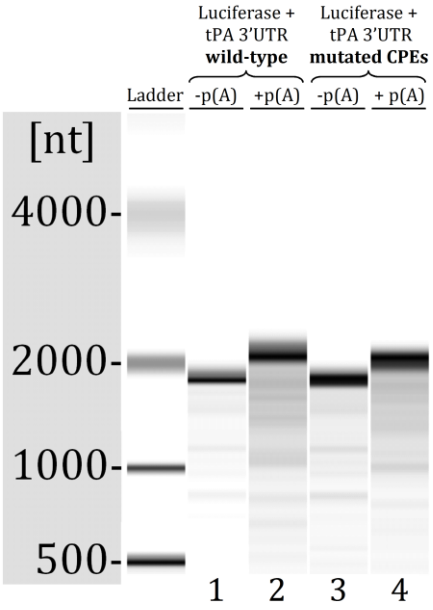

Fig. 4-22: ***In vitro*-transcribed mRNA integrity assessment by the Agilent 2100 Bioanalyzer.** The quality of the wild type and mutated fragments was comparable (lane 1: wild-type, lane 3: mutated). The in vitro polyadenylation efficacy was demonstrated by the significant shift in fragment size (lanes 1 and 3: before polyadenylation, lanes 2 and 4: after polyadenylation).

Normalized luciferase reporter activity in case of the wild-type construct amounted to 44% of the construct with mutated CPEs (Fig. 4-23). This shows, that in the presented experimental paradigm, the presence of CPEs leads to translational inhibition, probably mediated by the CPEB proteins endogenously present in HeLa cells (RT-PCR data, not shown).

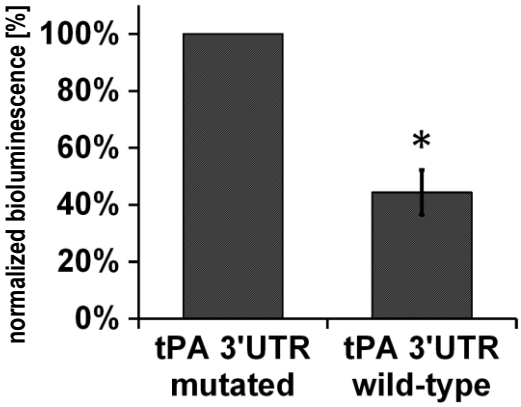

Fig. 4-23: **Repression of luciferase reporter tPA 3'UTR construct expression by CPEBs.** Results of the reporter assay shows that the luciferase with the wild-type CPEs shows normalized activity amounting to 44% of the mutated counterpart (with mutated CPEs). The effect is probably due to the expression of endogenous CPEBs in HeLa cells (RT-PCR data, not shown). Error bars represent SEM. (*) $p < 0.05$ (Student's t-test).

4.6 Expression of the DN-CPEB1-4 protein in ESdM cells

To study the function of CPEBs in microglia, a lentiviral gene delivery system was used to stably overexpress the CPEB-1-EGFP, DN-CPEB1-4-EGFP and CPEB3-EGFP fusion proteins in ESdM cells (Napoli *et al.*, 2009). To this end, CPEB-1, CPEB-3 and DN-CPEB1-4 ORFs were cloned into the 3rd generation lentiviral vector pFTM-3GW (section 3.9.5). Functionality of the expression cassette was proven by robust fluorescence of transiently transfected HeLa cells (not shown). The lentiviral particle production was performed with the ViraPower system (Invitrogen), using HEK-293 FT as a packaging cell line (section 3.24). The transduction efficacy obtained (as determined by FACS) was 45% in case of the DN-CPEB1-4-EGFP and 55% in case of the control (EGFP) vector.

Unfortunately, transduction with CPEB1-EGFP and CPEB3-EGFP constructs resulted in no or barely detectable signal, respectively. For CPEB3-EGFP, the transduction efficacy was considerably lower, compared with EGFP and DN-CPEB1-4. The fluorescence intensity of transduced cells was hardly distinguishable from background noise and cell auto-fluorescence. Analysis of the CPEB3-EGFP infected ESdM cells on a flow cytometer did not allow for defining any clear GFP-positive population. Taking this into account, the experiments with the CPEB1-EGFP and CPEB3-EGFP lentiviral transduction were discontinued at this stage.

To exclude from further culturing the cells not expressing the transgene, FACS-sorting was performed. Sorting gates were defined in the EGFP-channel, in a way that 80% of the brightest cells from the GFP-positive population were selected. Histogram overlays, showing GFP fluorescence distribution of the transduced cells and the negative (not transduced) controls, are shown on Fig. 4-24. In each case, a distinct population of GFP-fluorescent cells was present.

By comparing the forward scatter (FSC) versus side scatter (SSC) plots of the control and the infected ESdMs, it immediately became obvious, that transduced cells (both, EGFP-positive and DN-CPEB1-4-EGFP-positive) had an altered morphology. They were larger (FSC-A median for EGFP-positive and DN-CPEB1-4-EGFP-positive populations 6.47 x 10^4 a.u. and 6.01 x 10^4 a.u. respectively, compared with 2.82 x 10^3 a.u. for control cell population), as well as more complex/granular (SSC-A median for EGFP-positive and DN-CPEB1-4-EGFP-positive populations 1.03 x 10^4 a.u. and 1.28x 10^4 a.u. respectively, compared with 0.80 x 10^3 a.u. for control cell population). SSC/FSC plots of transduced and control ESdM cells were presented in Fig. 4-25.

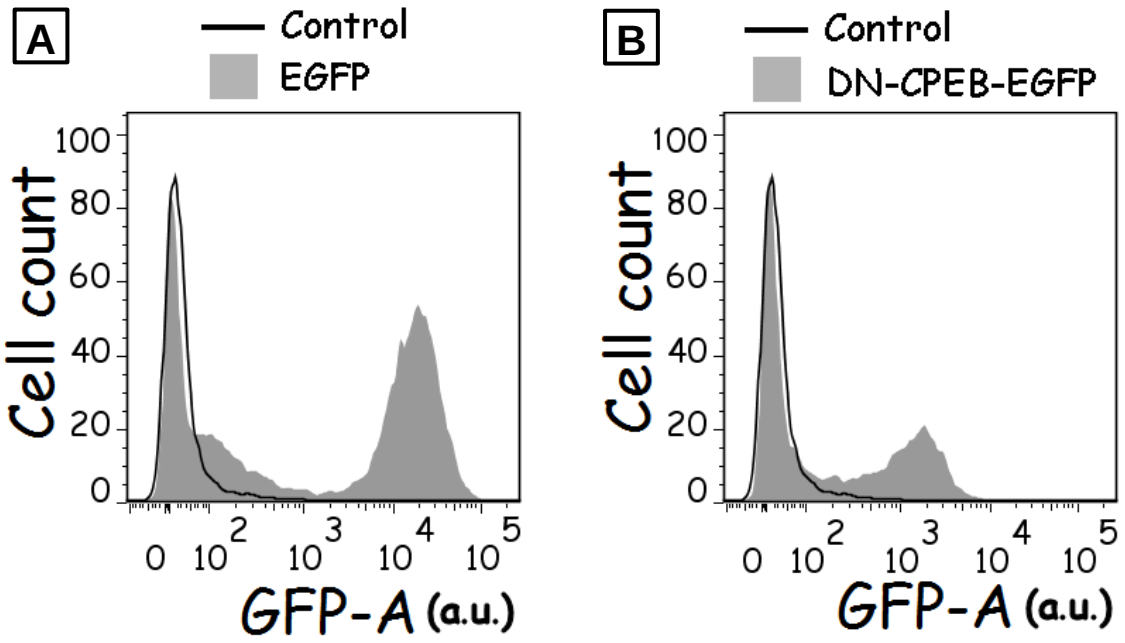

Fig. 4-24: FACS-sorting of the transduced ESdM cells. Histograms showing GFP fluorescence distribution for the ESdM cells transduced with EGFP (**A**) and DN-CPEB1-4-EGFP (**B**). Grey filled trace - transduced cells; overlaid black line – negative controls.

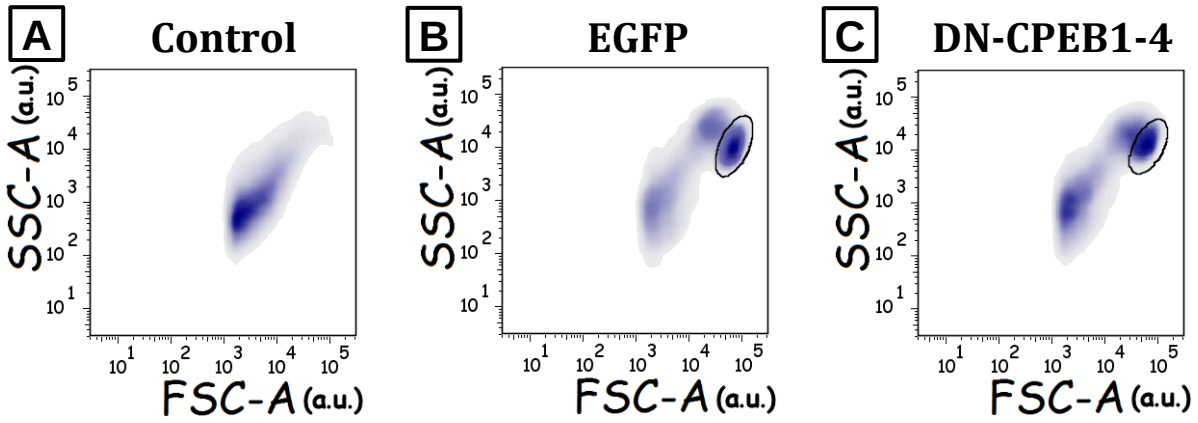

Fig. 4-25: Changed scattering properties of transduced ESdM cells. Forward scatter (FSC) versus side scatter (SSC) FACS plots of the control (**A**), EGFP-transduced (**B**) and DN-CPEB1-4-transduced (**C**) ESdM cells. Transduced cells appear as bigger and more granular/complex, compared with controls. In B and C, the GFP-positive population of cells was marked with an elliptical gate.

After sorting, the cells were brought back to culture conditions and cultivated for five passages. After that time, a sample of cells was FACS-analyzed, to confirm that the transgene expression was sustained at the expected level. Cells were analyzed for GFP fluorescence. Viable cells were identified using the Live/Dead Far-Red Fixable Stain (Invitrogen). The fraction of GFP-positive cells in the viable cell population of the DN-CPEB1-4- and EGFP-expressing cells was 93.5% and 98.8%, respectively (Fig. 4-26). Positivity for EGFP expression of nearly all cells was confirmed by fluorescence microscopy of living cells (Fig. 4-27).

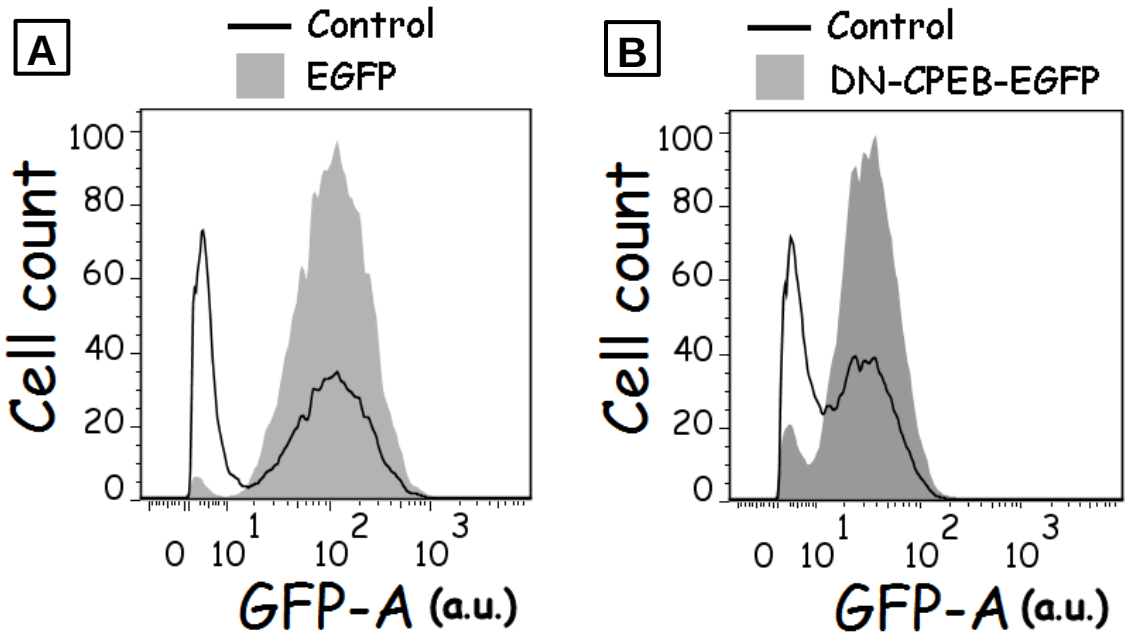

Fig. 4-26: Evaluation of FACS-sorted ESdM cells. After 5 passages >90% of transduced cells remained positive for the transgene. The fraction of positive cells in the living cell population of EGFP- (**A**) and DN-CPEB1-4-EGFP-expressing cells (**B**) was 98.8% and 93.5%, respectively. Grey filled trace – living cell population; overlaid black line – total cells (dead cells included).

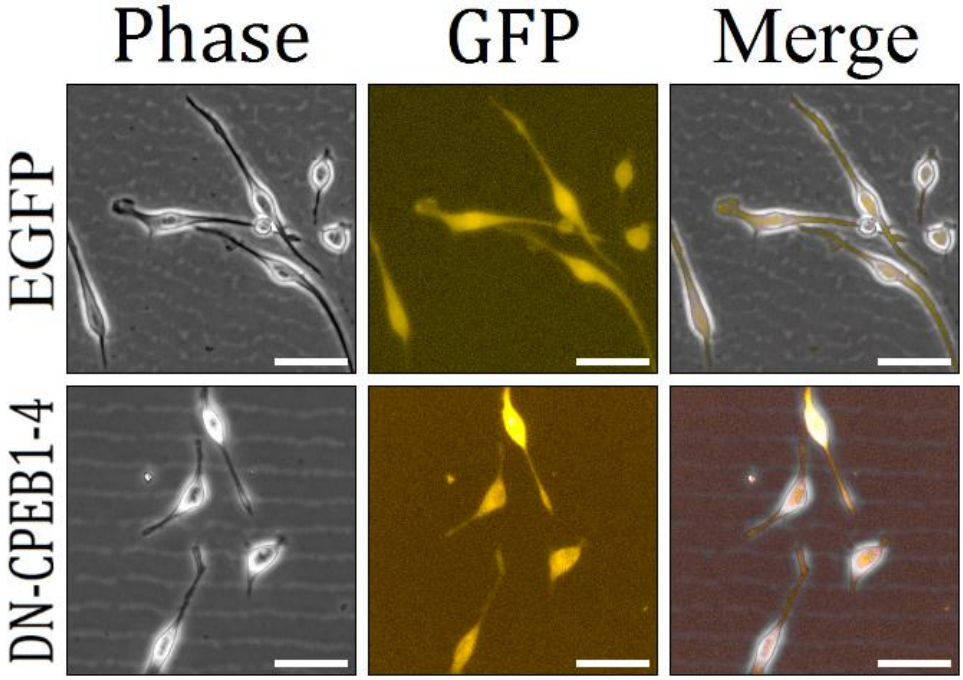

Fig. 4-27: ESdM cells after lentiviral transduction. Phase contrast and GFP fluorescence pictures of transduced EGFP (top) and DN-CPEB1-4 (bottom) ESdM cells. Scale bar: 50μm.

The CPEB-1 protein binds to the CPEs in the 3'UTR of tPA mRNA, as shown in the section 4.4.4. It was mentioned before that DN-CPEB1-4 is the N-terminally truncated variant of CPEB-1 protein, proven to functionally bind CPEB-1 targets: CaMKIIα and CPEB3 mRNAs (section 4.1.3 and 4.1.4, respectively). DN-CPEB functionally interferes

with CPEB function by constitutively repressing the translation of CPEB target mRNAs. Importantly, DN-CPEB1-4 protein was shown to be functional *in vivo*: overexpression of the protein in the principal neurons (the tet-off system, with the CaMKIIα-tTA driver) led to phenotypical changes on the molecular (translational regulation), cellular (LTP) and behavioral level (spatial memory) in transgenic mice (Theis *et al.*, in revision). Therefore, after establishing a stable overexpression of the DN-CPEB1-4 protein in ESdM cells, we aimed at evaluating its impact on the putative microglial CPEB target – tPA. Immunoblot analysis showed no significant difference in the tPA protein expression between control cells (transduced with the EGFP vector) and the DN-CPEB1-4-expressing cells (DN-CPEB: n=6, EGFP: n=6) (Fig. 4-28).

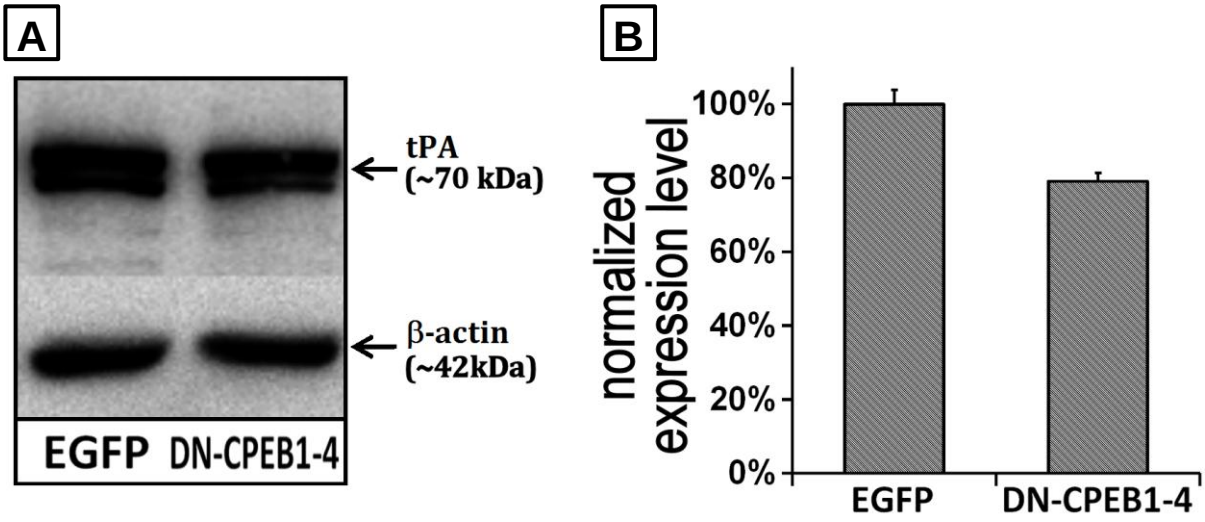

Fig. 4-28: Expression of tPA protein in ESdM cells transduced with the DN-CPEB1-4. (**A**) Representative immunoblot showing expression of tPA protein levels ESdM cells transduced with DN-CPEB1-4 and EGFP (control). β-actin and α-tubulin (not shown) were used as the internal control for normalizing expression levels. To bands observed in case of tPA blot might result from the heterogeneous glycosylation of the protein. (**B**) Densitometric analysis of the immunoblot shown in A. The observed decrease of tPA protein expression to 79.1 ± 2.2% of the EGFP control levels was not statistically significant. DN-CPEB1-4: n=6, EGFP (control): n = 6.

4.7 NG2 cells and astrocytes express all four CPEBs

To visualize NG2 cells and astrocytes simultaneously from one litter, homozygous $NG2^{kiYFP/kiYFP}$ mice (Karram *et al.*, 2008) were crossbred with $Cx43^{kiCFP/+}$ (Degen, Dublin *et al.*, unpublished) to generate double transgenic littermates, expressing YFP in NG2 cells and CFP in classical astrocytes. Mice were sacrificed at postnatal day 5, dissociated using the trypsin-based Neural Tissue Dissociation Kit (Miltenyi Biotec). After isolation of RNA, RT-PCR was performed, using Taq-Man sqRT-PCR primers/probes for CPEBs 1-4. All four CPEBs were detected in both, NG2 cell and astrocytes. Results for the NG2 cells and astrocytes are presented in Fig. 5-29 and 5-30, respectively. The comparison of NG2 cells and astrocytes with respect to CPEBs 1-4 expression was presented in Fig. 5-31.

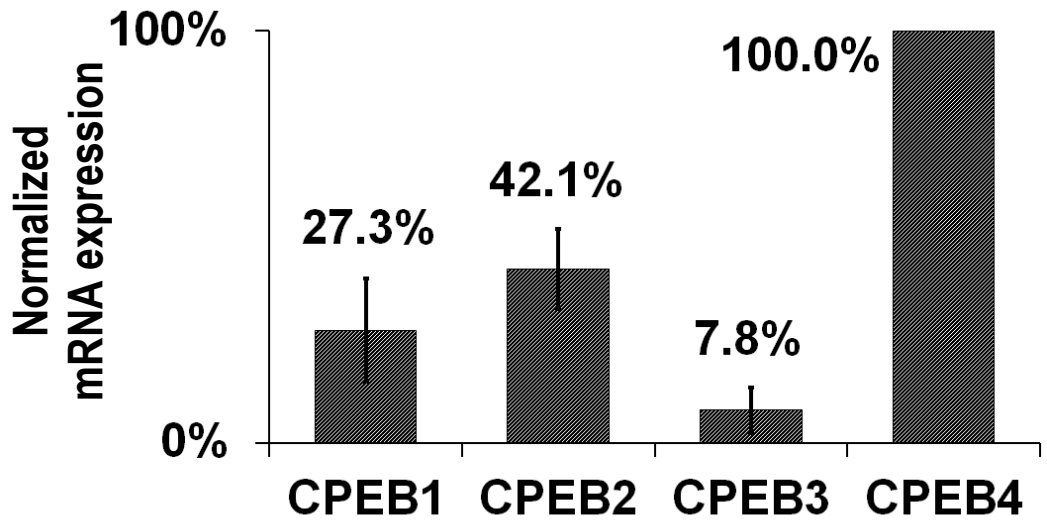

Fig. 4-29: sqRT-PCR analysis of relative expression of CPEBs -1 to -4 in FACS-sorted NG2 cells. Total RNA was extracted from FACS-sorted NG2 cells from mouse brain (postnatal day 5) and the relative expression of CPEBs -1 to -4 was analyzed using Taq-Man-based sqRT-PCR system. Highest level (CPEB4) was set to 100%. Error bars are SEM; n=4.

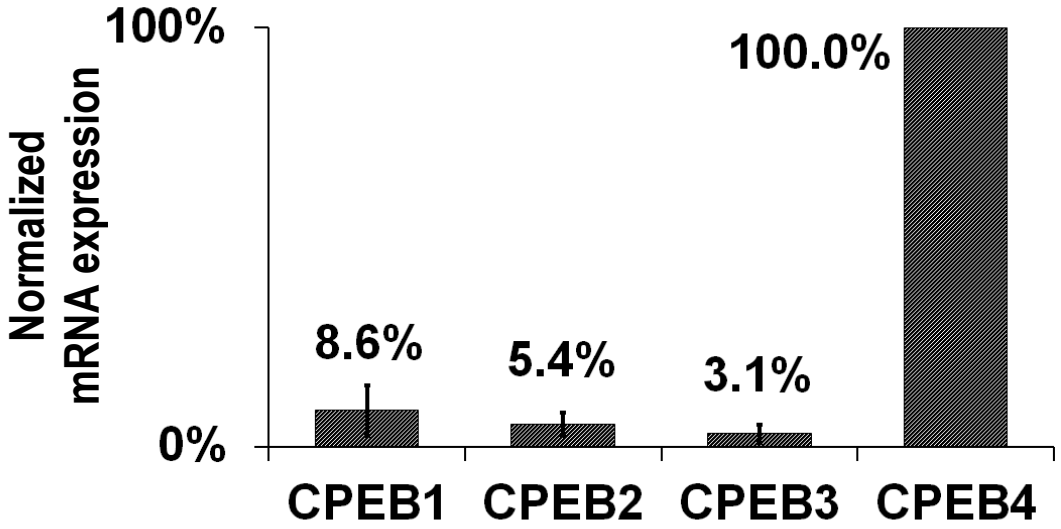

Fig. 4-30: sqRT-PCR analysis of relative expression of CPEBs -1 to -4 in FACS-sorted astrocytes. Total RNA was extracted from FACS-sorted astrocytes from mouse brain (postnatal day 5) and the relative expression of CPEBs -1 to -4 was analyzed using Taq-Man-based sqRT-PCR system. Highest level (CPEB4) was set to 100%. Error bars are SEM; n=4.

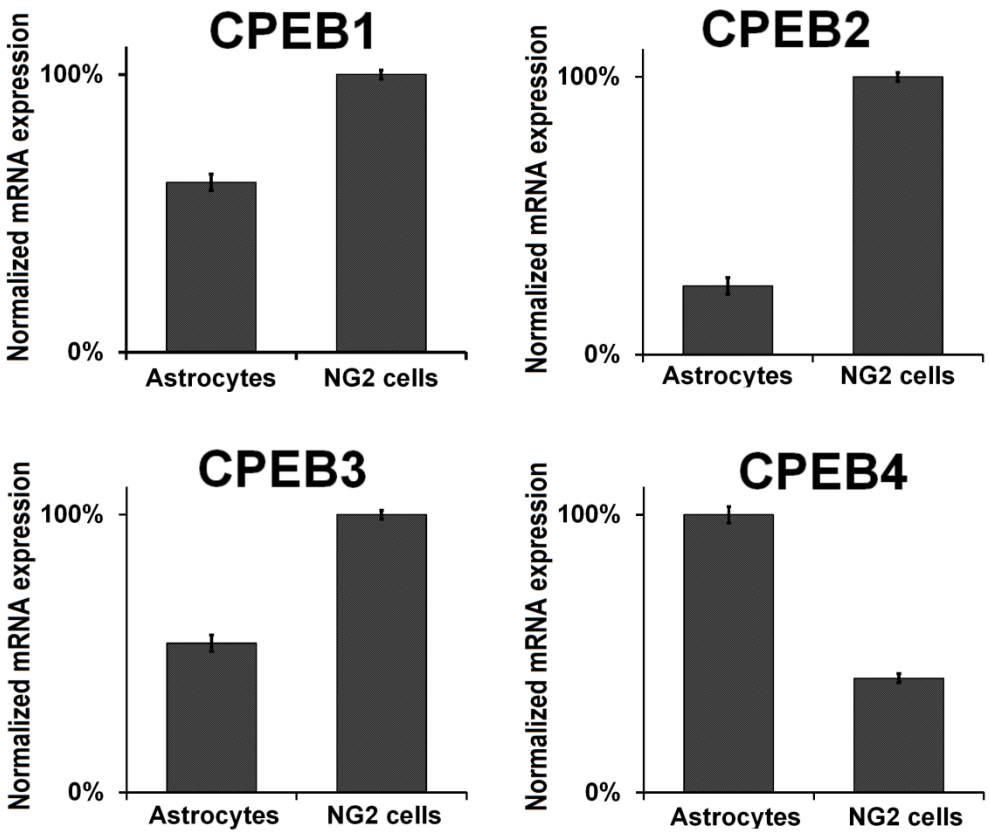

Fig. 4-31: Comparison of the relative expression or CPEBs 1-4 in astrocytes and NG2 cells. Total RNA was extracted from FACS-sorted astrocytes and NG2 cells from mouse brain (postnatal day 5) and the relative expression of CPEBs 1-4 was analyzed using Taq-Man-based sqRT-PCR system. In each graph the higher of the two values was set to 100%. Error bars are SEM; n=4.

4.8 Cx43 is a novel CPEB protein target

Sequence analysis of Cx43 3'UTR revealed the presence of a CPE element overlapping with the AAUAAA hexanucleotide, suggesting a strong translational inhibition (Pique *et al.*, 2008). Unlike to tPA, there was no experimental evidence to date that Cx43 mRNA is a CPEB target. With an approach similar to the one used to confirm the interaction between CPEB-1 and tPA mRNA, the putative interaction between CPEB-1 and Cx43 3'UTR was tested. As prey, we used the luciferase construct appended with a 202bp terminal fragment of Cx43 3'UTR, containing wild-type (WT) or mutated (MUT) CPE (Fig. 4-32B). Similar to tPA, CPEB-1 co-immunoprecipitated the Cx43 3'UTR WT fragment with significantly higher affinity than it did in case of the corresponding mutated 3'UTR. A control bait protein (FLAG-EGFP) did not interact with the Cx43 3'UTR (Fig. 4-32A).

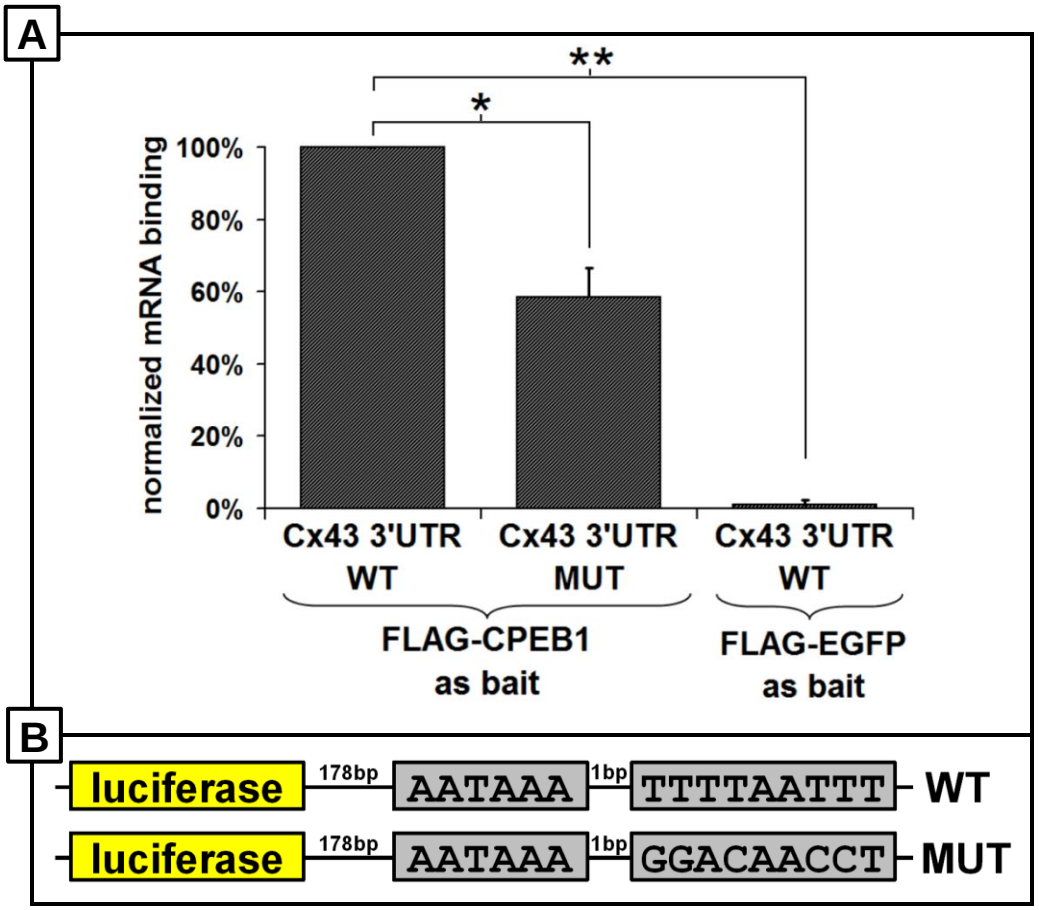

Fig. 4-32: CPEB-1 protein interacts with the Cx43 3'UTR. (**A**) Co-IP of overexpressed 3'UTR derived from Cx43 luciferase reporter mRNA appended with wild-type (WT) or mutated (MUT) 3'UTR (TaqMan-based sqRT-PCR quantification using luciferase-gene specific oligonucleotides). FLAG-CPEB1 or FLAG-EGFP (control) fusion proteins were used as baits. * P<0.05, ** P<0.01 (student's t-test); n=3. (**B**) Schematic of the wild-type and mutated 3'UTR constructs used in A.

4.9 Quality control of astrocyte-directed Connexin43 conditional gene deletion

4.9.1 Cx30/43 DKO mice require a quality control for experimental validation

The hGFAP-Cre transgene (Zhuo *et al.*, 2001) has one important drawback: a variable recombination efficacy caused by spontaneous downregulation (or loss) of Cre expression (Requardt, Kaczmarczyk *et al.*, 2009). This critical limitation required developing a reliable method of quality control in the transgenic animals. Here we embarked on assessing the hGFAP-Cre in mediating recombination in the conditional KO of Cx43 in $Cx30^{-/-};Cx43^{fl/fl}$ mice (Cx30/43 DKO mice). We developed a method in addition to a reporter gene activation, which is necessary due to the abovementioned variability of Cre expression, and which allows for assessing Cx43 ablation fidelity in $Cx30^{-/-};Cx43^{fl/fl}$:hGFAP-Cre. The method is immunoblot-based and can be used post-experimentally.

4.9.2 Cx30/43 DKO mice display a variable Cx43 ablation status

The brains of Cx30/43 DKO and littermate control mice were dissected. From one hemisphere, cerebellum, hippocampus and frontal cortex were isolated for Cx43 and Cre immunoblot analysis. The frontal tip of the cortex and cerebellum of the remaining hemisphere were used for DNA isolation to perform PCR analysis for i) the presence of the hGFAP-Cre transgene (Theis *et al.*, 2003a), ii) the recombined Gja1 flox allele (called Cx43del) allele (Theis *et al.*, 2001) and iii) the non-recombined Gja1 flox (called Cx43 flox) allele (Theis *et al.*, 2001). The remaining part of the hemisphere (containing the dorsal hippocampus) was used for (immuno-)histochemical detection of the recombination-activated β-galactosidase reporter. In addition, immunofluorescence analysis and immunoblotting for Cre recombinase were performed, to correlate its expression with the Cx43 ablation status. All three methods for monitoring recombination events were applied, i.e. immunoblot to assess recombination-mediated ablation of Cx43, PCR to examine recombination of the Cx43 flox allele and (immuno-) histochemistry to monitor recombination-activation of the reporter replacing Cx43 (immunohistochemistry was performed by Pavel Dublin, Institute of Cellular Neurosciences, Bonn, Germany). Immunoblot experiments with hippocampal lysates showed that in 6 DKO mice from 2 different litters (F_a, F_b), efficient hGFAP-Cre mediated loss of Cx43 expression occurred (Fig. 4-33A). Residual expression amounted to 4.4 ± 0.8% of the mean level observed in Cx30-/-;Cx43fl/fl control littermates (DKO: n=6; control: n=5). This was in line with previous reports (Theis *et al.*, 2003a; Theis *et al.*, 2004). In one remaining litter (F_c), out of the 4 putative DKO mice tested one did not show a decrease in Cx43 protein expression and 3 mice showed a partial decrease of Cx43 protein level (Fig. 4-33B). The mean decrease of Cx43 protein expression in hippocampus for all pseudo DKO mice tested amounted to 61.8 ± 21.0% of control (DKO: n=4; control: n=4; Fig. 4-33D). Interestingly, faithful hGFAP-Cre mediated recombination (or lack thereof) occurred independently of gender and was consistent and reliable within individual litters. This means that littermates can be used as sentinels to pre-experimentally assess hGFAP-Cre activity by immunoblotting for Cx43. Using the cerebellar material, it was examined whether the occurrence of faithful recombination or inefficient Cre activity was consistent across different litters from the same parents and across generations, that is, if pseudo DKOs were generated by pseudo DKO parents. 16 DKO animals, 2 each from 8 breedings and the corresponding 8 parental DKOs were analyzed. The parental DKO animal giving rise to the pseudo DKO litter Fc (Fig. 4-33B) turned out to be a pseudo DKO mouse, as did the mice from the second tested litter from the same breeding pair. Another litter from a separate breeding pair contained pseudo DKO mice, and the corresponding parent was likewise a pseudo DKO. The other six breeding pairs generated offspring with faithful and efficient deletion. Interestingly, two of the parents were pseudo DKOs, yet they gave rise to DKO

offspring (immunoblot data not shown, but included in the densitometric analysis in Fig. 4-33E). Consequently, the deletion status of siblings seems to be a better indicator for Cre efficacy than the deletion status of the parents.

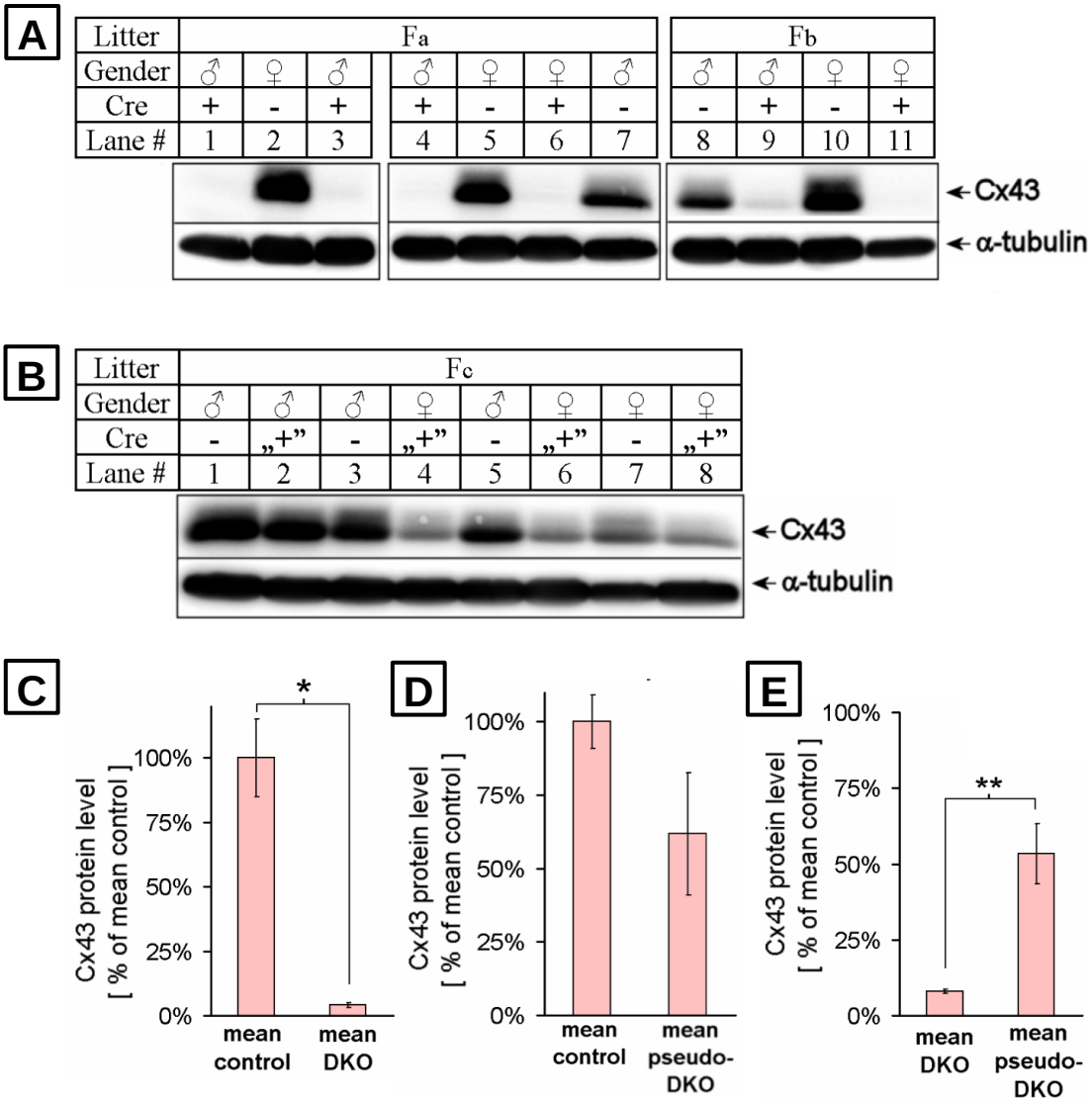

Fig. 4-33: Assessing the efficacy of hGFAP-Cre by immunoblot analysis for Cx43. (**A**) Two litters (Fa and Fb) displayed greater than 95% loss of Cx43 protein expression in $Cx30^{-/-}$;$Cx43^{fl/fl}$:hGFAP-Cre mice compared to $Cx30^{-/-}$;$Cx43^{fl/fl}$ littermates. (**B**) In another litter (Fc), pseudo DKO mice ("+"; #2, 4, 6, 8) showed an average decrease in Cx43 protein expression to about 62% of control levels. ♂ - male; ♀ - female. (**C** and **D**) Densitometric analysis of the immunoblots shown in A and B, respectively; (*) $P < 0.001$ (student's t-test). (**E**) Comparison of mean cerebellar levels of Cx43 protein expression in DKO and pseudo DKO mice; (**) $P < 0.0001$ (Mann–Whitney test).

4.9.3 Cx43 ablation status in Cx30/43 DKO mice is homogeneous across brain areas

As a next step, we tested by immunoblot analyses, whether faithful recombination or lack thereof occurred in a homogeneous fashion across brain areas and found that in hippocampus, frontal cortex, and cerebellum recombination was similarly efficient within individual mice of the DKO type and similarly inefficient within individual mice of the pseudo DKO type (Fig. 4-34A, B). When normalized to the respective, brain area-specific Cx43 levels of controls (n = 4), the residual Cx43 levels of DKO mice (n = 3) were higher in cortex 6.9 ± 0.7% and cerebellum 8.2 ± 1.6% compared to hippocampus 3.7 ± 0.4%. This may be due to the presence of leptomeningeal cells (difficult to separate from the brain tissue during surgery) in the samples that are not targeted by hGFAP-Cre (Theis *et al.*, 2003a; Theis *et al.*, 2004). Residual Cx43 protein levels of the pseudo DKO animals tested (n = 3) were much higher and were similar across brain areas within individual animals (Fig. 4-34B). This means that, in addition to the pre-experimental selection of DKO mice using littermates as sentinels, faithful recombination can also be investigated postexperimentally. This can be accomplished by assessing Cx43 ablation in brain areas (e.g. cerebellum), which were not immediately used for the experimental analysis (such as electrophysiological investigation of acute hippocampal slices). Cerebellar tissue seems to be a good choice for routine evaluation of hGFAP-Cre efficacy. Pseudo DKO mice showed a mean decrease of cerebellar Cx43 protein levels to 57.6 ± 8.4% of control, whereas DKO mice showed a decrease to 8.1 ± 0.8% of control levels (pseudo DKO: n = 9; DKO: n = 23; control: n = 17; Fig. 4-34E).

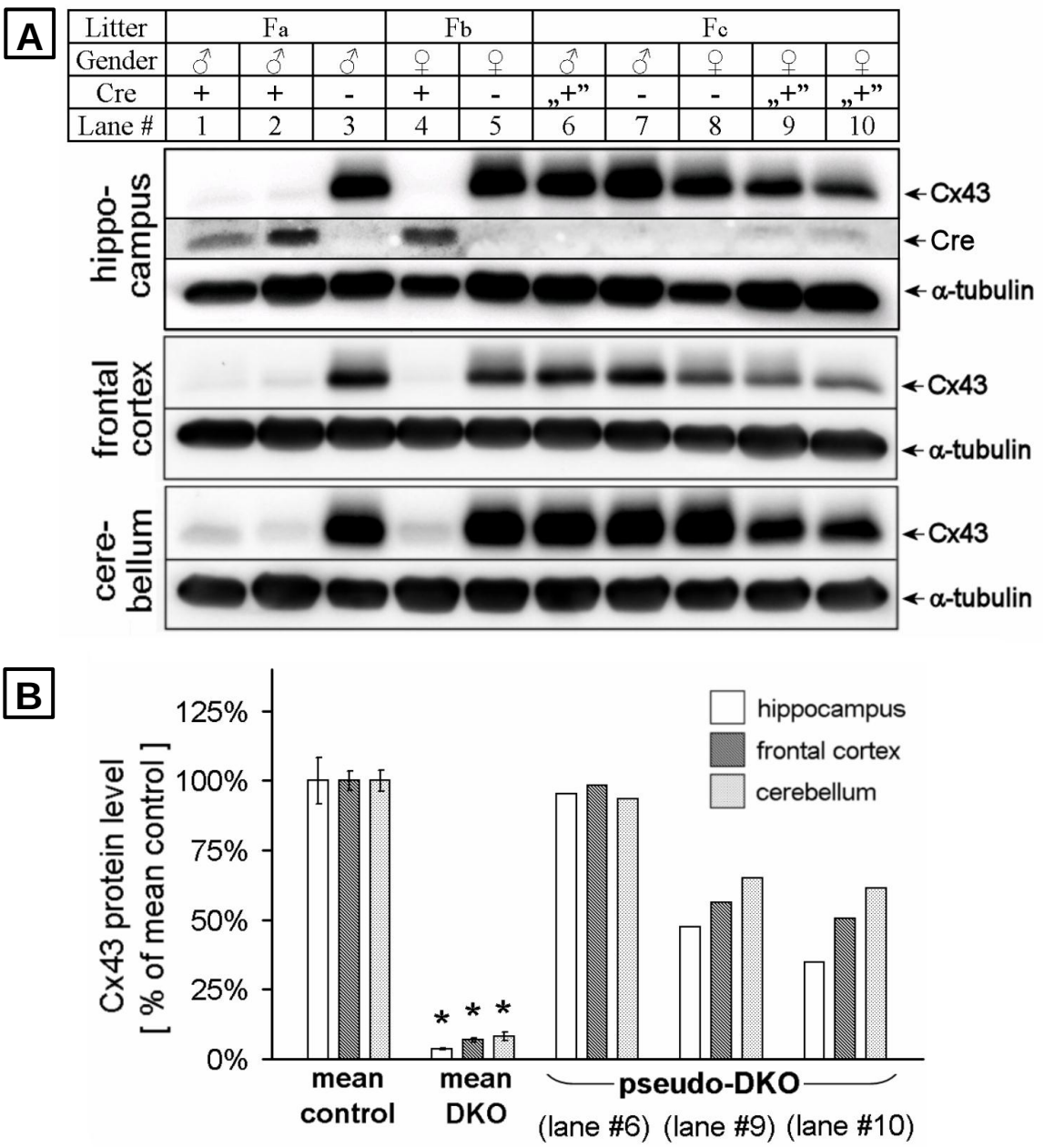

Fig. 4-34: Comparison of Cx43 ablation level across brain areas. (**A**) Immunoblots showing that within individual mice selected from litters Fa-c, the pattern of hGFAP-Cre mediated Cx43 ablation was similar across all brain regions examined (i.e., hippocampus, frontal cortex and cerebellum). A representative Cre immunoblot (hippocampus) shows the correlation of Cx43 ablation status with the abundance of Cre protein in all brain areas examined. +: active Cre; "+": partially active or inactive Cre; -: Cre not present. (**B**) Densitometric analysis of Cx43 immunoblots shown in A. (*) $P < 0.05$ (Mann–Whitney test).

4.9.4 In Cx30/43 DKO mice Cx43 levels positively correlate with Cre expression

By immunobloting, it was found that expression of Cre recombinase positively correlates with the extent of Cx43 ablation (Fig. 4-34A). When testing different brain regions from transgenic mice ($Cx30^{-/-}$;$Cx43^{fl/fl}$:hGFAPCre: n = 16; $Cx30^{-/-}$;$Cx43^{fl/fl}$ control: n = 10), three subpopulations of animals were distinguished (Fig. 4-35). One class of mice showed residual Cx43 protein levels below 20% of control level (19 samples from 9 animals; Cx43 = 6.6 ± 0.8%). These mice (termed DKO) were used for normalization of Cre levels (Cre = 100.0 ± 3.3%). A second class of mice showed Cx43 levels between 20% and 80% of control level (12 samples from 5 animals; Cx43 = 50.0 ± 3.0%. These mice, termed half pseudo-DKOs, displayed Cre levels amounting to 15.4 ± 2.8% of DKO mice. A third class of mice displayed a Cx43 abundance above 80% of control level (five samples from two animals; Cx43 = 102.7 ± 4.8%). These mice, termed full pseudo-DKOs, displayed Cre levels amounting to 21.4 ± 1.5%. Please note that the values mentioned above are mean ± SEM while the error bars in Fig. 4-35 depict the range, that is, the maximal deviations from the mean.

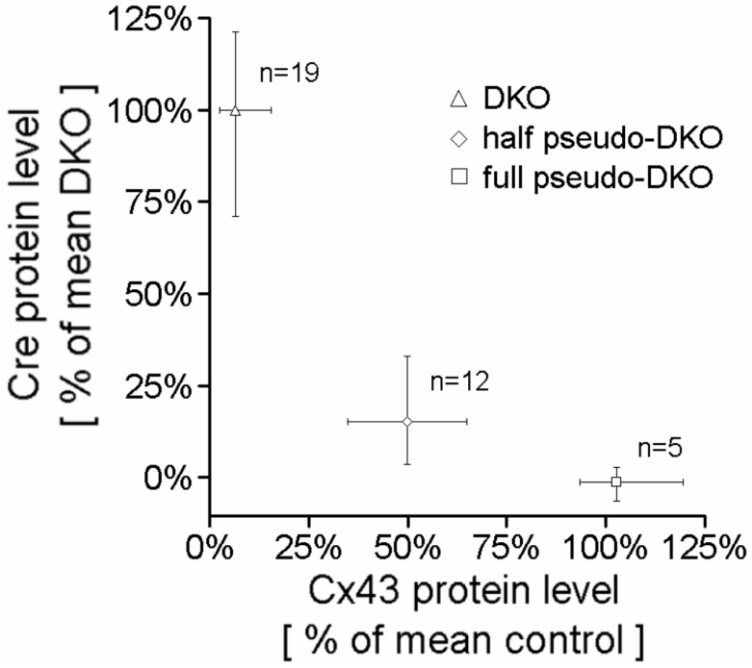

Fig. 4-35: Correlation of Cx43 and Cre protein levels. Densitometric analysis of Cx43 and Cre immunoblots, showing the correlation of Cx43 ablation with Cre recombinase expression. Data points represent three distinct subpopulations of $Cx30^{-/-}$;$Cx43^{fl/fl}$:hGFAP-Cre animals, which were separated on the basis of their Cx43 ablation status. Values for hippocampus, frontal cortex, and cerebellum were pooled and the mean was calculated. Bars represent the highest and the lowest value for each group. Note that there was no overlap of data obtained for DKOs vs. pseudo DKOs.

The results of the PCR analysis to monitor the recombination of the Cx43 flox allele in frontal cortex and cerebellum were consistent with the immunoblotting (for details see Requardt, Kaczmarczyk *et al.*, 2009).

5 Discussion and Conclusions

5.1 CPEB expression in mouse brain

CPEBs 1-4 are present in major brain cell populations: neurons (Theis *et al.*, 2003b), astrocytes, NG2 cells, and microglia. CPEBs1-4 were detected in microglial cell lines: BV-2 cells and ESdMs (immunoblot, ICC, RT-PCR) as well as the primary microglia from FACS-sorted brain dissociates (sqRT-PCR). This is in fact the first attempt to look at CPEB expression in microglial cells. CPEB-1 on the Western blot level was barely detectable (not shown), which may be explained by the low specificity of the antibody used (custom made, Eurogentec). Detailed analysis of CPEB-3 isoforms in ESdM cells revealed expression of only selected isoforms. In case of CPEB-3 and CPEB-4, only isoforms lacking the B-region were found expressed. It cannot be ruled out that these isoforms were not detected due to the limitation of the analysis used. To analyze expression of the different CPEBs (and their isoforms), a set of primers flanking the alternatively spliced region of each CPEB was used. The amplicon length varied between 144nt and 347nt, depending on the isoform amplified. Due to insufficient resolution of the DNA electrophoresis in that range, and as small as 24nt (B-region size) difference between isoforms, the PCR products were cumulatively (all obtained products) purified from gel and T/A-cloned. During T/A cloning of multiple PCR products, some PCR fragments may tend to ligate preferentially compared to others. Especially shorter fragments (i.e. the fragments lacking B- and/or C-domain) may ligate preferentially, leading to a bias in the outcome. To reliably dissect the isoform expression in different cell types, a high resolution DNA electrophoresis on polyacrylamide gel should be used. For semi quantitative assessment of isoform distribution in tested material, a DNA capillary electrophoresis should be applied, or selected isoform-specific Taq-Man sqRT-PCR primer and probe sets should be designed. Another likely explanation for the failure to detect certain isoforms in ESdM cells is the discrepancies occurring between the cultured cells (even primary cells) and the cells *in vivo*. Although ESdM cells show a clear microglial phenotype (Napoli *et al.*, 2009), they cannot be regarded as cells in the *in vivo* state, for they are derived from stem cell precursor cells in laboratory conditions. Thereby, the differentiation stimuli are limited and not physiological. As a consequence, phenotypical differences between these cells and their *in vivo* counterparts will unavoidably be present. Using FACS cell sorting, primary NG2 cells and astrocytes were purified from trypsin-dissociated mouse hippocampi (at postnatal day 5). Analysis of RNA purified from the FACS-sorted material revealed expression of all four CPEBs, with the CPEB-4 transcripts being the most abundant in both analyzed cell populations (see Fig. 4-29 and 4-30).

5.2 Phosphorylation and alternative splicing of CPEB-3

The CPEB-3 protein in mouse brain occurs in four splice isoforms, termed a, b, c, and d, differing by the presence (or absence) of the so called B-region and C-region (see Fig. 5-1) (Theis *et al.*, 2003b). The CPEB-3a isoform, containing both of the regions, is the most abundant. The occurrence of the B-region may have high physiological significance, as it harbors the PKA and the CaMKII phosphorylation sites.

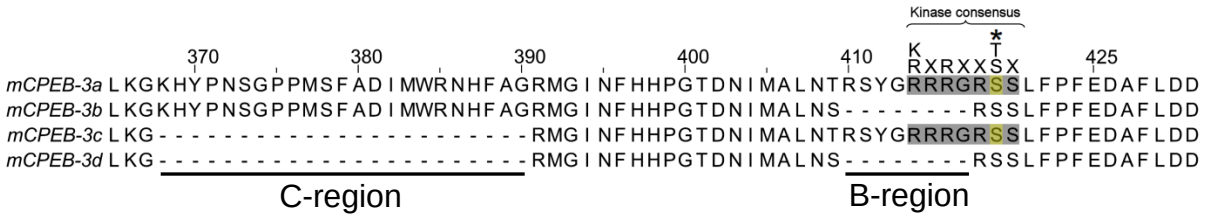

Fig. 5-1: CPEB-3 isoforms in mouse brain. Sequence comparison of a variable region in mouse CPEB-3 (mCPEB-3). Two regions, termed B and C, are alternatively spliced, leading to expression of four isoforms. Consensus phosphorylation sites for PKA and CaMKII kinase is shown above the alignment and the putative phosphorylated residue (S419) is marked by an asterisk.

The results of the *in vitro* peptide phosphorylation assays (see section 4.3.1) show that the a-isoform peptide (identical to the CPEB-3a/c sequence flanking the putative phosphorylation site) is (at least *in vitro*) indeed phosphorylated by PKA and CaMKII. The phosphorylation in case of the b-isoform peptide and the serine-to-alanine mutant was significantly reduced, as compared to the a-isoform. Moreover, HEK-293 cells transfected with CPEB-3a, followed by treatment with forskolin, showed a significant increase in the CPEB-3a phosphorylation level (see section 4.3.3). Therefore, a firm conclusion can be made that the presence of the B-region significantly affects the propensity of CPEB-3 protein for phosphorylation by PKA and CaMKII.

Inducing seizures in mice by intraperitoneal injection of kainic acid (a potent agonist of non NMDA-type glutamate receptors), leads to upregulation of CPEB-3 mRNAs (Theis *et al.*, 2003b). Interestingly, only the isoforms containing the phosphorylation consensus site (i.e. the B-region) are upregulated after kainate-induced stimulation (see Fig. 5-2). Epilepsy entails similar neuronal mechanisms as LTP, learning and memory. Therefore, it is conceivable that the CPEB-3 isoforms containing the B-region play an important role in these processes.

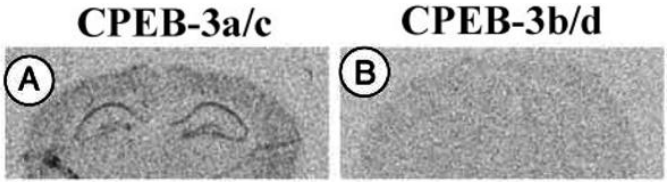

Fig. 5-2: Isoform-specific upregulation of mCPEB3a/c isoforms in the hippocampus. (**A**) mCPEB-3a/c detected by Northern blot 2 h after intraperitoneal kainate injection. (**B**) corresponding image obtained using mCPEB-3b/d-specific probe (adapted from Theis *et al.*, 2003b).

The sequence similarity between CPEBs -2 to -4 is substantial, especially in the RBD, where the proteins are almost identical (>98% similarity). It is therefore conceivable that they may share the propensity for being phosphorylated by the same set of protein kinases. Fig. 5-3 shows close to 100% similarity of the phosphorylation consensus site between the CPEBs -2 to -4.

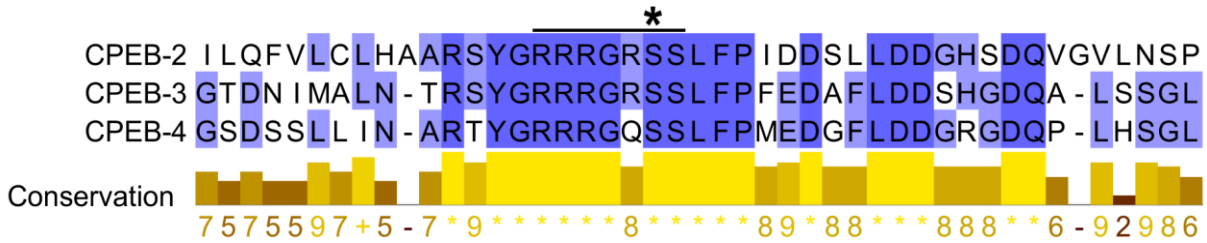

Fig. 5-3: Alignment of the regions flanking the phosphorylation site in CPEBs -2, -3, and -4. Sequence comparison shows, that although the flanking regions show moderate similarity, the phosphorylation consensus site is conserved between the paralogs. The putative phosphorylation site is marked with asterisk. Sequences aligned and analyzed using Jalview software.

Additionally, the splicing pattern of CPEB-2 and CPEB-4 is similar to CPEB-3: they both contain the C-region and the B-region, and the latter contains the part of the phosphorylation consensus site. Each of the CPEBs -2 to -4 occurs therefore as B region-containing isoforms (undergoing phosphorylation) and B region-lacking isoforms, which cannot be (at least at this particular site) phosphorylated. Studying the cell-type specific CPEB-3 phosphorylation mechanisms may shed new light on the physiological processes in which not only CPEB-3, but also CPEBs -2 and -4 are important players.

CONCLUSION

The presence of the B-region significantly affects the propensity of CPEB-3 protein to phosphorylation by PKA and CaMKII.

The alternative splicing of CPEBs adds complexity to that task of unraveling CPEB function. In case of CPEB3, in addition to the four isoforms herein mentioned (a, b, c, d), additional isoforms have been found in mouse retina (Wang and Cooper, 2009). It cannot be ruled out that these, and possibly other not yet described variants are present in other cells. The exact physiological significance of the multiple CPEB isoforms, as well as their expression pattern in brain, awaits elucidation.

5.3 CPEB-3 phosphorylation in cell signalling

5.3.1 Neurons

Regulation via phosphorylation by PKA and CaMKII places CPEB-3 (and, due to phosphorylation site conservation, also CPEB-2 and -4) as intracellular effector of signalling pathways. Synaptic plasticity, including hippocampal LTP, has been shown to be dependent on CaMKII (Atkins *et al.*, 2005) and PKA activity (Sweatt, 1999; Duffy *et al.*,

2001; Wikstrom *et al.*, 2003; Gelinas *et al.*, 2008). Both of these kinases are downstream targets of NMDA-R (Atkins *et al.*, 2005). CPEB-1 protein - the first described and the most extensively investigated member of the CPEB family – is phosphorylated at the Thr171 by the Aurora A kinase, upon NMDA-R stimulation (Huang *et al.*, 2002). CPEB-1 has also been shown to undergo phosphorylation by CaMKII (Atkins *et al.*, 2004). Regulation of CPEB-1 by phosphorylation and dephosphorylation by, respectively, CaMKII and **P**rotein **P**hosphatase **1** (PP1) (see Fig. 5-4), is involved in sustaining hippocampal LTP (Atkins *et al.*, 2005). This might be one of the explanations of LTP deficits observed in the CPEB-1 KO mice (Alarcon *et al.*, 2004).

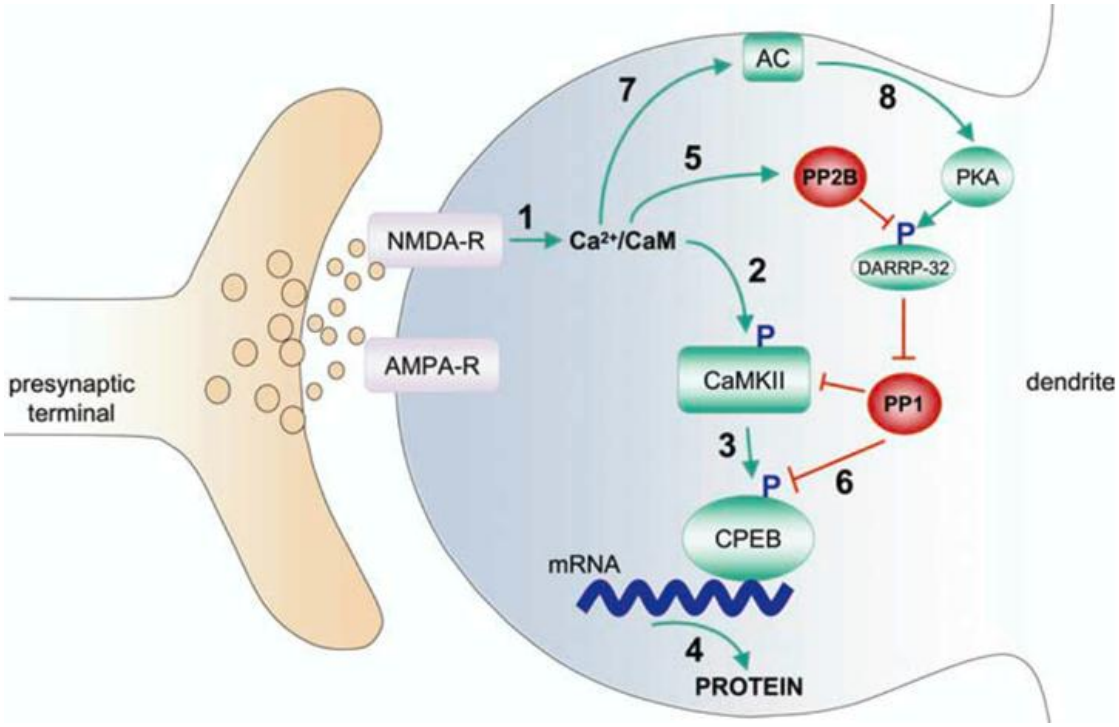

Fig. 5-4: Model for bidirectional regulation of CPEB1 by CaMKII and PP1. Modest LTP induction (1x100Hz) stimulates Ca^{2+} influx through the NMDA-R (**1**). Ca^{2+} binds to calmodulin (CaM) and activates CaMKII (**2**) through autophosphorylation. Activated CaMKII phosphorylates CPEB-1 (3) to stimulate protein synthesis (**4**). The elevated levels of Ca^{2+} also activate protein phosphatase 2B (PP2B) (5), which dephosphorylates **d**opamine- and cyclic **A**MP-**r**egulated **p**hospho**p**rotein (DARPP-32), thereby activating PP1, to dephosphorylate CPEB-1 (**6**) and limiting protein synthesis. However, robust LTP (4x100Hz) further elevates Ca^{2+}, stimulating **a**denylate **c**yclase (AC) (**7**) to generate cAMP. This activates PKA (**8**), which phosphorylates DARPP-32, thereby inhibiting PP1 to prolong CPEB phosphorylation and protein synthesis. Adapted from Atkins *et al.* (2005).

CPEB-3a overexpression in neurons leads to the translational repression of the GluR2 subunit of the AMPA-R (see section 4.2). Reports on the AMPA-Rs function in synaptic plasticity, and the role of the GluR2 subunit, has been extensively reviewed (Isaac *et al.*, 2007; Kessels and Malinow, 2009; Santos *et al.*, 2009). Considering the overlapping target mRNA specificity of CPEBs -1 and -3, one cannot exclude that they may functionally complement themselves. Amongst the putative CPEB targets (binding to CPEB-1 and -3, see section 4.1.3) is the mRNA of CaMKIIα – the kinase which is itself a

CPEB-1 and -3 regulator, as well as a key player in synaptic plasticity (Wu *et al.*, 1998; Lisman *et al.*, 2002). The functional ablation of CPEB-1 to -4 in DN-CPEB1-4 transgenic mice (discussed in more detail in section 5.4) leads to deficits in LTP, learning and memory (Theis *et al.*, in revision). Altogether, it is conceivable that CPEB-3 (and, due to sequence similarity, CPEBs -2 and -4) participates in synaptic plasticity mechanisms, and undergoes similar regulation, as CPEB-1 does (Fig. 5-5).

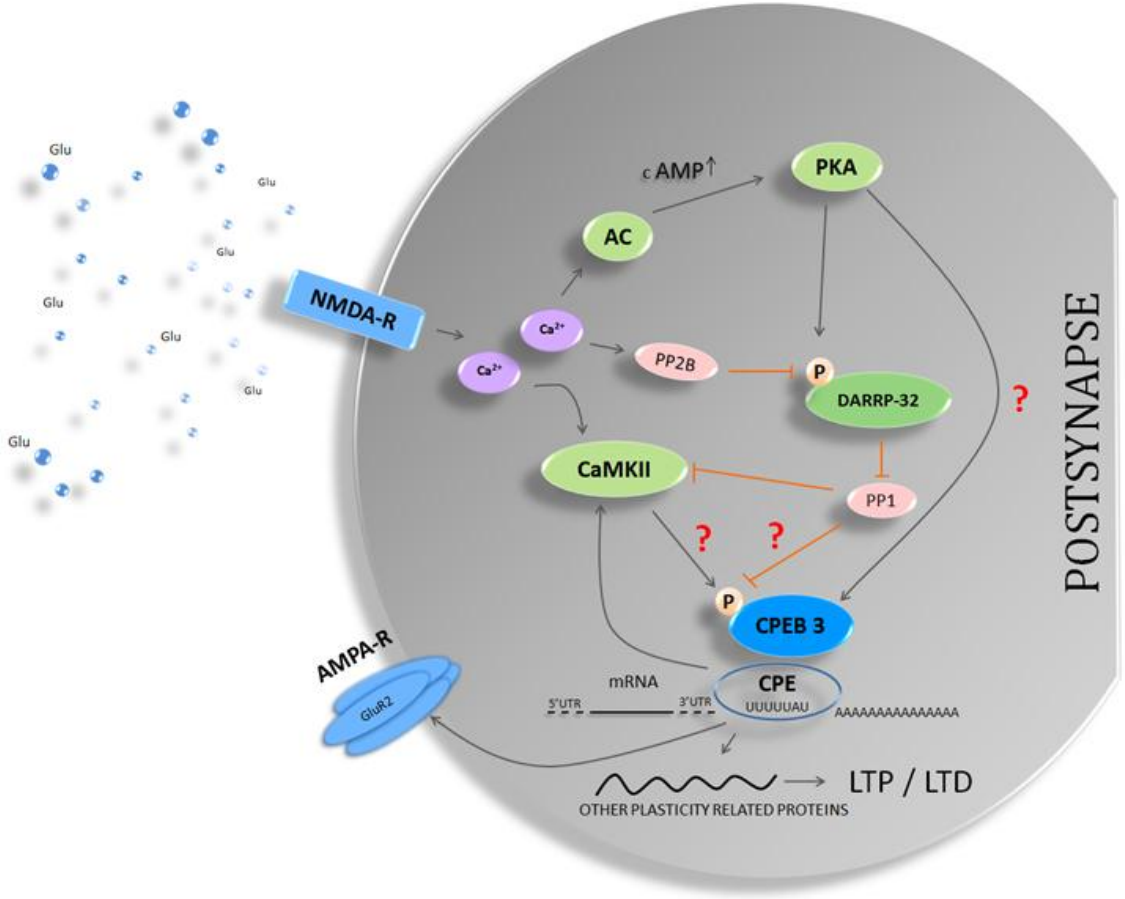

Fig. 5-5: Hypothetical model of the translational regulation by CPEB-3 in synaptic plasticity. CPEB-3 may be subjected to similar regulatory mechanisms, and control a similar set of targets, as CPEB-1 (see also Fig. 5-4). Adapted from Atkins *et al.* (2005), modified.

HYPOTHESIS

CPEBs -2 to -4 in neurons are regulated by PKA and CaMKII and are involved in NMDA-R-dependent forms of synaptic plasticity.

5.3.2 Astrocytes and microglia

CPEB-1 is involved in the control of astrocyte migration via translational regulation of β-catenin mRNA (Jones *et al.*, 2008). Since CPEBs -2 and -3 are binding to β-catenin mRNA as well (see section 4.1.2), they likewise might be involved in translational regulation of this protein. Using RNA co-immunoprecipitation, herein I confirmed that

CPEB-1 is binding tPA mRNA (see section 4.4.4), an established neuronal CPEB target (Shin *et al.*, 2004). tPA – a serine protease produced in brain by neurons and microglia – is a key player in synaptic plasticity (Samson and Medcalf, 2006). It has also been implicated in neurodegeneration following seizures in mouse brain (Tsirka *et al.*, 1995). As mentioned before, in neurons, production of tPA is translationally regulated by CPEB-1 protein (Shin *et al.*, 2004). However, it has been shown that specifically tPA of microglial origin is a factor causing neurodegeneration (Siao *et al.*, 2003). In this respect, it is worthwhile to investigate the binding of tPA mRNA by CPEBs 2-4 and the potential regulation of microglial CPEBs -2 to -4 by PKA. Microglial activation leads to activation of PKA. Hypothetically, PKA phosphorylation of CPEBs -2 to -4 in microglia might modulate the expression of tPA and thereby be crucial for microglial function in brain homeostasis and neurodegeneration in epilepsy.

HYPOTHESIS

CPEBs are involved in regulation of microglial tPA production and thereby implicated in neurodegeneration following epileptic seizures.

5.4 mRNA sequence specificity of CPEBs

As mentioned in section 5.3, one of the putative functions of the CPEB-3 protein may be regulation of local protein synthesis in dendritic spines, in response to stimulation. Such mechanism has already been reported in case of CPEB-1 protein, involved in hippocampal LTP (Alarcon *et al.*, 2004; Atkins *et al.*, 2005). Interestingly, ablation of CPEB-1 gene leads to deficits in single train theta-burst stimulation (TBS)-evoked LTP and LTP evoked by 1 train of 100 Hz stimulation. LTP evoked by other stimulation paradigms (4 trains of 100 Hz stimulation, 1 Hz stimulation) were not affected (Alarcon *et al.*, 2004). In contrast, overexpression of the DN-CPEB1-4 transgene in principal neurons (functionally interfering with all CPEBs constitutively repressing translation of CPE-containing mRNAs) did not result in changes in 1x TBS-evoked LTP, but led to significant deficits in late form of LTP (L-LTP) induced by repetitive TBS stimulation (Theis *et al.*, in revision). In addition, DN-CPEB1-4 mice showed deficits in captured LTP and modest enhancement of LTD induced by 1 Hz stimulation. The mRNA co-IP results showed that CPEB1 and CPEBs 2-4 have (at least to certain extent) overlapping specificity. Taken together, these results may suggest that in the CPEB-1 KO mice (Alarcon *et al.*, 2004), the CPEBs -2 to -4 may compensate the deficits caused by CPEB-1 gene ablation. The co-IP experiments of CaMKIIα, β-catenin, and CPEB3 mRNAs have shown that despite the differences in the RBD of CPEB-1 and CPEB-3, they may both bind to the same sequences. As already mentioned in the section 5.2, CPEBs -2 to -4 have >98% identical RBDs. Therefore it is conceivable that CPEBs -2 and -4 share the binding

specificity with CPEB-3. Consequently, it is possible that despite differences in the primary structure between CPEB-1 and CPEBs -2 to -4, they all could regulate translation of the same target mRNAs.

CONCLUSION

mRNA sequence specificity of CPEB-1 and CPEB-3 is overlapping.

HYPOTHESIS

All CPEBs share similar phosphorylation regulatory mechanisms and regulate expression of an overlapping set of target mRNAs.

5.5 Novel CPEB targets

Two potential novel CPEB target mRNAs have been identified by RNA co-IP: the astrocytic gap junction protein Cx43 and the CPEB-3 itself. The function of such a positive feedback loop in case of CPEB-3 has to be elucidated. The hypothesis that increased translation of CPEB-3 after neuronal stimulation leads to increased inhibition of target mRNA, thereby modulating synaptic efficacy, awaits experimental evidence. In turn, the function of Cx43 in the CNS is better understood. Cx43 together with Cx30 comprise the major astrocytic connexins (Nagy *et al.*, 2004). They mediate gap-junctional communication between astrocytes, thereby forming an interconnected syncytium. This was demonstrated by tracer-coupling experiments in transgenic mice with deletion of Cx30 (gjb6) and Cx43 (gja1) genes in astrocytes (the DKO mice, see also section 3.26) (Wallraff *et al.*, 2006; Requardt, Kaczmarczyk *et al.*, 2009). In these mice Cx30 is deleted in all cells of the body and the deletion of Cx43 is astrocyte-directed, achieved via the Cre/LoxP system using a hGFAP-Cre driver (Zhuo *et al.*, 2001) (deletion of Cx43 in all cells of the body leads to embryonic lethality due to heart failure) (see also section 1.8). These mice display complete ablation of astrocytic coupling – a property that has made them extensively used in research of astrocytic gap-junctional communication in brain (patho)physiology (Wallraff *et al.*, 2006; Rouach *et al.*, 2008; Lutz *et al.*, 2009). Interestingly, the DKO mice have a decreased threshold for epileptic seizure activity (Wallraff *et al.*, 2006). This is in line with the suggested role of glia in K^+ buffering and thereby regulation of K^+ homeostasis in the CNS (Orkand *et al.*, 1966). More recently, astrocytic networks were found to participate in metabolite delivery to neurons, essential for maintaining synaptic transmission (Rouach *et al.*, 2008). Altogether, these finding suggest the dysfunctions of astrocytic connexins may either promote excitability by impairment of K^+ homeostasis (fast onset effect) or decrease it by disruption of neuronal energy supply (delayed effect) (reviewed by Seifert *et al.*,

2010). Interestingly, both astrocytic gap junctions proteins - Cx43 and Cx30 - contain CPE elements in their mRNA 3'UTRs, as revealed by database sequence analysis. Immunohistochemical analysis of mice overexpressing CPEB-3a protein in astrocytes (tet-off system, hGFAP-driven tTA) show decreased expression of Cx30 and Cx43 proteins in double transgenic animals, as compared with the single transgenic littermate controls (Vangoor *et al.*, in preparation). Altogether, CPEB1, but possibly also CPEB2-4 might be involved in translational regulation of the major astrocytic connexins. The functional implications of this findings are to be elucidated.

5.6 The complexity of translational regulation by CPEB proteins

As mentioned before, the sequence specificity of CPEB proteins is not restricted to a specific and well defined consensus sequence. It is conceivable, that variations in CPEs are tolerated and that the number, sequence and positioning of CPEs on the mRNA affect CPEB function. Pique *et al.* (2008) hypothesize that position of CPE elements, their number and distance from the AAUAAA hexanucleotide, determine the magnitude and direction of regulation for a given transcript. CPEB- may either interact with other (mRNA binding) proteins, thereby requiring specific spatial distribution of binding sites. Huang *et al.* (2006) argue that in case of CPEBs -3 and -4, mRNA secondary structure is necessary for CPEB binding. This however would be difficult to explain in view of the overlapping specificity of CPEB-1 and CPEB-3. EMSA experiments showing CPEB binding to target mRNAs (Theis *et al.*, in revision) were usually performed on shorter fragments, which might not have the secondary structure they would have when incorporated into a full-length mRNA. In recent years several novel CPEB isoforms in addition to the ones previously reported (Theis *et al.*, 2003b) have been described (Wang and Cooper, 2009). *In silico* analysis of database information on CPEBs revealed existence of additional variants (Wang and Cooper, 2010). The significance of this variability, expression pattern of each isoform, and functions of alternatively spliced domains are in most cases to be disclosed. Unfortunately, such abundance of transcripts and protein variants renders the analysis with conventional molecular biology tools (e.g. immunoblotting or immunocytochemistry) highly difficult. Herein, a function of the B-region in CPEB -2 to -4 regulation by phosphorylation is proposed. The significance of the phosphorylation *in vivo* awaits to be described. An intriguing hypothesis would be that some unknown splicing factors modulate CPEB function via changing the domain composition as a response to stimulation/activation. Addressing the question if such mechanism exists in neurons and are activated upon kainite stimulation would require employment of global proteomic analysis of stimulated hippocampal cultures and

transgenic mice. Lack of well-defined specificity of CPEBs is making analysis of mRNA binding in co-IP assay a difficult task. In this thesis I have established an RNA co-IP assay using a recombinant, FLAG-tagged protein. To discriminate between specific binding and unspecific background, the immunoprecipitated material was analyzed using a quantitative RT-PCR, and the data normalized to unspecific protein control levels. Still, the binding specificity of CPEBs require further investigation, and alternative *in vitro* binding studies may likely prove to be required for interpretation of the *in vivo* observations.

5.7 Cre transgenic mice require experimental validation of floxed gene deletion

As already mentioned (section 1.8.1), Cre-transgenes are not free of limitations. One of the problem occurring with hGFAP-Cre is the spontaneous downregulation (or loss) of Cre expression (Requardt, Kaczmarczyk *et al.*, 2009). Several hypothetical mechanisms lying behind the heterogeneity of hGFAP-Cre mediated recombination were discussed and tested (Requardt, Kaczmarczyk *et al.*, 2009). The results remained inconclusive, and the question about the cause of observed vagaries remains open. In section 4.9 an immunoblot-based recombination fidelity control method of hGFAP-Cre-mediated gene deletions was described. The method enables the selection and evaluation of knockout animals bearing the hGFAP-Cre transgene. The presented quality control method is strongly recommended when working with the hGFAP-Cre transgene. An identical or similar approach may be applied as an additional control to other GFAP-Cre transgenes, widely used in the glial field. Immunoblot-determined Cx43 deletion status in Cx30/43 DKO mice was consistent within individual litters and breedings. Therefore, sibling can be used to initially determine the suitability of a given litter for experiments. Nonetheless, it is strongly recommended to post-experimentally validate the individual mice, to exclude the chances that observed phenotypical alterations are caused by incomplete recombination.

6 Summary

CPEBs are a family of evolutionary conserved auxiliary translational factors. They bind to CPEs in the 3'UTR of target mRNA and, by interacting with other members of the translational machinery, promote or decrease gene expression. Since the first description of CPEB protein as a key orchestrator of oocyte maturation in *Xenopus Laevis*, key functions of CPEBs in embryonic development, cellular senescence and synaptic plasticity have been described (reviewed by Richter, 2007). Local, postsynaptic modulation of synaptic efficacy is the most studied function of CPEBs in the CNS. However, the expression of CPEBs is not restricted to neurons and even 7% of total brain mRNAs possesses CPEs. Moreover, specific mRNAs are enriched in functionally distinct subcellular regions, like dendritic spines of neurons or complex cellular processes of astrocytes, where they might be translationally regulated. Herein, I embarked on further elucidating the role of CPEB translational regulators family in selected cell populations in mouse brain.

In the first part of the work, the target mRNA specificity of different CPEBs was tested. I argued with the hypothesis that CPEBs -3 and -4 require mRNA secondary structure (a stem-loop) for target recognition (Huang *et al.*, 2006). I showed that despite differences in the RBD primary structure, CPEB-1 shows a considerable sequence specificity overlap with CPEB-3 (and possibly, due to sequence similarity, with CPEBs -2 and -4 as well). This holds true for neuronal (CaMKIIα) and astrocytic (β-catenin) CPEB targets (Theis *et al.*, in revision). Additionally, RNA co-immunoprecipitation revealed two novel CPEB target mRNAs, encoding (1) an astrocytic gap junction protein (Connexin43) and (2) CPEB-3 protein itself.

In the second part of the thesis, CPEBs 1-4 gene expression in microglia, NG2 cells and astrocytes was assessed at the mRNA and protein level, confirming the ubiquitous nature of the CPEB expression. A more detailed analysis of CPEB-3 mRNA revealed expression of only certain isoforms of the protein in ESdM cells. Each CPEB family member occurs in several splice variants. Hitherto, only a handful of reports are dealing with the significance of alternative splicing of CPEBs. Interestingly, regulation of expression of CPEBs in neurons may happen in an isoform-specific fashion (Theis *et al.*, 2003b). Seeing this as a highly intriguing phenomenon, I focused on CPEB-3, containing a putative kinase recognition site on the alternatively spliced exon 5. In a cell-free systems and in cultured cells, I showed that CPEB-3 is a target of PKA and CaMKII – both critical for LTP/LTD (Grey and Burrell, 2010), and that exon 5 harbors a consensus sequence required for kinase recognition. *In vivo*, in a transgenic mouse overexpressing CPEB3 protein in principal neurons of the hippocampus, I found a significant decrease in GluR2 AMPA-R subunit protein levels. In view of the above, the stimulation-induced phosphorylation of CPEB-3 may very well be a novel mechanism of translational modulation of synaptic plasticity.

In the third part, I embarked on unraveling the function of CPEBs in microglial cells, using ESdM cells (Napoli *et al.*, 2009) as model system. I tried to test the hypothesis, that CPEB translationally regulates the production of microglial tPA – the major factor causing neurodegeneration following epileptic seizures in mouse brain (Tsirka *et al.*, 1995). Using retroviral gene targeting followed by FACS of cellular populations, I tried to interfere with the microglial CPEB function by expressing a DN-CPEB1-4 transgene. DN-CPEB1-4 expression was successfully established in ESdM cells. Despite that, I did not observe a significant impact of DN-CPEB1-4 overexpression on the microglial tPA production in cultured ESdM cells.

In the final part of the thesis, I aimed at establishing a quality control method for Cre-mediated gene deletions. Using $Cx30^{-/-};Cx43^{fl/fl}$ mice with hGFAP-Cre recombinase driver, I developed a reliable immunoblot-based tool for post-hoc control of recombination variability in hGFAP-Cre transgenic mice (Requardt, Kaczmarczyk *et al.*, 2009).

7 Future Outlook

7.1 Detailed analysis of CPEB expression

In view of the recent findings describing new CPEB1-4 splice isoforms (Wang and Cooper, 2009; Wang and Cooper, 2010), the CPEB1-4 splicing pattern should be investigated in more detail. Using (1) single cell RT-PCR and (2) (laser capture) microdissection of specific hippocampal subregions and FACS-separation of brain cell subpopulations, followed by Taq-Man-based sqRT-PCR and end-point RT-PCR followed by SNPplex electrophoresis, the distribution and region/cell specificity of individual isoforms could be determined. In addition, it awaits confirmation if activity-induced increases of CPEB-3 and -4 mRNA following intraperitoneal kainate injection (Theis *et al.*, 2003b) are indeed isoform-specific. This can be tested with the abovementioned methods as well. If so, then one could conclude that neuronal activity-induced splicing may modulate CPEB expression and properties (e.g. presence or absence of phosphorylation sites) in synapse-specific manner.

7.2 Elucidating the significance of alternative splicing

The significance of the multitude of splice isoforms of CPEBs in unknown. Herein I propose the hypothesis that the presence of the B-domain in CPEB-2 to -4 affects the propensity of those proteins for PKA and CaMKII phosphorylation. Both of these kinases are critical in synaptic plasticity (Wang *et al.*, 2006; Wu *et al.*, 2006; Anwyl, 2009; Lucchesi *et al.*, 2011). CPEBs have been shown to be involved in synaptic plasticity (Wu *et al.*, 1998; Alarcon *et al.*, 2004; Aslam *et al.*, 2009; Theis *et al.*, in revision). It is therefore reasonable to investigate the putative implication of CPEB splicing and phosphorylation in learning and memory. And what about other CPEB isoforms? Do they contain regulatory elements? Or maybe interaction domains, binding to translational factors or scaffold proteins? Coupling *in vitro* (interaction studies) and *in vivo* (mouse transgenics and detailed mRNA and protein isoform expression analysis) might shed some light on this intriguing phenomenon.

7.3 Testing mRNA sequence specificity determinants

In view or the mRNA co-IP results, CPEBs-1 to -4 may have overlapping specificity, as shown herein for the CaMKIIα and β-catenin mRNAs. On the other hand, CPEB-3 was shown to require mRNA secondary structure for target recognition (Huang *et al.*, 2006). Targets of CPEBs differ in the positioning and sequence of the CPE elements present. Hypothetically, the position of CPEs with respect to the AAUAAA hexanucleotide (and other regulatory elements) may influence CPEB binding and activity (Pique *et al.*, 2008). We might be still far away from understanding the molecular mechanism of CPEB

function and its determinants. Protein – RNA interaction experiments (using EMSA, Surface Plasmon Resonance (SPR), etc.) involving recombinant CPEBs and artificial or real mRNA sequences containing CPEs in different (i) number, (ii) composition, (iii) relative placement, or (iv) secondary structure might be helpful to shed some light on this issue. On the other hand, it is conceivable that CPEBs require binding partners (e.g. CPSF) to recognize/bind target mRNA. Altogether, this seems to be the property of CPEBs which is the hardest to study, yet without answering this question the molecular picture of CPE-dependent polyadenylation will remain incomplete.

7.4 Studying the function of neuronal CPEBs in vivo

Transgenic mice overexpressing CPEB isoforms, as well as phosphorylation site mutants (constitutively active or kinase-dead) may be used to address the CPEB function *in vivo*. Using electrophysiological methods coupled with two-photon LSCM (transgenes are EGFP-tagged), together with the biochemical analysis, it might be possible to dissect how translational regulation contributes to local changes of synaptic plasticity in brain. How are CPEBs (trans)located and how stimulation affects their subcellular localization? Finally, how does the presence or absence of alternatively spliced domains and regulatory sites affect the CPEB function? And how this relates to the overall morphology (and properties) of the postsynapse?

7.4.1 Regulation of the GluR2 subunit of the AMPA-R

Herein I have shown that overexpression of CPEB-3 in forebrain neurons leads to a decrease in GluR2 protein levels (see section 4.2). This corroborates earlier findings, showing increase of GluR2 expression in primary hippocampal neurons, following siRNA-mediated knock-down of CPEB-3 (Huang *et al.*, 2006). The GluR2 subunit critically determines the properties of the AMPA-R function, affecting receptor kinetics, Ca^{2+} permeability, conductance and sensitivity to endogenous polyamines (Isaac *et al.*, 2007). Using the patch-clamp technique, one could look at how expression of CPEB-3 and its mutants affect AMPA-R expression and Ca^{2+} permeability. Using NMDA-R agonists and antagonists on acute slice preparation, and two-photon LSCM with UV laser based glutamate uncaging, one could look *in vivo* at how synapse morphology and calcium transients are affected in CPEB-3 overexpressing mice. Finally, using electrophysiological paradigms to induce LTP (repeated TBS trains) one could investigate whether mice expressing CPEB-3 and its kinase-dead mutant show altered LTP.

7.5 Studying the function of glial CPEBs in vivo

RNA co-IP revealed mRNA encoding the astrocytic gap junction protein connexin43 as a CPEB target. In addition, glial cells express proteins reported to undergo translational regulation in neurons, like β-catenin in astrocytes, GluR2 in NG2 glia, or tPA in microglia. β-catenin is an astrocytic CPEB-1 target (Jones *et al.*, 2008). Herein I showed by RNA co-IP, that CPEB-3 binds to the β-catenin mRNA as well. Therefore, this mRNA may be regulated by other members of CPEB family as well, which is likely to be the case for neuronal and glial CPEBs. And what about other CPE-containing astrocytic transcripts? The astrocyte-specific GFAP-tTA transgene already serves as a tool to dissect CPEB function by overexpression of CPEBs in these cells (Vangoor *et al.*, in preparation). Moreover, I have embarked on generating a microglia-specific tTA mouse line (expressing tTA driven by the iba1 promoter). These mice are currently under screening and, if suitable, may be used to elucidate potential function of CPEBs in the regulation of microglial tPA production.

7.6 CPEBs in the context of temporal lobe epilepsy (TLE)

Epileptiform activity entails molecular mechanisms similar to those correlated with learning and memory, including LTP. Are neuronal or glial CPEBs involved in epileptogenesis? Is defective translation one of the reasons for disappearance of astrocytes in the epileptic hippocampus? CPEB transcripts are strongly upregulated in the hippocampus upon induction of status epilepticus (SE) in mice (Theis *et al.*, 2003b). In the intracortical kainate injection model, mice expressing a DN-CPEB1-4 in forebrain neurons (Theis *et al.*, in revision) show significantly weaker SE, but develop more generalized, recurrent seizures at a later timepoint (Dr. Peter Bedner, unpublished data). The mechanism behind this observation is to be disclosed, yet it is probable that CPEBs, being to a significant extent implicated in L-LTP formation, have likewise a function in TLE pathology. The DN-CPEB1-4 transgene leads to translational repression of CPE-containing mRNAs. It is worthwhile to investigate if overexpression of CPEB-3 and/or a CPEB-3 constitutively active mutant (S419D) would have the opposite effects.

References

Alarcon, J. M., R. Hodgman, M. Theis, Y. S. Huang, E. R. Kandel and J. D. Richter (2004). "Selective modulation of some forms of schaffer collateral-CA1 synaptic plasticity in mice with a disruption of the CPEB-1 gene." Learn Mem **11**(3): 318-327.

Anwyl, R. (2009). "Metabotropic glutamate receptor-dependent long-term potentiation." Neuropharmacology **56**(4): 735-740.

Ashkenas, J. (1997). "Gene regulation by mRNA editing." Am J Hum Genet **60**(2): 278-283.

Aslam, N., Y. Kubota, D. Wells and H. Z. Shouval (2009). "Translational switch for long-term maintenance of synaptic plasticity." Mol Syst Biol **5**: 284.

Atkins, C. M., M. A. Davare, M. C. Oh, V. Derkach and T. R. Soderling (2005). "Bidirectional regulation of cytoplasmic polyadenylation element-binding protein phosphorylation by Ca2+/calmodulin-dependent protein kinase II and protein phosphatase 1 during hippocampal long-term potentiation." J Neurosci **25**(23): 5604-5610.

Atkins, C. M., N. Nozaki, Y. Shigeri and T. R. Soderling (2004). "Cytoplasmic polyadenylation element binding protein-dependent protein synthesis is regulated by calcium/calmodulin-dependent protein kinase II." J Neurosci **24**(22): 5193-5201.

Barnard, D. C., K. Ryan, J. L. Manley and J. D. Richter (2004). "Symplekin and xGLD-2 are required for CPEB-mediated cytoplasmic polyadenylation." Cell **119**(5): 641-651.

Bassani, S., P. Valnegri, F. Beretta and M. Passafaro (2009). "The GLUR2 subunit of AMPA receptors: synaptic role." Neuroscience **158**(1): 55-61.

Berger-Sweeney, J., N. R. Zearfoss and J. D. Richter (2006). "Reduced extinction of hippocampal-dependent memories in CPEB knockout mice." Learn Mem **13**(1): 4-7.

Blasi, E., R. Barluzzi, V. Bocchini, R. Mazzolla and F. Bistoni (1990). "Immortalization of murine microglial cells by a v-raf/v-myc carrying retrovirus." J Neuroimmunol **27**(2-3): 229-237.

Bliss, T. V. and G. L. Collingridge (1993). "A synaptic model of memory: long-term potentiation in the hippocampus." Nature **361**(6407): 31-39.

Bodian, D. (1965). "A Suggestive Relationship of Nerve Cell Rna with Specific Synaptic Sites." Proc Natl Acad Sci U S A **53**: 418-425.

Cajigas, I. J., T. Will and E. M. Schuman (2010). "Protein homeostasis and synaptic plasticity." EMBO J **29**(16): 2746-2752.

Cao, Q., Y. S. Huang, M. C. Kan and J. D. Richter (2005). "Amyloid precursor proteins anchor CPEB to membranes and promote polyadenylation-induced translation." Mol Cell Biol **25**(24): 10930-10939.

Capecchi, M. R. (2001). "Generating mice with targeted mutations." Nat Med **7**(10): 1086-1090.

Casper, K. B., K. Jones and K. D. McCarthy (2007). "Characterization of astrocyte-specific conditional knockouts." Genesis **45**(5): 292-299.

Copeland, P. R. and M. Wormington (2001). "The mechanism and regulation of deadenylation: identification and characterization of Xenopus PARN." RNA **7**(6): 875-886.

Corpet, F. (1988). "Multiple sequence alignment with hierarchical clustering." Nucleic Acids Res **16**(22): 10881-10890.

Curtis, D., R. Lehmann and P. D. Zamore (1995). "Translational regulation in development." Cell **81**(2): 171-178.

Derkach, V. A., M. C. Oh, E. S. Guire and T. R. Soderling (2007). "Regulatory mechanisms of AMPA receptors in synaptic plasticity." Nat Rev Neurosci **8**(2): 101-113.

Doetschman, T., N. Maeda and O. Smithies (1988). "Targeted mutation of the Hprt gene in mouse embryonic stem cells." Proc Natl Acad Sci U S A **85**(22): 8583-8587.

Du, L. and J. D. Richter (2005). "Activity-dependent polyadenylation in neurons." RNA **11**(9): 1340-1347.

Duffy, S. N., K. J. Craddock, T. Abel and P. V. Nguyen (2001). "Environmental enrichment modifies the PKA-dependence of hippocampal LTP and improves hippocampus-dependent memory." Learn Mem **8**(1): 26-34.

Eberwine, J., B. Belt, J. E. Kacharmina and K. Miyashiro (2002). "Analysis of subcellularly localized mRNAs using in situ hybridization, mRNA amplification, and expression profiling." Neurochem Res **27**(10): 1065-1077.

Eckardt, D., M. Theis, B. Doring, D. Speidel, K. Willecke and T. Ott (2004). "Spontaneous ectopic recombination in cell-type-specific Cre mice removes loxP-flanked marker cassettes in vivo." Genesis **38**(4): 159-165.

Emini, E. A., J. V. Hughes, D. S. Perlow and J. Boger (1985). "Induction of hepatitis A virus-neutralizing antibody by a virus-specific synthetic peptide." J Virol **55**(3): 836-839.

Evans, M. J. and M. H. Kaufman (1981). "Establishment in culture of pluripotential cells from mouse embryos." Nature **292**(5819): 154-156.

Gainey, M. A., J. R. Hurvitz-Wolff, M. E. Lambo and G. G. Turrigiano (2009). "Synaptic scaling requires the GluR2 subunit of the AMPA receptor." J Neurosci **29**(20): 6479-6489.

Gelinas, J. N., G. Tenorio, N. Lemon, T. Abel and P. V. Nguyen (2008). "Beta-adrenergic receptor activation during distinct patterns of stimulation critically modulates the PKA-dependence of LTP in the mouse hippocampus." Learn Mem **15**(5): 281-289.

Geller, S. F., P. S. Ge, M. Visel, K. P. Greenberg and J. G. Flannery (2007). "Functional promoter testing using a modified lentiviral transfer vector." Mol Vis **13**: 730-739.

Gosejacob, D., P. Dublin, P. Bedner, K. Huttmann, J. Zhang, O. Tress, K. Willecke, F. Pfrieger, C. Steinhauser and M. Theis (2011). "Role of astroglial connexin30 in hippocampal gap junction coupling." Glia **59**(3): 511-519.

Gossen, M. and H. Bujard (1992). "Tight control of gene expression in mammalian cells by tetracycline-responsive promoters." Proc Natl Acad Sci U S A **89**(12): 5547-5551.

Grey, K. B. and B. D. Burrell (2010). "Co-induction of LTP and LTD and its regulation by protein kinases and phosphatases." J Neurophysiol **103**(5): 2737-2746.

Hake, L. E., R. Mendez and J. D. Richter (1998). "Specificity of RNA binding by CPEB: requirement for RNA recognition motifs and a novel zinc finger." Mol Cell Biol **18**(2): 685-693.

Hall, T. A. (1999). "BioEdit: a user-friendly biological sequence alignment editor and analysis program for Windows 95/98/NT." Nucl. Acids. Symp. Ser. **41**: 95-98.

Hansson, E. and L. Ronnback (2003). "Glial neuronal signaling in the central nervous system." FASEB J **17**(3): 341-348.

Higuchi, R., C. Fockler, G. Dollinger and R. Watson (1993). "Kinetic PCR analysis: real-time monitoring of DNA amplification reactions." Biotechnology (N Y) **11**(9): 1026-1030.

Hinterkeuser, S., W. Schroder, G. Hager, G. Seifert, I. Blumcke, C. E. Elger, J. Schramm and C. Steinhauser (2000). "Astrocytes in the hippocampus of patients with temporal lobe epilepsy display changes in potassium conductances." Eur J Neurosci **12**(6): 2087-2096.

Hirrlinger, J., R. P. Requardt, U. Winkler, F. Wilhelm, C. Schulze and P. G. Hirrlinger (2009). "Split-CreERT2: temporal control of DNA recombination mediated by split-Cre protein fragment complementation." PLoS One **4**(12): e8354.

Hirrlinger, P. G., A. Scheller, C. Braun, J. Hirrlinger and F. Kirchhoff (2006). "Temporal control of gene recombination in astrocytes by transgenic expression of the tamoxifen-inducible DNA recombinase variant CreERT2." Glia **54**(1): 11-20.

Hovland, R., J. E. Hesketh and I. F. Pryme (1996). "The compartmentalization of protein synthesis: importance of cytoskeleton and role in mRNA targeting." Int J Biochem Cell Biol **28**(10): 1089-1105.

Huang, Y. S., J. H. Carson, E. Barbarese and J. D. Richter (2003). "Facilitation of dendritic mRNA transport by CPEB." Genes Dev **17**(5): 638-653.

Huang, Y. S., M. Y. Jung, M. Sarkissian and J. D. Richter (2002). "N-methyl-D-aspartate receptor signaling results in Aurora kinase-catalyzed CPEB phosphorylation and alpha CaMKII mRNA polyadenylation at synapses." EMBO J **21**(9): 2139-2148.

Huang, Y. S., M. C. Kan, C. L. Lin and J. D. Richter (2006). "CPEB3 and CPEB4 in neurons: analysis of RNA-binding specificity and translational control of AMPA receptor GluR2 mRNA." EMBO J **25**(20): 4865-4876.

Huber, K. M., M. S. Kayser and M. F. Bear (2000). "Role for rapid dendritic protein synthesis in hippocampal mGluR-dependent long-term depression." Science **288**(5469): 1254-1257.

Isaac, J. T., M. C. Ashby and C. J. McBain (2007). "The role of the GluR2 subunit in AMPA receptor function and synaptic plasticity." Neuron **54**(6): 859-871.

Jabs, R., T. Pivneva, K. Huttmann, A. Wyczynski, C. Nolte, H. Kettenmann and C. Steinhauser (2005). "Synaptic transmission onto hippocampal glial cells with hGFAP promoter activity." J Cell Sci **118**(Pt 16): 3791-3803.

Jackson, R. J., C. U. Hellen and T. V. Pestova (2010). "The mechanism of eukaryotic translation initiation and principles of its regulation." Nat Rev Mol Cell Biol **11**(2): 113-127.

Jameson, B. A. and H. Wolf (1988). "The antigenic index: a novel algorithm for predicting antigenic determinants." Comput Appl Biosci **4**(1): 181-186.

Jansen, R. P. (2001). "mRNA localization: message on the move." Nat Rev Mol Cell Biol **2**(4): 247-256.

Jia, Z., N. Agopyan, P. Miu, Z. Xiong, J. Henderson, R. Gerlai, F. A. Taverna, A. Velumian, J. MacDonald, P. Carlen, W. Abramow-Newerly and J. Roder (1996). "Enhanced LTP in mice deficient in the AMPA receptor GluR2." Neuron **17**(5): 945-956.

Johnstone, O. and P. Lasko (2001). "Translational regulation and RNA localization in Drosophila oocytes and embryos." Annu Rev Genet **35**: 365-406.

Jones, K. J., E. Korb, M. A. Kundel, A. R. Kochanek, S. Kabraji, M. McEvoy, C. Y. Shin and D. G. Wells (2008). "CPEB1 regulates beta-catenin mRNA translation and cell migration in astrocytes." Glia **56**(13): 1401-1413.

Jung, M. Y., L. Lorenz and J. D. Richter (2006). "Translational control by neuroguidin, a eukaryotic initiation factor 4E and CPEB binding protein." Mol Cell Biol **26**(11): 4277-4287.

Jung, S., J. Aliberti, P. Graemmel, M. J. Sunshine, G. W. Kreutzberg, A. Sher and D. R. Littman (2000). "Analysis of fractalkine receptor CX(3)CR1 function by targeted deletion and green fluorescent protein reporter gene insertion." Mol Cell Biol **20**(11): 4106-4114.

Kandel, E. R. (2001). "The molecular biology of memory storage: a dialogue between genes and synapses." Science **294**(5544): 1030-1038.

Kang, H. and E. M. Schuman (1996). "A requirement for local protein synthesis in neurotrophin-induced hippocampal synaptic plasticity." Science **273**(5280): 1402-1406.

Karram, K., S. Goebbels, M. Schwab, K. Jennissen, G. Seifert, C. Steinhauser, K. A. Nave and J. Trotter (2008). "NG2-expressing cells in the nervous system revealed by the NG2-EYFP-knockin mouse." Genesis **46**(12): 743-757.

Keleman, K., S. Kruttner, M. Alenius and B. J. Dickson (2007). "Function of the Drosophila CPEB protein Orb2 in long-term courtship memory." Nat Neurosci **10**(12): 1587-1593.

Kellendonk, C., F. Tronche, E. Casanova, K. Anlag, C. Opherk and G. Schutz (1999). "Inducible site-specific recombination in the brain." J Mol Biol **285**(1): 175-182.

Kessels, H. W. and R. Malinow (2009). "Synaptic AMPA receptor plasticity and behavior." Neuron **61**(3): 340-350.

Klann, E. and T. E. Dever (2004). "Biochemical mechanisms for translational regulation in synaptic plasticity." Nat Rev Neurosci **5**(12): 931-942.

Kyte, J. and R. F. Doolittle (1982). "A simple method for displaying the hydropathic character of a protein." J Mol Biol **157**(1): 105-132.

Laemmli, U. K. (1970). "Cleavage of structural proteins during the assembly of the head of bacteriophage T4." Nature **227**(5259): 680-685.

Laird, P. W., A. Zijderveld, K. Linders, M. A. Rudnicki, R. Jaenisch and A. Berns (1991). "Simplified mammalian DNA isolation procedure." Nucleic Acids Res **19**(15): 4293.

Lein, E. S., M. J. Hawrylycz, N. Ao, M. Ayres, A. Bensinger, A. Bernard, A. F. Boe, M. S. Boguski, K. S. Brockway, E. J. Byrnes, L. Chen, T. M. Chen, M. C. Chin, J. Chong, B. E. Crook, A. Czaplinska, C. N. Dang, S. Datta, N. R. Dee, A. L. Desaki, T. Desta, E. Diep, T. A. Dolbeare, M. J. Donelan, H. W. Dong, J. G. Dougherty, B. J. Duncan, A. J. Ebbert, G. Eichele, L. K. Estin, C. Faber, B. A. Facer, R. Fields, S. R. Fischer, T. P. Fliss, C. Frensley, S. N. Gates, K. J. Glattfelder, K. R. Halverson, M. R. Hart, J. G. Hohmann, M. P. Howell, D. P. Jeung, R. A. Johnson, P. T. Karr, R. Kawal, J. M. Kidney, R. H. Knapik, C. L. Kuan, J. H. Lake, A. R. Laramee, K. D. Larsen, C. Lau, T. A. Lemon, A. J. Liang, Y. Liu, L. T. Luong, J. Michaels, J. J. Morgan, R. J. Morgan, M. T. Mortrud, N. F. Mosqueda, L. L. Ng, R. Ng, G. J. Orta, C. C. Overly, T. H. Pak, S. E. Parry, S. D. Pathak, O. C. Pearson, R. B. Puchalski, Z. L. Riley, H. R. Rockett, S. A. Rowland, J. J. Royall, M. J. Ruiz, N. R. Sarno, K. Schaffnit, N. V. Shapovalova, T. Sivisay, C. R. Slaughterbeck, S. C. Smith, K. A. Smith, B. I. Smith, A. J. Sodt, N. N. Stewart, K. R. Stumpf, S. M. Sunkin, M. Sutram, A. Tam, C. D. Teemer, C. Thaller, C. L. Thompson, L. R. Varnam, A. Visel, R. M. Whitlock, P. E. Wohnoutka, C. K. Wolkey, V. Y. Wong, M. Wood, M. B. Yaylaoglu, R. C. Young, B. L. Youngstrom, X. F. Yuan, B. Zhang, T. A. Zwingman and A. R. Jones (2007). "Genome-wide atlas of gene expression in the adult mouse brain." Nature **445**(7124): 168-176.

Lin, S. C. and D. E. Bergles (2004). "Synaptic signaling between neurons and glia." Glia **47**(3): 290-298.

Lisman, J., H. Schulman and H. Cline (2002). "The molecular basis of CaMKII function in synaptic and behavioural memory." Nat Rev Neurosci **3**(3): 175-190.

Lucchesi, W., K. Mizuno and K. P. Giese (2011). "Novel insights into CaMKII function and regulation during memory formation." Brain Res Bull **85**(1-2): 2-8.

Luscher, C. and K. M. Huber (2010). "Group 1 mGluR-dependent synaptic long-term depression: mechanisms and implications for circuitry and disease." Neuron **65**(4): 445-459.

Lutz, S. E., Y. Zhao, M. Gulinello, S. C. Lee, C. S. Raine and C. F. Brosnan (2009). "Deletion of astrocyte connexins 43 and 30 leads to a dysmyelinating phenotype and hippocampal CA1 vacuolation." J Neurosci **29**(24): 7743-7752.

Macdonald, P. (2001). "Diversity in translational regulation." Curr Opin Cell Biol **13**(3): 326-331.

Malys, N. and J. E. McCarthy (2011). "Translation initiation: variations in the mechanism can be anticipated." Cell Mol Life Sci **68**(6): 991-1003.

Martens, K., A. Bottelbergs and M. Baes (2010). "Ectopic recombination in the central and peripheral nervous system by aP2/FABP4-Cre mice: implications for metabolism research." FEBS Lett **584**(5): 1054-1058.

Matthias, K., F. Kirchhoff, G. Seifert, K. Huttmann, M. Matyash, H. Kettenmann and C. Steinhauser (2003). "Segregated expression of AMPA-type glutamate receptors and glutamate transporters defines distinct astrocyte populations in the mouse hippocampus." J Neurosci **23**(5): 1750-1758.

Mayford, M., M. E. Bach, Y. Y. Huang, L. Wang, R. D. Hawkins and E. R. Kandel (1996). "Control of memory formation through regulated expression of a CaMKII transgene." Science **274**(5293): 1678-1683.

Mayford, M. and E. R. Kandel (1999). "Genetic approaches to memory storage." Trends Genet **15**(11): 463-470.

McEvoy, M., G. Cao, P. Montero Llopis, M. Kundel, K. Jones, C. Hofler, C. Shin and D. G. Wells (2007). "Cytoplasmic polyadenylation element binding protein 1-mediated mRNA translation in Purkinje neurons is required for cerebellar long-term depression and motor coordination." J Neurosci **27**(24): 6400-6411.

Mendez, R. and J. D. Richter (2001). "Translational control by CPEB: a means to the end." Nat Rev Mol Cell Biol **2**(7): 521-529.

Merrick, W. C. (1992). "Mechanism and regulation of eukaryotic protein synthesis." Microbiol Rev **56**(2): 291-315.

Miniaci, M. C., J. H. Kim, S. V. Puthanveettil, K. Si, H. Zhu, E. R. Kandel and C. H. Bailey (2008). "Sustained CPEB-dependent local protein synthesis is required to stabilize synaptic growth for persistence of long-term facilitation in Aplysia." Neuron **59**(6): 1024-1036.

Moon, A. M., A. M. Boulet and M. R. Capecchi (2000). "Normal limb development in conditional mutants of Fgf4." Development **127**(5): 989-996.

Mori, T., K. Tanaka, A. Buffo, W. Wurst, R. Kuhn and M. Gotz (2006). "Inducible gene deletion in astroglia and radial glia--a valuable tool for functional and lineage analysis." Glia **54**(1): 21-34.

Muckenthaler, M., N. K. Gray and M. W. Hentze (1998). "IRP-1 binding to ferritin mRNA prevents the recruitment of the small ribosomal subunit by the cap-binding complex eIF4F." Mol Cell **2**(3): 383-388.

Nagy, J. I., F. E. Dudek and J. E. Rash (2004). "Update on connexins and gap junctions in neurons and glia in the mammalian nervous system." Brain Res Brain Res Rev **47**(1-3): 191-215.

Napoli, I., K. Kierdorf and H. Neumann (2009). "Microglial precursors derived from mouse embryonic stem cells." Glia **57**(15): 1660-1671.

Odeh, F., T. B. Leergaard, J. Boy, T. Schmidt, O. Riess and J. G. Bjaalie (2011). "Atlas of transgenic Tet-Off Ca2+/calmodulin-dependent protein kinase II and prion protein promoter activity in the mouse brain." Neuroimage **54**(4): 2603-2611.

Orkand, R. K., J. G. Nicholls and S. W. Kuffler (1966). "Effect of nerve impulses on the membrane potential of glial cells in the central nervous system of amphibia." J Neurophysiol **29**(4): 788-806.

Ostareck, D. H., A. Ostareck-Lederer, I. N. Shatsky and M. W. Hentze (2001). "Lipoxygenase mRNA silencing in erythroid differentiation: The 3'UTR regulatory complex controls 60S ribosomal subunit joining." Cell **104**(2): 281-290.

Pique, M., J. M. Lopez, S. Foissac, R. Guigo and R. Mendez (2008). "A combinatorial code for CPE-mediated translational control." Cell **132**(3): 434-448.

Radford, H. E., H. A. Meijer and C. H. de Moor (2008). "Translational control by cytoplasmic polyadenylation in Xenopus oocytes." Biochim Biophys Acta **1779**(4): 217-229.

Requardt, R. P., L. Kaczmarczyk, P. Dublin, A. Wallraff-Beck, T. Mikeska, J. Degen, A. Waha, C. Steinhauser, K. Willecke and M. Theis (2009). "Quality control of astrocyte-directed Cre transgenic mice: the benefits of a direct link between loss of gene expression and reporter activation." Glia **57**(6): 680-692.

Richter, J. D. (2007). "CPEB: a life in translation." Trends Biochem Sci **32**(6): 279-285.

Richter, J. D. and P. Lasko (2011). "Translational Control in Oocyte Development." Cold Spring Harb Perspect Biol.

Rouach, N., A. Koulakoff, V. Abudara, K. Willecke and C. Giaume (2008). "Astroglial metabolic networks sustain hippocampal synaptic transmission." Science **322**(5907): 1551-1555.

Rouhana, L., L. Wang, N. Buter, J. E. Kwak, C. A. Schiltz, T. Gonzalez, A. E. Kelley, C. F. Landry and M. Wickens (2005). "Vertebrate GLD2 poly(A) polymerases in the germline and the brain." RNA **11**(7): 1117-1130.

Routtenberg, A. and J. L. Rekart (2005). "Post-translational protein modification as the substrate for long-lasting memory." Trends Neurosci **28**(1): 12-19.

Rozen, S. and H. Skaletsky (2000). "Primer3 on the WWW for general users and for biologist programmers." Methods Mol Biol **132**: 365-386.

Salehi-Ashtiani, K., A. Luptak, A. Litovchick and J. W. Szostak (2006). "A genomewide search for ribozymes reveals an HDV-like sequence in the human CPEB3 gene." Science **313**(5794): 1788-1792.

Sambrook, J. and D. W. Russell (2001). Molecular cloning : a laboratory manual. Cold Spring Harbor, N.Y., Cold Spring Harbor Laboratory Press.

Samson, A. L. and R. L. Medcalf (2006). "Tissue-type plasminogen activator: a multifaceted modulator of neurotransmission and synaptic plasticity." Neuron **50**(5): 673-678.

Santos, S. D., A. L. Carvalho, M. V. Caldeira and C. B. Duarte (2009). "Regulation of AMPA receptors and synaptic plasticity." Neuroscience **158**(1): 105-125.

Sauer, B. and N. Henderson (1988). "Site-specific DNA recombination in mammalian cells by the Cre recombinase of bacteriophage P1." Proc Natl Acad Sci U S A **85**(14): 5166-5170.

Schmidt-Supprian, M. and K. Rajewsky (2007). "Vagaries of conditional gene targeting." Nat Immunol **8**(7): 665-668.

Seifert, G., G. Carmignoto and C. Steinhauser (2010). "Astrocyte dysfunction in epilepsy." Brain Res Rev **63**(1-2): 212-221.

Shin, C. Y., M. Kundel and D. G. Wells (2004). "Rapid, activity-induced increase in tissue plasminogen activator is mediated by metabotropic glutamate receptor-dependent mRNA translation." J Neurosci **24**(42): 9425-9433.

Si, K., Y. B. Choi, E. White-Grindley, A. Majumdar and E. R. Kandel (2010). "Aplysia CPEB can form prion-like multimers in sensory neurons that contribute to long-term facilitation." Cell **140**(3): 421-435.

Si, K., M. Giustetto, A. Etkin, R. Hsu, A. M. Janisiewicz, M. C. Miniaci, J. H. Kim, H. Zhu and E. R. Kandel (2003). "A neuronal isoform of CPEB regulates local protein synthesis and stabilizes synapse-specific long-term facilitation in aplysia." Cell **115**(7): 893-904.

Siao, C. J., S. R. Fernandez and S. E. Tsirka (2003). "Cell type-specific roles for tissue plasminogen activator released by neurons or microglia after excitotoxic injury." J Neurosci **23**(8): 3234-3242.

Slezak, M., C. Goritz, A. Niemiec, J. Frisen, P. Chambon, D. Metzger and F. W. Pfrieger (2007). "Transgenic mice for conditional gene manipulation in astroglial cells." Glia **55**(15): 1565-1576.

Souaze, F., A. Ntodou-Thome, C. Y. Tran, W. Rostene and P. Forgez (1996). "Quantitative RT-PCR: limits and accuracy." Biotechniques **21**(2): 280-285.

Steward, O. and W. B. Levy (1982). "Preferential localization of polyribosomes under the base of dendritic spines in granule cells of the dentate gyrus." J Neurosci **2**(3): 284-291.

Sweatt, J. D. (1999). "Toward a molecular explanation for long-term potentiation." Learn Mem **6**(5): 399-416.

Tadros, W. and H. D. Lipshitz (2005). "Setting the stage for development: mRNA translation and stability during oocyte maturation and egg activation in Drosophila." Dev Dyn **232**(3): 593-608.

Takagaki, Y., J. L. Manley, C. C. MacDonald, J. Wilusz and T. Shenk (1990). "A multisubunit factor, CstF, is required for polyadenylation of mammalian pre-mRNAs." Genes Dev **4**(12A): 2112-2120.

Tarun, S. Z., Jr. and A. B. Sachs (1996). "Association of the yeast poly(A) tail binding protein with translation initiation factor eIF-4G." EMBO J **15**(24): 7168-7177.

Teubner, B., V. Michel, J. Pesch, J. Lautermann, M. Cohen-Salmon, G. Sohl, K. Jahnke, E. Winterhager, C. Herberhold, J. P. Hardelin, C. Petit and K. Willecke (2003). "Connexin30 (Gjb6)-deficiency causes severe hearing impairment and lack of endocochlear potential." Hum Mol Genet **12**(1): 13-21.

Theis, M., C. de Wit, T. M. Schlaeger, D. Eckardt, O. Kruger, B. Doring, W. Risau, U. Deutsch, U. Pohl and K. Willecke (2001). "Endothelium-specific replacement of the connexin43 coding region by a lacZ reporter gene." Genesis **29**(1): 1-13.

Theis, M., Gael Malleret, Juan Marcos Alarcon, Luana Fioriti, Yi-Shuian Huang, Lech Kaczmarczyk, Kevin Karl, Pierre Trifilieff, Kausik Si, Joel D. Richter and Eric R. Kandel (in revision). "Expression of a dominant negative CPEB in forebrain neurons impairs stimulation-induced translation, protein synthesis-dependent forms of hippocampal synaptic plasticity and long-term spatial reference memory."

Theis, M., R. Jauch, L. Zhuo, D. Speidel, A. Wallraff, B. Doring, C. Frisch, G. Sohl, B. Teubner, C. Euwens, J. Huston, C. Steinhauser, A. Messing, U. Heinemann and K. Willecke (2003a). "Accelerated hippocampal spreading depression and enhanced locomotory activity in mice with astrocyte-directed inactivation of connexin43." J Neurosci **23**(3): 766-776.

Theis, M., K. Si and E. R. Kandel (2003b). "Two previously undescribed members of the mouse CPEB family of genes and their inducible expression in the principal cell layers of the hippocampus." Proc Natl Acad Sci U S A **100**(16): 9602-9607.

Theis, M., D. Speidel and K. Willecke (2004). "Astrocyte cultures from conditional connexin43-deficient mice." Glia **46**(2): 130-141.

Thomas, K. R., K. R. Folger and M. R. Capecchi (1986). "High frequency targeting of genes to specific sites in the mammalian genome." Cell **44**(3): 419-428.

Tsien, J. Z., D. F. Chen, D. Gerber, C. Tom, E. H. Mercer, D. J. Anderson, M. Mayford, E. R. Kandel and S. Tonegawa (1996a). "Subregion- and cell type-restricted gene knockout in mouse brain." Cell **87**(7): 1317-1326.

Tsien, J. Z., P. T. Huerta and S. Tonegawa (1996b). "The essential role of hippocampal CA1 NMDA receptor-dependent synaptic plasticity in spatial memory." Cell **87**(7): 1327-1338.

Tsirka, S. E., A. Gualandris, D. G. Amaral and S. Strickland (1995). "Excitotoxin-induced neuronal degeneration and seizure are mediated by tissue plasminogen activator." Nature **377**(6547): 340-344.

Vangoor, V., S. L. Turimella, J. Zhang, L. Kaczmarczyk, P. Bedner, E. von Staden, A. Derouiche, R. Jabs, G. Seifert, C. Steinhäuser and M. Theis (in preparation). "Overexpression of CPEB3 in astrocytes represses the basal translation of the major gap junction proteins Connexin43 and Connexin30.".

Vogler, C., K. Spalek, A. Aerni, P. Demougin, A. Muller, K. D. Huynh, A. Papassotiropoulos and D. J. de Quervain (2009). "CPEB3 is associated with human episodic memory." Front Behav Neurosci **3**: 4.

Wallraff, A., R. Kohling, U. Heinemann, M. Theis, K. Willecke and C. Steinhauser (2006). "The impact of astrocytic gap junctional coupling on potassium buffering in the hippocampus." J Neurosci **26**(20): 5438-5447.

Wang, H., Y. Hu and J. Z. Tsien (2006). "Molecular and systems mechanisms of memory consolidation and storage." Prog Neurobiol **79**(3): 123-135.

Wang, X. P. and N. G. Cooper (2009). "Characterization of the transcripts and protein isoforms for cytoplasmic polyadenylation element binding protein-3 (CPEB3) in the mouse retina." BMC Mol Biol **10**: 109.

Wang, X. P. and N. G. Cooper (2010). "Comparative in silico analyses of cpeb1-4 with functional predictions." Bioinform Biol Insights **4**: 61-83.

Waterhouse, A. M., J. B. Procter, D. M. Martin, M. Clamp and G. J. Barton (2009). "Jalview Version 2--a multiple sequence alignment editor and analysis workbench." Bioinformatics **25**(9): 1189-1191.

Wells, S. E., P. E. Hillner, R. D. Vale and A. B. Sachs (1998). "Circularization of mRNA by eukaryotic translation initiation factors." Molecular cell **2**(1): 135-140.

Wicksteed, B., M. Brissova, W. Yan, D. M. Opland, J. L. Plank, R. B. Reinert, L. M. Dickson, N. A. Tamarina, L. H. Philipson, A. Shostak, E. Bernal-Mizrachi, L. Elghazi, M. W. Roe, P. A. Labosky, M. G. Myers, Jr., M. Gannon, A. C. Powers and P. J. Dempsey (2010). "Conditional gene targeting in mouse pancreatic ss-Cells: analysis of ectopic Cre transgene expression in the brain." Diabetes **59**(12): 3090-3098.

Wikstrom, M. A., P. Matthews, D. Roberts, G. L. Collingridge and Z. A. Bortolotto (2003). "Parallel kinase cascades are involved in the induction of LTP at hippocampal CA1 synapses." Neuropharmacology **45**(6): 828-836.

Wilhelm, J. E. and C. A. Smibert (2005). "Mechanisms of translational regulation in Drosophila." Biol Cell **97**(4): 235-252.

Wu, C. W., F. Zeng and J. Eberwine (2007). "mRNA transport to and translation in neuronal dendrites." Anal Bioanal Chem **387**(1): 59-62.

Wu, J., M. J. Rowan and R. Anwyl (2006). "Long-term potentiation is mediated by multiple kinase cascades involving CaMKII or either PKA or p42/44 MAPK in the adult rat dentate gyrus in vitro." J Neurophysiol **95**(6): 3519-3527.

Wu, L., D. Wells, J. Tay, D. Mendis, M. A. Abbott, A. Barnitt, E. Quinlan, A. Heynen, J. R. Fallon and J. D. Richter (1998). "CPEB-mediated cytoplasmic polyadenylation and the regulation of experience-dependent translation of alpha-CaMKII mRNA at synapses." Neuron **21**(5): 1129-1139.

Xiao, X. and J. H. Lee (2010). "Systems analysis of alternative splicing and its regulation." Wiley Interdiscip Rev Syst Biol Med **2**(5): 550-565.

Zhuo, L., M. Theis, I. Alvarez-Maya, M. Brenner, K. Willecke and A. Messing (2001). "hGFAP-cre transgenic mice for manipulation of glial and neuronal function in vivo." Genesis **31**(2): 85-94.

Appendix

DECLARATION

I hereby declare, that this Doctoral Thesis, entitled "Many facets of CPEB proteins in neurons and beyond: expression, mRNA recognition and phosphorylation", is original and was written independently, using no other sources and aids than stated. This document - in the current or similar form - has not and will not be submitted to any other institution, apart from the University of Bonn.

Bonn, November 2011

(Lech Kaczmarczyk)